UNIVERSIDAD AUTÓNOMA DE MADRID

DOCTORAL THESIS

Light induced interactions between nanoparticles in complex fields

Author:
Jorge LUIS HITA

Supervisor:
Prof. Juan José SÁENZ
Prof. Manuel Ignacio MARQUÉS

A thesis submitted in fulfillment of the requirements for the degree of Doctor of Philosophy

in the

MoLE Group
Departmento de Física de la Materia Condensada
and IFIMAC

June 26, 2017

Declaration of Authorship

I, Jorge LUIS HITA, declare that this thesis titled, "Light induced interactions between nanoparticles in complex fields" and the work presented in it are my own. I confirm that:

- This work was done wholly or mainly while in candidature for a research degree at this University.
- Where any part of this thesis has previously been submitted for a degree or any other qualification at this University or any other institution, this has been clearly stated.
- Where I have consulted the published work of others, this is always clearly attributed.
- Where I have quoted from the work of others, the source is always given. With the exception of such quotations, this thesis is entirely my own work.
- I have acknowledged all main sources of help.
- Where the thesis is based on work done by myself jointly with others, I have made clear exactly what was done by others and what I have contributed myself.

Signed:

Date:

"Se empieza por ver los vínculos. Cada vez estará más claro que no hay problemas concretos que puedan identificarse o resolverse aisladamente. En el fondo, todo está relacionado, no hay nada que no dependa de otra cosa."

Wassily Kandinsky

Universidad Autónoma de Madrid

Abstract

Facultad de Ciencias
Departmento de Física de la Materia Condensada
and IFIMAC

Doctor of Philosophy

Light induced interactions between nanoparticles in complex fields

by Jorge LUIS HITA

In this Thesis a theoretical investigation of the properties of interactions mediated by light and a quest for different setups in which new features of these interactions arise have been accomplished.

During last decades, strong research efforts have been committed to this field. From the original experimental measurement of a picoNewton optical force made by Ashkin in the mid-80s, showing for the first time how a highly focused laser beam can be used to trap a micron-size particles, to the modern extensive experimental and theoretical investigations on photonics and optical manipulation.

Within the advances in the understanding of light's mechanical effects on nanoparticles, a huge number of different research lines have recently emerged. The Brownian dynamical analysis based on the information extracted from optical forces and torques on a particle in an optical tweezer, the analysis of the fulfillment of actio and reactio in the interaction between two nanoparticles with different polarizabilities or the discovery of enhanced diffusion of nanoparticles in optical vortex fields are just three examples showing how diverse and rich is the investigation in the field of optical manipulation.

Also, during the last decades, the manipulation of dispersion forces have played a crucial role in fundamental fields of research such as Physics, Biology, Chemistry and Colloidal Sciences. These interaction forces found between two objects arise from fluctuations with different physical origin such as thermal fluctuations or fluctuations in a critical fluid mixture. Dispersion forces have been recently analyzed from an optical manipulation perspective yielding to a new, very promising, research line.

Based on this previous knowledge of the effect of optical forces on nanoparticles, four different targets have been deemed in the design of this Thesis:

First, the study of how diffusion can be manipulated by the optical interactions between two particles have been carried out. To isolate the effect of the optical interaction among particles a setup in which a single nanoparticle experiences no force at all has been proposed. Then, the properties of the diffusion of a dimer have been investigated. Although the interactions are known to be non-conservative, a potential that captures the main features of the dynamics has been proposed.

Secondly, the properties of many-particle optical interactions have been analyzed. From simple setups of three identical nanoparticles illuminated by either a linearly polarized plane wave or an optical lattice to systems with a large number of hydrodynamic particles diffusing through an optical vortex field.

Thirdly, the optical interactions between two identical non-absorbing particles under random light illumination has been analyzed in detail, and the main features of the interaction have been tested by using a physical model for the electric permittivity. The use of a realistic model allow us to understand the different interaction's regimes and their main characteristics. As a main contribution, an analytical equation describing the interaction between two absorbing particles, has been obtained for the first time.

Finally, some novel effects on the interaction between particles under random light illumination have been investigated by means of the new analytical expression cited above. The specific conditions for the electric polarizability of two identical particles needed to obtain a fluctuation induced gravitational-like interaction have been established. Also, for the particular case of two different absorbing nanoparticles, a notable particular case with non-reciprocal and non-conservative optical forces coming from a homogeneous and isotropic field has been identified.

Universidad Autónoma de Madrid

Abstract

Facultad de Ciencias
Departmento de Física de la Materia Condensada
and IFIMAC

Doctor of Philosophy

Light induced interactions between nanoparticles in complex fields

by Jorge LUIS HITA

En esta Tesis se ha desarrollado una investigación teórica de las propiedades de las interacciónes mediadas por luz y se ha realizado una búsqueda de diferentes montajes en los que se puedan obtener nuevos efectos producidos por estas interacciones.

En las últimas décadas, se ha realizado un enorme esfuerzo investigador dentro de este campo. Desde la primera medida experimental de una fuerza óptica de picoNewton realizada por Ashkin a mediados de los años 80, mostrando cómo se podía usar un haz láser colimado para atrapar partículas micrométricas, hasta la enorme investigación teórica y experimental actual en fotónica y manipulación óptica.

Entre los avances en el entendimiento de los efectos mecánicos de la luz en nanopartículas han emergido recientemente un enorme número de líneas de investigación. El análisis de la dinámica Browniana obtenida de las fuerzas y torques sobre una partícula en una trampa óptica, el análisis de la validez del principio de acción y reacción entre dos partículas de diferente polarizabilidad o el descubrimiento del aumento de la difusión de nanopartículas en redes ópticas de vórtices son sólo tres ejemplos que muestran cómo de rica y diversa es la investigación en el campo de la manipulación óptica.

La manipulación de las fuerzas de dispersión han jugado también un papel crucial en las últimas décadas en campos fundamentales como la física, la biología, la química o las ciencias coloidales. Estas interacciones entre dos objetos emergen de fluctuaciones de diversos origenes físicos, tales como fluctuaciones térmicas o flucuaciones en mezclas críticas de fluidos. Estas fuerzas de dispersión han sido recientemente analizadas desde la perspectiva de la manipulación óptica, dando lugar a una nueva y muy prometedora línea de investigación.

Basada en este conocimiento previo de los efectos de las fuerzas ópticas en nanopartículas, esta Tesis se propone la consecución de cuatro objetivos principales:

Primero, se ha realizado el estudio de cómo pueden las propiedades de difusión ser manipuladas mediante interacciones ópticas. Para aislar el efecto de las interacciones entre partículas se propone un montaje en el que una única nanopartícula no experimentaría ninguna fuerza. Se estudia entonces la difusión de un dímero en dicho montaje óptico. Aunque se sabe que las interacciones son no conservativas, se propone un potencial que capture las principales propiedades de la dinámica del sistema.

En segundo lugar, se han analizado las propiedades de las interacciones entre muchas partículas. Se han estudiado diversos casos, desde montajes simplificados de tres nanopartículas idénticas iluminadas bien por una onda plana linealmente polarizada, bien por una red óptica, hasta sistemas con gran número de partículas difundiendo en una red óptica de vórtices sujetas a interacciones ópticas e hidrodinámicas.

En tercer lugar, se ha analizado en detalle la interacción óptica entre dos partículas idénticas sin absorción bajo iluminaci"on con luz aleatoria, y se han comprobado, utilizando un modelo físico de la permitividad eléctrica, las principales características de dicha interacción. El uso de un modelo realista permite entender los diferentes regímenes de la interacción y sus principales propiedades. Como contribución principal, se ha obtenido por primera vez una expresión analítica que describe la interacción entre dos partículas con absorción en dichos campos de luz aleatoria.

Finalmente, se han investigado algunos resultados novedosos de la interacción entre dos partículas con absorción bajo iluminación con luz aleatoria, utilizando la expresión analítica antes mencionada. Se han caracterizado las condiciones específicas para la polarizabilidad eléctrica de dos partículas idénticas necesarias para obtener una interacción tipo gravitatoria inducida por fluctuaciones. Además, se ha identificado, para el caso de dos partículas con absorción y con diferente polarizabilidad, el

caso notable en el que la interacción muestra no reciprocidad y no conservatividad para un campo fluctuante homogéneo e isótropo.

Acknowledgements

Supongo que es difícil escribir una única sección de agradecimientos. No tanto por recordar y nombrar a tanta o cuánta gente que, a lo largo de todos estos años ha contribuido a ser lo que soy y hacer lo que hago, sino más bien porque, debido a la ingente variedad de maneras en las que las personas con las que he compartido camino a lo largo de estos años han tenido de dejar una impronta en mí, debería haber una ingente cantidad de formas de agradecimientos, para poder obrar con la debida justicia. Haré un intento, aunque ya de antemano pido perdón por las posibles omisiones o inexactitudes, espero que no sean muchas.

A mis directores de tesis, Juan José Sáez y Manuel Marqués, por la dedicación (y la paciencia) que han tenido durante estos años, lo que me han enseñado no sólo sobre óptica sino sobre este complejo y particular mundo académico. Por el cercano trato personal con el que la realización de esta Tesis se ha hecho sin duda mucho más llevadera. Y por el esfuerzo titánico de leer y proponer mejoras al manuscrito de la Tesis. Todos los fallos que se puedan encontrar serán de mi autoría, pero gran parte de los aciertos se deben sin duda a ellos.

A Nuno de Sousa y Pedro García Mochales, con quienes he compartido infinidad de horas y conversaciones en mi paso por la Autónoma, y a quienes siempre he podido recurrir en busca de ayuda cuando me atascaba en el manejo de estos ordenadores a los que nunca terminaré de entender.

A la gente del Donostia International Physics Center, CIC Nanogune y el Centro de Física de Materiales de Donosti, en particular a Nieves Morquillas, Diego Romero, Maia García y Aitzol García. Por las tardes de sagardotegi, las cervezas por lo viejo, los debates a la hora del café y las apariciones en TeleDonosti. Ya sé a dónde volver cuando tenga la oportunidad, espero que sea pronto. Mila esker bihotzez!

A la gente del Departamento de Física de la Universidad de Fribourg. A Frank Scheffold, por darme la oportunidad de realizar una estancia en tu grupo. A Luis Froufe-Pérez por tu hospitalidad, por tus consejos y por las conversaciones que mantuvimos durante horas sobre física y sobre nuestras visiones del mundo. Y a Isabelle Spühler, Gora Conley y Giuseppe Scalia, por las todas las comidas y coloquios que compartimos en la sala de reuniones del grupo.

Del periodo previo a embarcarme en la tesis, quisiera agradecer a José Luis Vicent y Elvira González, por el tiempo que pasé en vuestro laboratorio y todo lo que aprendí en él. Con especial cariño a Javier del Valle, Alicia Gómez, Luis Ruiz-Valdepeñas y Fernando Gálvez. Con vosotres

descubrí lo colaborativa (y divertida) que podía ser la ciencia. Los vídeos ochenteros del Chimo Bayo, las conversaciones sobre el liberalismo y, por supuesto, la danza del helio marcaron una etapa que recordaré mientras el destino me siga llevando cual hoja arrastrada por el viento en medio de este océano de poesía llamado mundo. Ahhh, la vita!

A José María Ortiz de Zárate y Mohamed Khayet, con quienes tuve el privilegio de empezar mi labor investigadora. Por las oportunidades que me disteis, por todo lo que me enseñásteis y por contagiarme vuestra enorme pasión por la ciencia.

En el plano puramente personal, no podría sino empezar por mi familia. Mi padre y mi madre, mi hermana Inma, mis hermanos Mario y Nacho y mi sobrina Beatriz. Por todo el apoyo que me habéis dado durante toda mi vida, y por dejaros la piel en darme oportunidades de las que en su momento no gozásteis. Por el amor con el que me habéis cuidado, por todo lo que me habéis enseñado (y seguís enseñándome), por la paciencia que habéis tenido en mis épocas difíciles (que han sido muchas y variadas, y alguna no del todo terminada) y por inculcarme una enorme inquietud y curiosidad hacia absolutamente todo, parte de la cual ha acabado desembocando en este manuscrito. Esta tesis es vuestra.

A Nicolás, Vero, Luis, Álvaro y Yuste, con quienes compartí buena parte de mi paso por la Complutense. Siempre me acuerdo de todos los ratos en el parque de las ciencias, de los días de biblioteca, de los exámenes y apuntes, de las cervezas de después, las pizzas del Picadilly, las conversaciones sobre el mundo y a veces hasta de la física. ¡Triviaaaaaal!

A Piter, Mery, Charku, Ville, Sil, Víctor, ... a les Ruteres, por todo este tiempo. Por vuestra amistad y compañía. Es difícil resumir todas las andanzas y correrías que he tenido el lujo de compartir con vosotres, y las que aún quedan por llegar.

A Marimar Martínez-Falero, Félix Prats, Bárbara Méndez y Santos Lora, por su infinita vocación, comprensión y paciencia. Y a Carlos Machín de Soignie, y a nuestro amigo Manolito.

Contents

List of Figures

List of Abbreviations

FRC	**F**rohlich **R**esonant **C**ondition
MSP	**M**ultiple **S**cattering **P**roblem
MSD	**M**ean **S**quare **D**isplacement
NP	**N**ano **P**article
PEL	**P**otential **E**nergy **L**andscape
RLI	**R**andom **L**ight **I**llumination
SIBA	**S**elf-**I**nduced **B**ack-**A**ction
WSA	**W**eak **S**cattering **A**pproximation

List of Symbols

a	particle's radius	m
R	separation between two particles	m
k	wavenumber	m^{-1}
$\boldsymbol{E}_0$	applied electric field	$\mathrm{N\,C}^{-1}$
$\boldsymbol{E}$	incident electric field	$\mathrm{N\,C}^{-1}$
I	laser intensity	$\mathrm{W/m}^2$
G	Green dyadic function	m^{-1}
T	temperature	K
ω	angular frequency	$\mathrm{rad\,s}^{-1}$
λ	wavelength	m
ϵ_0	electric permittivity of vacuum	$\mathrm{F\,m}^{-1}$
ϵ	particle's relative permittivity	$\mathrm{F\,m}^{-1}$
ϵ_m	medium's relative permittivity	$\mathrm{F\,m}^{-1}$
α_0	Lorentz-Lorenz particle's polarizability	m^3
α	particle's polarizability	m^3
α'	real part of α	m^3
α''	imaginary part of α	m^3
η	viscosity	$\mathrm{kg\,m}^{-1}\,\mathrm{s}^{-1}$
γ	friction coefficient	$\mathrm{kg\,s}^{-1}$

A mi familia.

Chapter 1

Introduction

The mechanical effect of light on matter was long time ago proposed when Kepler, in 1619, explained how the tail of comets always points away from the Sun, despite its direction of motion. Centuries after, based in the seminal work of James Maxwell published in 1873, the development of electromagnetism showed that these forces could be calculated analytically on arbitrary objects, using the formalism of the Maxwell stress tensor.

Experimental determination of optical forces on micro- and nano- particles was not possible until the development of lasers as intense light sources. In his pioneering work, (Ashkin, 1970) experimentally tested how radiation pressure exerts force on a particle, and in (Ashkin et al., 1986) proposed and proved that a highly focused laser beam is able to trap a micron sized particle. This led to the development of the so called Optical Tweezers (Jones et al., 2015; Padgett et al., 2010). In the theoretical counterpart, Maxwell stress tensor formalism were used to calculate optical forces on micron-sized particles in such highly focused beams (Barton et al., 1989).

Inspired by the novel fabrication of nanoparticles, new formulas for optical forces on particles much smaller than the radiation's wavelength were obtained. That lead to both a simplification on the calculation of the optical force and to the possibility of theoretically analyze the different contributions to the optical force. In (Chaumet et al., 2000), the total averaged force on a dipolar particle as a function of the incident electric field and its derivatives is obtained. In (Arias-González et al., 2003), the optical force on a dipolar particle is written as the sum of a gradient contribution and a scattering contribution, in which a radiation pressure term can be identified. In (Albaladejo et al., 2009b), a new manner to express the contribution to the scattering force that comes from the curl of the spin of angular momentum is obtained.

The study of the different contributions to the force lead to different applications of optical manipulation of dipolar particles. In the case of

diffusion of single nanoparticles, (Albaladejo et al., 2009a) studied the enhancement of the effective diffusion constant of gold nanoparticles in an optical vortex lattice and (Albaladejo et al., 2011) investigated the control on the diffusion of silver nanoparticles due to the characteristic behavior of its electric polarizability.

Trapping techniques have been stunningly profitable in the study of applications to other related fields during the last years, such as Statistical Physics or Biology. Relaxation from a non-equilibrium state towards equilibrium (Gieseler et al., 2015) and non-equilibrium diffusion processes (Roichman et al., 2008; Wu et al., 2009; Gieseler et al., 2014), hydrodynamic synchronization of an ensemble of oblate particles (Arzola et al., 2014), ultrasensitive sound detection techniques based in a trapped gold nanoparticle (Ohlinger et al., 2012), the resemble of the Schrödinger equation of a two-level system by means of the modulation of an optical trapping potential (Frimmer et al., 2017) or mapping the accessible space by Photonic Force Microscopy (Rohrbach et al., 2004) are examples of how prosperous are currently the optical trapping techniques in a wide variety of investigations. Optical forces have been widely exploited to understand, manipulate and control the statistical properties (Bechinger et al., 2001; Mikhael et al., 2008) and dynamics (Zurita-Sánchez et al., 2004; Šiler et al., 2010) of colloidal particles by optically induced potential energy landscapes (PEL) (Evers et al., 2013). Randomly modulated intensity patterns, so-called speckle patterns, can also be used to create a random Potential Energy Landscape (PEL) (Volpe et al., 2014; Bewerunge et al., 2016).

Counter intuitive phenomena like the giant diffusion induced by an oscillating periodic potential (Reimann et al., 2001) or kinetically locked-in states in driven diffusive transport (Reichhardt et al., 1999) have been realized by using optically induced Potential Energy Landscapes (PELs) (Korda et al., 2002; Lee et al., 2006), demonstrating optical guiding and sorting of particles in microfluidic flows (MacDonald et al., 2003; Ladavac et al., 2004; Xiao et al., 2010). The intriguing properties of Brownian motion under periodic landscapes of non-conservative "curl forces" (optical vortex lattices (Hemmerich et al., 1992; Albaladejo et al., 2009b; Gómez-Medina et al., 2011)) is also a subject of increasing interest (Albaladejo et al., 2009a; Zapata et al., 2009; Albaladejo et al., 2011; Berry et al., 2013; Berry et al., 2015; Zapata et al., 2016).

Also, optical torques is a very new and rich field of research. Torque detection from statistical analysis of Brownian fluctuations (Volpe et al., 2006), understanding the orientation dynamics of a single upconverting

particle into an optical trap (Rodríguez-Sevilla et al., 2016), analysis of conservativeness of optical torques as a function of the polarization (Haefner et al., 2009) of incident light or the theoretical study of the torque on small bi-isotropic particles under general light fields (Nieto-Vesperinas, 2015) are a few examples of how wide this field can be.

On the other hand, particles are able to interact by means of electromagnetic scattering. The study of the features and effects of these interactions is a present topic of intense investigation. Superdiffusion of a system of particles in a self-generated speckle pattern (Douglass et al., 2012), Self-Induced Back-Action optical forces generated between a particle and a nanoaperture (Juan et al., 2009) or optical interactions in plasmonic nanoparticle dimers (Miljković et al., 2010) and the enhancement of optical interactions in silver nanoaggregates due to surface-plasmon effects (Xu et al., 2002) are a variety of examples of this active field of research.

Multiple scattering effects are also behind unexpected phenomena that could not be explain by a single dipolar particle. By means of complex light beams, other different unexpected effects were studied in the field of optical forces. The theoretical work on negative forces (Dogariu et al., 2013) and tractor beams (Sukhov et al., 2011), together with its experimental demostration (Brzobohatỳ et al., 2013), gives an idea of how complex and rich can be the investigation of optical forces on single nanoparticles.

Optical binding is an interesting feature of optical interactions between nanoparticles (Thirunamachandran, 1980). First experimentally investigated in (Burns et al., 1990), it is theoretically studied based in the dipolar approximation by (Depasse et al., 1994). Special features of optical interactions like the fulfillment of actio and reactio have been investigated using this approach (Sukhov et al., 2015). Optical binding manifest itself in the extent of Brownian fluctuations of particles optically linked (Han et al., 2015). A comprehensive review in experimental and theoretical developments in optical binding is presented in (Dholakia et al., 2010).

Finally, dispersion forces are ubiquous in nature. They are produced from fluctuating fields, thermal fluctuations (Gómez-Santos, 2009), fluctuations in reaction-diffusion problems (Brito et al., 2007) or fluctuations driven by Soret effect (Kirkpatrick et al., 2016). The study of these forces due to the fluctuations of the electromagnetic field has been a topic of investigation during the last decades. Proposed for molecules in (Thirunamachandran, 1980) and extended to objects of ellipsoidal shape in (Stiles, 1979; Schiller et al., 2011), different formalisms have been used from quantum to classical electrodynamics (McLachlan, 1963). It has been brought

to the field of nanoparticles by (Sukhov et al., 2013), where the correlations of electromagnetic field in a chaotic cavity were used (Eckhardt et al., 1999), and by (Brügger et al., 2015), where both experimental results and a different formalism for calculating the forces were presented.

1.1 Motivation and aims

Despite the huge activity of research in the topic of optical forces during the last decades, there is still plenty of room to investigate new applications and new fundamental features of optical forces and interactions in different kinds of complex fields.

During the development of this Thesis, several aspects have been tackled. First, we wonder about the influence of optical interactions on the diffusion process of a system of particles. To start investigating this topic, we study the diffusion of a dimer in an optical lattice. The configuration is such that the only optical forces acting on the particles are interaction forces. In this manner, we make sure that every deviation from the free Brownian diffusion of the dimer is produced by interactions between the particles that formed the dimer.

We study and characterize the contribution of many-particle interactions to the dynamics of a system of several particles. To study this, we propose the simple case of a system formed by three identical particles, illuminated with different light fields. The contribution of three-particle terms in the force exerted on one of them is discussed, as well as the influence of three-particle interactions in the force on the center of mass of the system.

We analyze in detail the interaction between two nanoparticles under random light illumination and, by proposing a physical model of the electric permittivity we see that, in the expansion within the weak scattering approximation, the terms proportional to $R^{-3,-5,-7}$ are always present. We also tackle the probelm of the interaction between two identical absorbing particles, and we obtain an analytical expression for the interation in the presence of absorption.

The features of this interaction between absorbing particles can be deeply investigated, searching new effects of the interaction that were not expected in the nonabsorbing case. Specifically, the possibility of a gravitational-like interaction mediated by absorption is an aim of this work. Moreover, the characterization of the reciprocity and conservativity of this interaction in two different cases, when the two particles are identical and when they have different polarizability has been tackled.

In particular, the main objectives of this thesis are

- To study and characterize optical interactions between two dipolar particles, taking as a system a dimer formed by two nanoparticles moving in a optical lattice of wells.
- To study the influence of optical forces on the dynamics of a system of many dipolar particles subject to hydrodynamic interactions. In particular, to investigate the role of optical interactions between particles due to Multiple Scattering.
- To investigate the interaction between two dipolar particles due to random light illumination. In particular, to extend the method for nonabsorbing particles to a system of two particles when absorption contributes to their electric polarizability.
- To study and characterize new features of this interaction that can not be obtained without absorption.
- To investigate the conservativeness of interactions between dipolar particles in random light illumination. In particular, to analize the cases of identical and non-identical pair of particles and the case of three body forces.

1.2 Structure of the Thesis

This Thesis has been structured in the following manner:

In Chapter 2, the theoretical methods used along the Thesis are described. The models for electric parmittivity and electric polarizability are described, as well as the expressions for the scattering, absorption and extinction cross sections. The dipolar force on a NP and the interaction between two and several nanoparticles for non random light fields are discussed in detail. The computation of the force between two nanoparticles under RLI is explained, starting from the filed-field correlations of an homogeneous, isotropic random electromagnetic field.

In Chapter 3, the case of a dimer formed by NPs diffusing through an optical well lattice is discussed. Statistical properties such as the effective diffusion constant are studied for several values of parameters like the dimer length and the intensity of the applied optical field. A simplified model is proposed to capture the essential features of the trapping in non-conservative landscapes. The Langevin dynamics method used to perform the simulations is described, as well as analytical results of the

Brownian diffusion of the dimer used to check the validity of the Langevin dynamics simulations.

In Chapter 4, the features of several particle optical interactions are analyzed, and applied to an investigation where the dynamic phase transition of a system of several optical NPs subjected to hydrodynamic interactions is studied. In particular, the influence of optical interactions in Brownian hydrodynamic simulations is studied.

In Chapter 5, the interaction between two dipolar NPs in an homogeneous, isotropic random light field is studied. First, the interaction between two nonabsorbing NP is analized. By studying the different limits of this interaction it is found that the terms depending on the imaginary part of the polarizability, usually neglected in the literature, change drastically the behaviour of the interaction at short distances. Then, a new analytical expression for the interaction between two identical absorbing NP under RLI is obtained, and the expansions of this interaction in different separation limits are obtained and analized.

In Chapter 6, different features of the interaction between two NPs under RLI are studied. First, by analyzing the expansions of the interaction between two identical NPs, the particular conditions needed to obtain a full-range gravitational-like behaviour are determined. Two specific conditions for the electric polarizability are obtained, and the results are tested using model particles, with an electric permittivity given by a Lorentz model, and realistic particles, with an electric permittivity given by the ones of gold and silver. Then, the case of the interaction between two different particles is analyzed analytically and numerically. Nonreciprocity of the interaction is found, leading to a new scenario in which actio and reactio is not fulfilled. Conservativity of the forces is also studied. For two identical particles, it is shown that the system is fully conservative, while for two different particles (although the force on each particle is irrotational) the system as a whole is shown to be nonconservative, and the work performed along a closed path is found to be different from zero.

Chapter 2

Theoretical methods

In this Chapter some basic theoretical concepts that will be used along the Thesis will be defined. The specific methods that have been used in the calculations will be described, as well as the limitations and advantages of these methods. The relations between these different sets of ideas will be described in detail.

2.1 Electromagnetism in a nutshell

Electromagnetism is based in the time-dependent electric field $\boldsymbol{E}(\boldsymbol{r},t)$, electric displacement $\boldsymbol{D}(\boldsymbol{r},t)$, magnetic field $\boldsymbol{H}(\boldsymbol{r},t)$ and magnetic induction $\boldsymbol{B}(\boldsymbol{r},t)$ that are related by constitutive relations (Novotny et al., 2006). A particular case is the time-harmonic fields that, for a monochromatic field of frequency ω, can be expressed as

$$\boldsymbol{E}(\boldsymbol{r},t) = \mathrm{Re}\{\boldsymbol{E}(\boldsymbol{r})e^{-i\omega t}\} \tag{2.1}$$

and analogously for all the other fields.

2.1.1 Maxwell equations

The Maxwell equations relating all time-harmonic fields can be written as (Novotny et al., 2006)

$$\nabla \times \boldsymbol{E}(\boldsymbol{r}) = i\omega \boldsymbol{B}(\boldsymbol{r}) \tag{2.2a}$$

$$\nabla \times \boldsymbol{H}(\boldsymbol{r}) = -i\omega \boldsymbol{D}(\boldsymbol{r}) + \boldsymbol{j}(\boldsymbol{r}) \tag{2.2b}$$

$$\nabla \cdot \boldsymbol{D}(\boldsymbol{r}) = \rho(\boldsymbol{r}) \tag{2.2c}$$

$$\nabla \cdot \boldsymbol{B}(\boldsymbol{r}) = 0 \tag{2.2d}$$

being $\boldsymbol{E}(\boldsymbol{r})$ the electric field, $\boldsymbol{D}(\boldsymbol{r})$ the electric displacement, $\boldsymbol{H}(\boldsymbol{r})$ the magnetic field, $\boldsymbol{B}(\boldsymbol{r})$ the magnetic induction, $\boldsymbol{j}(\boldsymbol{r})$ the current density and $\rho(\boldsymbol{r})$ the charge density.

Instead of six different functions, it is convenient to define the vector potential $\boldsymbol{A}(\boldsymbol{r})$ and the scalar potential $\phi(\boldsymbol{r})$. These potentials are defined by

$$\boldsymbol{E}(\boldsymbol{r}) = i\omega\boldsymbol{A}(\boldsymbol{r}) - \nabla\phi(\boldsymbol{r}) \tag{2.3a}$$

$$\boldsymbol{H}(\boldsymbol{r}) = \frac{1}{\mu\mu_0}\nabla \times \boldsymbol{A}(\boldsymbol{r}) \tag{2.3b}$$

and by using Maxwell equations and the property $\nabla \times \nabla\times = -\nabla^2 + \nabla\nabla$ together with the Lorentz gauge $\nabla \cdot \boldsymbol{A} + 1/c^2\partial_t\phi = 0$ we get to

$$\left[\nabla^2 + k^2\right]\boldsymbol{A}(\boldsymbol{r}) = -\mu\mu_0\boldsymbol{j}(\boldsymbol{r}) \tag{2.4a}$$

$$\left[\nabla^2 + k^2\right]\phi(\boldsymbol{r}) = -\frac{\rho(\boldsymbol{r})}{\epsilon\epsilon_0} \tag{2.4b}$$

being ϵ_0, ϵ the electric permittivity of vacuum and of the medium, respectively, and μ_0, μ the magnetic permeability of vacuum and of the medium, respectively. These equations are known as Helmholtz equations. We will use the Green functions of the Helmholtz equation to obtain the electric field produced at $\boldsymbol{r}$ by a point-like source at $\boldsymbol{r}'$.

2.1.2 The Green dyadic function

The Green scalar function $g(\boldsymbol{r}_i, \boldsymbol{r}_j)$ is defined as the solution of the Helmholtz equation with a delta-like source

$$\left[\nabla^2 + k^2\right]g(\boldsymbol{r}_i, \boldsymbol{r}_j) = -\delta(\boldsymbol{r}_i - \boldsymbol{r}_j) \tag{2.5}$$

and has the form

$$g(\boldsymbol{r}_i, \boldsymbol{r}_j) = \frac{e^{\pm ik|\boldsymbol{r}_i - \boldsymbol{r}_j|}}{4\pi|\boldsymbol{r}_i - \boldsymbol{r}_j|} \tag{2.6}$$

For the calculation of the electric field, we must consider the Green dyadic function, which is obtained from Green scalar function as

$$G(\boldsymbol{r}_i, \boldsymbol{r}_j) = \left[\mathbb{I} + \frac{1}{k^2}\nabla\nabla\right]g(\boldsymbol{r}_i, \boldsymbol{r}_j) \tag{2.7}$$

And can be written explicitly as

$$G(\boldsymbol{r}_i, \boldsymbol{r}_j) = \frac{e^{ikR}}{4\pi R}\left[\left(1 + \frac{i}{kR} - \frac{1}{k^2R^2}\right)\mathbb{I} - \left(1 + \frac{i3}{kR} - \frac{3}{k^2R^2}\right)\frac{\boldsymbol{R}\otimes\boldsymbol{R}}{R^2}\right] \tag{2.8}$$

where $\boldsymbol{R} = \boldsymbol{r}_1 - \boldsymbol{r}_2$ is the separation vector, $R = |\boldsymbol{r}_1 - \boldsymbol{r}_2|$ is its modulus and $\boldsymbol{R}\otimes\boldsymbol{R}$ is the outer product of the separation vector by itself, which is defined as

$$\boldsymbol{R}\otimes\boldsymbol{R} = \begin{bmatrix} (x_1-x_2)^2 & (x_1-x_2)(y_1-y_2) & (x_1-x_2)(z_1-z_2) \\ (y_1-y_2)(x_1-x_2) & (y_1-y_2)^2 & (y_1-y_2)(z_1-z_2) \\ (z_1-z_2)(x_1-x_2) & (z_1-z_2)(y_1-y_2) & (z_1-z_2)^2 \end{bmatrix} \tag{2.9}$$

The calculation of the derivatives of the Green dyadic function and some properties that will be usefull in the computation of the optical forces will be discussed in Appendix A.

2.2 Permittivity and polarizability

The response of a material to an external electric or optical field is described by the electric permittivity and the electric polarizability. These properties can be experimentally measured for a certain sample, with a certain size and shape. However, in many cases it is useful to describe them by a model that depends on the wavelength of the applied field, as well as on parameters that describe phenomena such as scattering and absorption.

2.2.1 Drude and Lorentz permittivity

The Lorentz model describes the interaction between light and matter by supposing that the binding force between electrons and nuclei is similar to a mass-spring system. Electrons vibrate like damped harmonic oscillators when an electromagnetic field is applied.

The dielectric function for a material with a single resonance in a Lorentz model is given by (Ashcroft et al., 1976)

$$\epsilon(\omega) = \epsilon_\infty + \frac{(\epsilon_s - \epsilon_\infty)\omega_0^2}{\omega_0^2 - \omega^2 - i\omega\Gamma_0} \quad \epsilon_s = \epsilon_\infty + \frac{\omega_p^2}{\omega_0^2} \tag{2.10}$$

being $\epsilon_\infty, \epsilon_s, \omega_p, \omega_0, \Gamma_0$ parameters that can be adjusted to mimic the behavior of different materials.

The Drude model assumes that the material has motionless nuclei and electrons move through the material without interaction. It was developed to explain the transport properties of conduction electrons in metals and heavily-doped semiconductors. The Drude oscillator is a specific case of Lorentz oscillator in which the restoring force vanishes and then $\omega_0 = 0$.

The Drude model for electric permitivitty is written as

$$\epsilon(\omega) = \epsilon_\infty + \frac{\omega_p^2}{\omega^2 - i\omega\Gamma_0} \tag{2.11}$$

where $\epsilon_\infty, \epsilon_s, \omega_p, \Gamma_0$ are again parameters that can be adjusted to mimic a certain material.

2.2.2 Electric polarizability

The electric polarizability describes how a scatterer disperses or absorbs an incident electric field. If scattering is not taken into account, the so called Lorentz-Lorenz polarizability of the particle is obtained via the Clausius-Mossotti relation as (Jackson, 1999)

$$\alpha_0 = 4\pi a^3 \frac{\epsilon(\omega) - \epsilon_m}{\epsilon(\omega) + 2\epsilon_m} \tag{2.12}$$

where a is the particle radius, $\epsilon(\omega)$ is the permittivity of the particle's material and ϵ_m is the permittivity of the medium the particle is immersed in.

When scattering is considered, a radiative correction to the polarizability is needed. For small particles, the polarizability can be expressed as (Draine et al., 1993)

$$\alpha = \frac{\alpha_0}{1 - i\alpha_0 \frac{6\pi}{k^3}} \tag{2.13}$$

A different way to write this relation is

$$\frac{1}{\alpha} = \frac{1}{\alpha_0} - i\frac{k^3}{6\pi} \tag{2.14}$$

written in this form, we see that $k^3/6\pi$ accounts for the scattering part. So the absorption part is going to be given by $\mathrm{Im}\{1/\alpha_0\}$. If α_0 is real, then the particle has no absorption. For a detailed discussion of the Physics of the radiative correction and the optical theorem see (Albaladejo et al., 2010).

The particle will be at Frohlich Resonance Condition when the applied wavelength is such that the polarizability given by Equation (2.13) is purely imaginary (Markel et al., 2007).

2.2.3 Scattering, absorption and extinction cross sections

To calculate the rate at which energy is extinguished from an incident plane wave by the presence of a single scatterer, the extinction σ_{ext}, scattering σ_{sca} and absorption σ_{abs} cross sections are obtained through the following relations (Jones et al., 2015)

$$\sigma_{ext} = k_0 \operatorname{Im}\left\{\alpha\right\} \tag{2.15a}$$

$$\sigma_{sca} = \frac{k_0^4}{6\pi}|\alpha|^2 \tag{2.15b}$$

$$\sigma_{abs} = \sigma_{ext} - \sigma_{sca} = k_0 \operatorname{Im}\left\{\alpha\right\} - \frac{k_0^4}{6\pi}|\alpha|^2 \tag{2.15c}$$

Note how, if α_0 is real, then the absorption cross section vanishes $\sigma_{abs} = 0$.

When more than one scatterer is considered, multiple scattering between the particles must be taken into account. Then, for a system of N dipolar scatterers, the cross sections are given by (de Sousa et al., 2016)

$$\sigma_{ext} = \frac{k}{\epsilon_0 \epsilon |E_0|^2} \sum_{n=1}^{N} \operatorname{Im}\left\{\boldsymbol{E}_0^*(\boldsymbol{r}_n) \cdot \boldsymbol{p}_n\right\} \tag{2.16a}$$

$$\sigma_{sca} = \frac{k^3}{(\epsilon_0 \epsilon)^2 |E_0|^2} \sum_{n,m=1}^{N} \boldsymbol{p}_n^* \cdot \operatorname{Im}\left\{G(\boldsymbol{r}_n, \boldsymbol{r}_m)\right\} \boldsymbol{p}_m \tag{2.16b}$$

$$\sigma_{abs} = \frac{k}{(\epsilon_0 \epsilon)^2 |E_0|^2} \sum_{n=1}^{N} \operatorname{Im}\left\{\boldsymbol{p}_n \cdot [\alpha_{n0}^{-1} \cdot \boldsymbol{p}_n]^*\right\} \tag{2.16c}$$

where $\boldsymbol{p}_i = \epsilon_m \epsilon_0 \alpha_i \boldsymbol{E}(\boldsymbol{r}_i)$ is the dipole moment on particle i.

2.3 Optical forces

For a general scatterer, once the electric field has been obtained in its surrounding medium, the electromagnetic force exerted on the scatterer is obtained by integrating the time averaged Maxwell stress tensor $\langle T_M \rangle$ over

a closed surface S around the scatterer (Jones et al., 2015)

$$\langle \boldsymbol{F} \rangle = \oint_S \hat{\boldsymbol{n}} \cdot \langle T_M \rangle \, dS \tag{2.17}$$

with

$$T_M = \frac{1}{4\pi}\Big[\boldsymbol{E}_t \otimes \boldsymbol{E}_t + \boldsymbol{B}_t \otimes \boldsymbol{B}_t - \frac{1}{2}\Big(\boldsymbol{E}_t \cdot \boldsymbol{E}_t + \boldsymbol{B}_t \cdot \boldsymbol{B}_t\Big)\mathbb{I}\Big] \tag{2.18}$$

and being $\hat{\boldsymbol{n}}$ a unitary vector normal to the surface. The fields $\boldsymbol{E}_t, \boldsymbol{B}_t$ are the total electric field and the total magnetic induction defined by

$$\boldsymbol{E}_t = \boldsymbol{E}^0 + \boldsymbol{E}, \quad \boldsymbol{B}_t = \boldsymbol{B}^0 + \boldsymbol{B}, \tag{2.19}$$

being $\boldsymbol{E}^0, \boldsymbol{B}^0$ and $\boldsymbol{E}, \boldsymbol{B}$ the applied and incident fieds, respectively. They will be defined in Subsection 2.3.2.

In a similar manner, the optical torque can be obtained by performing the integration

$$\langle \boldsymbol{\Gamma} \rangle = -\oint_S \hat{\boldsymbol{n}} \cdot \langle T_M \rangle \times \boldsymbol{r} \, dS \tag{2.20}$$

2.3.1 Optical force on a dipolar particle

When the radius of the nanoparticle is much smaller than the incident wavelenght $a \ll \lambda$ we can assume Rayleigh scattering and the ϕ-component of optical force exerted on the particle becomes (Chaumet et al., 2000)

$$\langle F^{\phi} \rangle = \frac{\epsilon\epsilon_0}{2} \operatorname{Re}\{\alpha \boldsymbol{E} \cdot \partial_{\phi} \boldsymbol{E}^*\} \tag{2.21}$$

with $\phi = x, y, z$.

It can be shown that this expression for the optical force can be splited in three different terms (Albaladejo et al., 2009b). If $\alpha = \alpha' + i\alpha''$ then

$$\langle \boldsymbol{F} \rangle = \alpha' \nabla \langle U \rangle + k\alpha'' \frac{n}{c} \langle \boldsymbol{S} \rangle + k\alpha'' \frac{c}{n} \nabla \times \langle \boldsymbol{L_S} \rangle. \tag{2.22}$$

where the first term is proportional to the gradient of the electric energy density

$$\langle U \rangle = -\frac{\epsilon\epsilon_0}{4} |\boldsymbol{E}|^2 \tag{2.23}$$

the second term is proportional to the time-averaged Poynting vector

$$\langle \boldsymbol{S} \rangle = \frac{1}{2} \operatorname{Re}\{\boldsymbol{E} \times \boldsymbol{H}^*\} \tag{2.24}$$

and the third term accounts for the curl of the spin density of the light field

$$\langle \boldsymbol{L_S} \rangle = \frac{\epsilon\epsilon_0}{4\omega i} \{\boldsymbol{E} \times \boldsymbol{E}^*\} \tag{2.25}$$

which vanishes for linearly polarized light.

2.3.2 Optical interaction between nanoparticles

We start by defining the two electric fields that will be used in the following discussions: The applied electric field $\boldsymbol{E}^0(\boldsymbol{r})$ and the incident field $\boldsymbol{E}(\boldsymbol{r})$.

The applied field is the field that would be at point $\boldsymbol{r}$ if there were no scatterers in the system. It is produced by an external independent source. The incident field is the field at position $\boldsymbol{r}$ due to the applied field at this point and to the scattered field from the scatterers located at positions $\boldsymbol{r}_i \neq \boldsymbol{r}$.

Thus, if in a system of N particles, a particle is located at position $\boldsymbol{r}_i$, the incident field on this particle will be given by the applied field at $\boldsymbol{r}_i$ plus the contributions from all the other particles located at $\boldsymbol{r}_j$, propagated via the Green dyadic function

$$\boldsymbol{E}(\boldsymbol{r}_i) = \boldsymbol{E}^0(\boldsymbol{r}_i) + \sum_{j \neq i} k^2 G(\boldsymbol{r}_i, \boldsymbol{r}_j)\alpha_j \, \boldsymbol{E}(\boldsymbol{r}_j) \tag{2.26}$$

The force between two particles

When the system is composed by two dipolar particles an analytical solution for the scattered fields can be obtained

$$\boldsymbol{E}(\boldsymbol{r}_1) = \mathbb{H}_1^{-1}\Big(\boldsymbol{E}^0(\boldsymbol{r}_1) + k^2 G(\boldsymbol{r}_1, \boldsymbol{r}_2)\alpha_2 \boldsymbol{E}^0(\boldsymbol{r}_2)\Big) \tag{2.27a}$$

$$\boldsymbol{E}(\boldsymbol{r}_2) = \mathbb{H}_2^{-1}\Big(\boldsymbol{E}^0(\boldsymbol{r}_2) + k^2 G(\boldsymbol{r}_2, \boldsymbol{r}_1)\alpha_1 \boldsymbol{E}^0(\boldsymbol{r}_1)\Big) \tag{2.27b}$$

where

$$\mathbb{H}_1 = \mathbb{I} - k^4 G(\boldsymbol{r}_1, \boldsymbol{r}_2)\alpha_2 \, G(\boldsymbol{r}_2, \boldsymbol{r}_1)\alpha_1$$
$$\mathbb{H}_2 = \mathbb{I} - k^4 G(\boldsymbol{r}_2, \boldsymbol{r}_1)\alpha_1 \, G(\boldsymbol{r}_1, \boldsymbol{r}_2)\alpha_2$$

In these equations, it has been taken into account that the polarizabilities of particles 1 and 2 can be different and that they can be non-diagonal

tensors, which will be useful to perform computations in which magneto-optical effects have to be included, or if the particles are nonspherical, such as prolate or oblate spheroids.

In the particular case of two spherical particles with identical diagonal polarizability α

$$\boldsymbol{E}(\boldsymbol{r}_1) = \left[\mathbb{I} - \left(k^2 G(\boldsymbol{r}_1, \boldsymbol{r}_2)\alpha\right)^2\right]^{-1} \left(\boldsymbol{E}^0(\boldsymbol{r}_1) + k^2 G(\boldsymbol{r}_1, \boldsymbol{r}_2)\alpha \boldsymbol{E}^0(\boldsymbol{r}_2)\right) \quad (2.28a)$$

$$\boldsymbol{E}(\boldsymbol{r}_2) = \left[\mathbb{I} - \left(k^2 G(\boldsymbol{r}_1, \boldsymbol{r}_2)\alpha\right)^2\right]^{-1} \left(\boldsymbol{E}^0(\boldsymbol{r}_2) + k^2 G(\boldsymbol{r}_2, \boldsymbol{r}_1)\alpha \boldsymbol{E}^0(\boldsymbol{r}_1)\right) \quad (2.28b)$$

To compute the force, we also need to calculate the partial derivative of the field with respect to a coordinate of the position vector. For coordinate $\phi = x, y, z$ we have

$$\partial_{\phi_1} \boldsymbol{E}(\boldsymbol{r}_1) = \partial_{\phi_1} \boldsymbol{E}^0(\boldsymbol{r}_1) + k^2 \left[\partial_{\phi_1} G(\boldsymbol{r}_1, \boldsymbol{r}_2)\right] \alpha \, \boldsymbol{E}(\boldsymbol{r}_2) \quad (2.29a)$$

$$\partial_{\phi_2} \boldsymbol{E}(\boldsymbol{r}_2) = \partial_{\phi_2} \boldsymbol{E}^0(\boldsymbol{r}_2) + k^2 \left[\partial_{\phi_2} G(\boldsymbol{r}_2, \boldsymbol{r}_1)\right] \alpha \, \boldsymbol{E}(\boldsymbol{r}_1) \quad (2.29b)$$

where $\boldsymbol{E}(\boldsymbol{r}_{1,2})$ are the incident fields given by Equations 2.28. Note that, even though the incident field $\boldsymbol{E}(\boldsymbol{r}_2)$ depends on the coordinate ϕ_1, the partial derivative does not apply on it. This is because if we take the actual derivative $\partial_{\phi_1}\left[k^2 G(\boldsymbol{r}_1, \boldsymbol{r}_2)\alpha \boldsymbol{E}(\boldsymbol{r}_2)\right]$, the force is not equal to the force obtained from the integration of the Maxwell stress tensor (Haefner et al., 2009; Barton et al., 1989).

With these fields and field derivatives, Equation (2.21) can be used to obtain

$$\begin{aligned} \langle F^{\phi}(\boldsymbol{r}_1)\rangle = \frac{\epsilon\epsilon_0}{2} \operatorname{Re}\Big\{ &\left(\boldsymbol{E}^0(\boldsymbol{r}_1) + k^2 G(\boldsymbol{r}_1, \boldsymbol{r}_2)\alpha \boldsymbol{E}^0(\boldsymbol{r}_2)\right)^t \mathbb{H}_1^{-1t} \alpha^t \\ &\cdot \Big(\partial_{\phi_1} \boldsymbol{E}^0(\boldsymbol{r}_1) + k^2 \left[\partial_{\phi_1} G(\boldsymbol{r}_1, \boldsymbol{r}_2)\right] \alpha \cdot \\ &\cdot \mathbb{H}_2^{-1} \left[\boldsymbol{E}^0(\boldsymbol{r}_2) + k^2 G(\boldsymbol{r}_2, \boldsymbol{r}_1)\alpha \boldsymbol{E}^0(\boldsymbol{r}_1)\right]\Big)^*\Big\} \end{aligned} \quad (2.30)$$

Note that these results are valid only within the dipolar approximation, in which the interparticle separation is larger than three times the particle's radius $R > 3a$. For shorter distances higher order multipoles become relevant (Miljković et al., 2010).

The force between several particles

When several particles are considered, numerical or approximation methods are required to get a solution of the MSP. If the system is composed by N particles, the equations for the incident electric fields on every particle would be

$$\begin{aligned}
\boldsymbol{E}(\boldsymbol{r}_1) &= \boldsymbol{E}^0(\boldsymbol{r}_1) + k^2 G(\boldsymbol{r}_1, \boldsymbol{r}_2)\, \alpha_2 \boldsymbol{E}(\boldsymbol{r}_2) + \ldots + k^2 G(\boldsymbol{r}_1, \boldsymbol{r}_N)\, \alpha_N \boldsymbol{E}(\boldsymbol{r}_N) \\
\boldsymbol{E}(\boldsymbol{r}_2) &= k^2 G(\boldsymbol{r}_2, \boldsymbol{r}_1)\, \alpha_1 \boldsymbol{E}(\boldsymbol{r}_1) + \boldsymbol{E}^0(\boldsymbol{r}_2) + \ldots + k^2 G(\boldsymbol{r}_2, \boldsymbol{r}_N)\, \alpha_N \boldsymbol{E}(\boldsymbol{r}_N) \\
&\vdots \\
\boldsymbol{E}(\boldsymbol{r}_N) &= k^2 G(\boldsymbol{r}_N, \boldsymbol{r}_1)\, \alpha_1 \boldsymbol{E}(\boldsymbol{r}_1) + k^2 G(\boldsymbol{r}_N, \boldsymbol{r}_2)\, \alpha_2 \boldsymbol{E}^0(\boldsymbol{r}_2) + \ldots + \boldsymbol{E}^0(\boldsymbol{r}_N)
\end{aligned}$$

Then, the set of incident fields $\boldsymbol{E}(\boldsymbol{r}_i)$ can be obtained using, for example, the Couple Dipole Approximation described in the Appendix B

The set of field derivatives is computed in an analogous manner than in the case of two particles. Being $\phi_i = x_i, y_i, z_i$ a component of the position vector of particle i we write

$$\partial_{\phi_i} \boldsymbol{E}(\boldsymbol{r}_i) = \partial_{\phi_i} \boldsymbol{E}^0(\boldsymbol{r}_i) + \sum_{i \neq j} k^2 \Big[\partial_{\phi_i} G(\boldsymbol{r}_i, \boldsymbol{r}_j)\Big] \alpha_j\, \boldsymbol{E}(\boldsymbol{r}_j) \tag{2.31}$$

Again, we have not derived $\boldsymbol{E}(\boldsymbol{r}_j)$ with respect to the variable ϕ_i, since it would yield to an incorrect result of the optical force.

Then, the ϕ-component of the optical force on particle i can be written as

$$\begin{aligned}
\langle F_i^{\phi} \rangle = \frac{\epsilon\epsilon_0}{2} \operatorname{Re} \Big\{ \alpha_i \boldsymbol{E}(\boldsymbol{r}_i) \cdot \partial_{\phi_i} \boldsymbol{E}^{0*}(\boldsymbol{r}_i) \Big\} \\
+ \frac{\epsilon\epsilon_0}{2} \operatorname{Re} \left\{ \alpha_i \boldsymbol{E}(\boldsymbol{r}_i) \cdot k^2 \sum_{i \neq j}^{N} \left[\partial_{\phi_i} G^*(\boldsymbol{r}_i, \boldsymbol{r}_j)\right] \alpha_j^* \boldsymbol{E}^*(\boldsymbol{r}_j) \right\}
\end{aligned} \tag{2.32}$$

2.4 Forces due to random light illumination

It is well known that in nature, fluctuations can lead to net interactions between objects. Casimir-like forces due to geometry mediated by quantum or thermal fluctuations, and van der Waals forces due to polarization of nearby particles are two examples of this kind of interactions. In this section, we will describe the interaction force between dipolar particles due to the classical fluctuations of an applied electromagnetic field.

2.4.1 The field-field correlation functions

Since the force that is going to be induced between the dipoles is due to a random electromagnetic field, it can not be computed directly from the values of the electric field and its derivatives, as we did in the case of forces exerted by non-random forces. Instead, we are going to make use of the statistical properties of the fluctuations of the electromagnetic field to calculate the averaged value of these forces.

In the case of a free, homogeneous, isotropic random electromagnetic field, the field field correlation can be obtained as (Setälä et al., 2003)

$$\left\langle \boldsymbol{E}^*(\boldsymbol{r}_1) \otimes \boldsymbol{E}(\boldsymbol{r}_2) \right\rangle = \frac{4\pi u_E(\omega)}{k} \operatorname{Im}\left\{ G(\boldsymbol{r}_1, \boldsymbol{r}_2, \omega) \right\} \tag{2.33}$$

being $u_E(\omega)$ the energy density of the applied light field.

And the correlation between the electric field and its derivative is

$$\left\langle \left[\partial_{\phi_1} \boldsymbol{E}^*(\boldsymbol{r}_1) \right] \otimes \boldsymbol{E}(\boldsymbol{r}_2) \right\rangle = \frac{4\pi u_E(\omega)}{k} \operatorname{Im}\left\{ \partial_{\phi_1} G(\boldsymbol{r}_1, \boldsymbol{r}_2, \omega) \right\} \tag{2.34}$$

Then we have, for the inner products

$$\left\langle \boldsymbol{E}^*(\boldsymbol{r}_1) \cdot \boldsymbol{E}(\boldsymbol{r}_2) \right\rangle = \frac{4\pi u_E(\omega)}{k} \operatorname{Tr}\left[\operatorname{Im}\left\{ G(\boldsymbol{r}_1, \boldsymbol{r}_2, \omega) \right\} \right] \tag{2.35}$$

and

$$\left\langle \left[\partial_{\phi_1} \boldsymbol{E}^*(\boldsymbol{r}_1) \right] \cdot \boldsymbol{E}(\boldsymbol{r}_2) \right\rangle = \frac{4\pi u_E(\omega)}{k} \operatorname{Tr}\left[\operatorname{Im}\left\{ \partial_{\phi_1} G(\boldsymbol{r}_1, \boldsymbol{r}_2, \omega) \right\} \right] \tag{2.36}$$

Finally, if $\mathbb{C}$ and $\mathbb{D}$ are two arbitrary 3×3 matrices, we have the following relations

$$\begin{aligned} \left\langle \boldsymbol{E}^*(\boldsymbol{r}_1)\mathbb{C} \cdot \mathbb{D}\boldsymbol{E}(\boldsymbol{r}_2) \right\rangle &= \frac{4\pi u_E(\omega)}{k} \operatorname{Tr}\left[\mathbb{C}\mathbb{D} \operatorname{Im}\left\{ G(\boldsymbol{r}_1, \boldsymbol{r}_2, \omega) \right\} \right] \\ &= \frac{4\pi u_E(\omega)}{k} \operatorname{Tr}\left[\mathbb{D} \operatorname{Im}\left\{ G(\boldsymbol{r}_1, \boldsymbol{r}_2, \omega) \right\} \mathbb{C} \right] \\ &= \frac{4\pi u_E(\omega)}{k} \operatorname{Tr}\left[\operatorname{Im}\left\{ G(\boldsymbol{r}_1, \boldsymbol{r}_2, \omega) \right\} \mathbb{C}\mathbb{D} \right]. \end{aligned} \tag{2.37}$$

2.4.2 The two-particle force

For a two particle system, we can express the solution of the MSP as (see Equation (2.27))

$$T_A \boldsymbol{E}(\boldsymbol{r}_A) = A^{-1}\Big(\boldsymbol{E}^0(\boldsymbol{r}_A) + G(\boldsymbol{r}_A, \boldsymbol{r}_B) T_B \boldsymbol{E}^0(\boldsymbol{r}_B)\Big) \tag{2.38a}$$

$$T_B \boldsymbol{E}(\boldsymbol{r}_B) = B^{-1}\Big(\boldsymbol{E}^0(\boldsymbol{r}_B) + G(\boldsymbol{r}_B, \boldsymbol{r}_A) T_A \boldsymbol{E}^0(\boldsymbol{r}_A)\Big) \tag{2.38b}$$

where, for spherical particles,

$$T_{A,B} = k^2 \alpha_{A,B} = k^2 \begin{bmatrix} \alpha_{A,B} & 0 & 0 \\ 0 & \alpha_{A,B} & 0 \\ 0 & 0 & \alpha_{A,B} \end{bmatrix} \tag{2.39}$$

are the polarizability matrices and

$$A = T_A^{-1} - G(\boldsymbol{r}_A, \boldsymbol{r}_B) T_B G(\boldsymbol{r}_B, \boldsymbol{r}_A) \tag{2.40a}$$

$$B = T_B^{-1} - G(\boldsymbol{r}_B, \boldsymbol{r}_A) T_A G(\boldsymbol{r}_A, \boldsymbol{r}_B) \tag{2.40b}$$

To evaluate the interaction force between particles A and B, we will need the relations

$$\operatorname{Im}\Big\{\partial_{\phi_i} G(\boldsymbol{r}_i, \boldsymbol{r}_j)\Big\}\Big|_{\boldsymbol{r}_j = \boldsymbol{r}_i} = 0_{3\times 3} \tag{2.41}$$

$$T_A G(\boldsymbol{r}_A, \boldsymbol{r}_B) B^{-1} = A^{-1} G(\boldsymbol{r}_A, \boldsymbol{r}_B) T_B \tag{2.42}$$

and, in the case of particles with no absorption,

$$\operatorname{Im}\Big\{T_i^{-1}\Big\} = -\operatorname{Im}\Big\{G(\boldsymbol{r}_i, \boldsymbol{r}_i)\Big\} \tag{2.43}$$

where $i = A, B$.

Then, taking into account the correlations given by Equations (2.35) and (2.36), the interaction force on particle B can be written as

$$\Big\langle F(\boldsymbol{r}_B)\Big\rangle = \frac{2\pi u_E(\omega)}{k^3} \operatorname{Im}\Big\{ \operatorname{Tr}\Big[[\partial_{z_B} G(\boldsymbol{r}_B, \boldsymbol{r}_A)] T_A G(\boldsymbol{r}_A, \boldsymbol{r}_B) B^{-1}\Big]\Big\}. \tag{2.44}$$

This force can be written in terms of a potential which, under WSA, takes the form (Brügger et al., 2015)

$$U(R) = \frac{2\pi u_E(\omega)}{k^3} \operatorname{Tr}\Big[\operatorname{Im}\Big\{G(\boldsymbol{r}_B, \boldsymbol{r}_A) T_A G(\boldsymbol{r}_A, \boldsymbol{r}_B) T_B\Big\}\Big] \tag{2.45}$$

where $R = |\boldsymbol{r}_B - \boldsymbol{r}_A|$ is the separation between the particles.

Note that, in the particular case of a system of several particles illuminated by a random light field, the computation of the force is different from the computation of forces in systems of several particles illuminated by non-random light fields. In the case of non-random fields, we may solve the MSP to obtain the incident fields on every particle, and then use these incident fields to compute the force.

In the case of random fields we can not use this procedure since we can not assign a value of the applied field on any particle. We must use the field-field correlations defined by Equations (2.35) and (2.36). This will make the simulation code to be computationally more expensive.

Chapter 3

Arrested dimer's diffusion in Optical Lattices

Understanding Brownian motion in spatially periodic and random landscapes has long been of great interest from a fundamental and practical point of view (Risken et al., 1996; Bouchaud et al., 1990; Sahimi, 1993; Reimann, 2002; Hänggi et al., 2009). The ability of light to exert significant forces on small particles (Ashkin, 1970) offers the opportunity to sculpt potential energy profiles enabling the study of Brownian dynamics in complex landscapes. Extended periodic landscapes, known as optical lattices, can be generated by the periodic intensity maxima arising in the interference pattern of several crossed laser beams (Chowdhury et al., 1985; Burns et al., 1990; Hemmerich et al., 1993) or by an array of optical tweezers (Ashkin et al., 1986; Jones et al., 2015) generated by holographic techniques (Polin et al., 2005).

In order to understand the interplay between the optically induced Potential Energy Landscapes (PELs) and multiple scattering in the diffusion of dimers or other aggregates we have analyzed a simple system consisting of a dimer made out of two non-absorbing particles at Frohlich Resonance Condition (FRC) diffusing on a two-dimensional optical lattice. In an optical potential energy landscape, the electromagnetic forces on small particles are conservative gradient interactions (Chaumet et al., 2000; Albaladejo et al., 2009b) proportional to the real part of the particle's polarizability. At resonance, the real part of the polarizability is negligible and, as a consequence, a single resonant nanoparticle does not see the underlying optical lattice and undergoes free thermal Brownian motion. However, as we will show, when two resonant monomers link into a dimer, multiple scattering among them induces both a torque and a net force on the dimer's center of mass.

The actual torques and forces are not driven directly by the external

PEL but they are sustained by the dimer itself. Related self-induced forces arising in the mechanical action of light on a nanoparticle in a confined geometry (Gómez-Medina et al., 2001; Gómez-Medina et al., 2004; Juan et al., 2009; Descharmes et al., 2013) are called "self-induced back-action" (SIBA) forces (Juan et al., 2009). The multiple scattering between the monomer and the confining walls are replaced here by the back-action induced by the mirror monomers in the dimer. Interestingly, while a monomer can freely diffuse, the SIBA forces can be strong enough to arrest the dimer's diffusion. These results suggest interesting applications in the manipulation of diffusion-limited aggregation (Witten et al., 1981) under optical fields.

3.1 SIBA forces on a dimer in an Optical Lattice

Let us consider a dimer formed by two linked resonant electric dipoles of mass m, radius a, separated by a fixed distance L and moving in the xy-plane. The dimer is immersed in water and is illuminated by a superposition of two standing waves in the x and y directions as sketched in Figure 3.1. The external illuminating electric field is given by

$$\boldsymbol{E}^0(x,y,z) = E_z^0 \hat{\boldsymbol{e}}_z = i2E_0(\sin kx + \sin ky)\,\hat{\boldsymbol{e}}_z \tag{3.1}$$

where $k = n\omega/c = 2\pi/\lambda$ is the wave number, λ is the wavelength in water, n the refractive index, E_0 is the amplitude of the electric field, Ψ is a real function and $\hat{\boldsymbol{e}}_z$ is the unitary vector in the z-direction.

For a single electric dipolar particle moving through a field $\boldsymbol{E} = E_z\hat{\boldsymbol{e}}_z$, linearly polarized along z, the time averaged optical force is given by (Chaumet et al., 2000)

$$\boldsymbol{F} = \frac{\epsilon\epsilon_0}{2}\,\mathrm{Re}\left\{\alpha^* E_z^* \nabla E_z\right\} = \frac{\epsilon\epsilon_0}{2}\left\{\frac{\alpha'}{2}\nabla|E_z|^2 + \alpha''\,\mathrm{Im}\left\{E_z^*\nabla E_z\right\}\right\}. \tag{3.2}$$

At Frohlich resonance $\alpha = i\frac{6\pi}{k^3}$, i.e. $\alpha' = 0$, and the total force on a single monomer moving through an external field given by Equation (3.1) is identically zero: there are no forces coming from the gradient force term (proportional to α') and the "scattering force" (proportional to $\mathrm{Im}\left\{E_z^{0*}\nabla E_z^0\right\} = 0$) vanishes.

However, when a dimer is formed, the actual field that polarises each monomer comes not only from the external field but also from the radiation scattered by the other dipole . This scattered light contributes to the optical force and may alter some dynamical properties of the system such

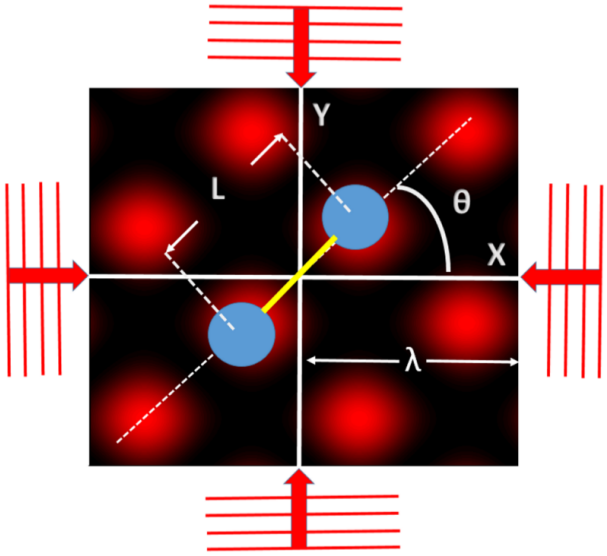

FIGURE 3.1: Sketch of the model system to analyze the Brownian motion of a dimer of length L in a two-dimensional optical lattice. The optical lattice is made up of two perpendicular standing waves with wavelength λ. The dimer configuration is given by the position (x, y) of the center of mass and the angle θ with respect to the x-axis.

as the diffusion. The optical polarising fields on particles located at positions $\boldsymbol{r}_1$ and $\boldsymbol{r}_2$, respectively, are expressed as

$$\begin{aligned} \boldsymbol{E}(\boldsymbol{r}_1) &= \boldsymbol{E}^0(\boldsymbol{r}_1) + k^2 G(\boldsymbol{r}_1, \boldsymbol{r}_2)\alpha \boldsymbol{E}(\boldsymbol{r}_2) \\ \boldsymbol{E}(\boldsymbol{r}_2) &= \boldsymbol{E}^0(\boldsymbol{r}_2) + k^2 G(\boldsymbol{r}_2, \boldsymbol{r}_1)\alpha \boldsymbol{E}(\boldsymbol{r}_1) \end{aligned} \tag{3.3}$$

where $G(\boldsymbol{r}_i, \boldsymbol{r}_j)$ is the Green dyadic function. Since the motion of the dimer in our system is restricted to the xy-plane and the external electric field is oriented along the z-axis, the only relevant component of the Green dyadic function is

$$G_{zz}(\boldsymbol{r}_i, \boldsymbol{r}_j) = G_{zz}(L) = \frac{e^{ikL}}{4\pi L}\left(1 + i\frac{1}{kL} - \frac{1}{k^2L^2}\right) \tag{3.4}$$

being $L = |\boldsymbol{r}_1 - \boldsymbol{r}_2| = \sqrt{(x_1 - x_2)^2 + (y_1 - y_2)^2}$ the distance between the particles.

Defining, $\mathrm{G} \equiv G_{zz}(\boldsymbol{r}_1, \boldsymbol{r}_2) = G_{zz}(\boldsymbol{r}_2, \boldsymbol{r}_1)$, the system of equations (3.3) admits a simple analytic solution given by

$$\begin{aligned} E_z(\boldsymbol{r}_1) &= \frac{E_z^0(\boldsymbol{r}_1) + k^2\,\mathrm{G}\,\alpha\,E_z^0(\boldsymbol{r}_2)}{1 - k^4\,\mathrm{G}^2\,\alpha^2} \\ E_z(\boldsymbol{r}_2) &= \frac{E_z^0(\boldsymbol{r}_2) + k^2\,\mathrm{G}\,\alpha\,E_z^0(\boldsymbol{r}_1)}{1 - k^4\,\mathrm{G}^2\,\alpha^2}. \end{aligned} \tag{3.5}$$

Note how the field polarising the particles always point along z and, from Eq. (3.2), the force on the resonant monomers "1" and "2" is given by

$$\begin{aligned} \boldsymbol{F}_1 &= \frac{\epsilon\epsilon_0}{2}\alpha''\,\mathrm{Im}\left\{E_z^*(\boldsymbol{r}_1)\nabla_1 E_z(\boldsymbol{r}_1)\right\} \\ \boldsymbol{F}_2 &= \frac{\epsilon\epsilon_0}{2}\alpha''\,\mathrm{Im}\left\{E_z^*(\boldsymbol{r}_2)\nabla_2 E_z(\boldsymbol{r}_2)\right\} \end{aligned} \tag{3.6}$$

where $E_z^*(\boldsymbol{r}_i)$ is given by Eq. (3.5), $\nabla_i \equiv \{\partial/\partial x_i, \partial/\partial y_i\}$ and by taking into account that $\nabla_2\,\mathrm{G} = -\nabla_1\,\mathrm{G}$,

$$\begin{aligned} \nabla_1 E_z(\boldsymbol{r}_1) &= \nabla_1 E_z^0(\boldsymbol{r}_1) + i\alpha'' k^2\Big[\nabla_1\,\mathrm{G}\Big]E_z(\boldsymbol{r}_2) \\ \nabla_2 E_z(\boldsymbol{r}_2) &= \nabla_2 E_z^0(\boldsymbol{r}_2) - i\alpha'' k^2\Big[\nabla_1\,\mathrm{G}\Big]E_z(\boldsymbol{r}_1). \end{aligned} \tag{3.7}$$

These expressions will be used to perform the molecular dynamics simulations discussed below. Notice that they are exact only within the dipolar approximation which is known to be valid for L larger than approximately three times the monomer radius (Miljković et al., 2010). At smaller inter-particle separations, higher order multipoles become relevant in the computation of the forces.

3.1.1 Analytical approach

In order to gain some insight into the problem, let us consider Equations (3.5) and (3.7) in the limit $k^2\,\mathrm{G}\,\alpha'' = 3\lambda\,\mathrm{G} \ll 1$ (a good approximation for $R \geq \lambda/2$),

$$\begin{aligned} E_z(\boldsymbol{r}_1) &\approx E_z^0(\boldsymbol{r}_1) + ik^2\,\mathrm{G}\,\alpha'' E_z^0(\boldsymbol{r}_2) + \cdots \\ \nabla_1 E_z(\boldsymbol{r}_1) &\approx \nabla_1 E_z^0(\boldsymbol{r}_1) + ik^2\Big[\nabla_1\,\mathrm{G}\Big]\alpha'' E_z^0(\boldsymbol{r}_2) + \cdots. \end{aligned}$$

Analogous expressions are obtained for monomer "2".

Then, at lowest order in $[k^2\,\mathrm{G}\,\alpha'']$, the forces defined in Equation (3.2) are given by

$$\begin{aligned}\boldsymbol{F}_1 = \frac{\epsilon\epsilon_0}{2}\,\mathrm{Re}\Big\{ &- i\alpha'' E_z^{0*}(\boldsymbol{r}_1)\nabla_1 E_z^0(\boldsymbol{r}_1) + k^2\alpha''^2\Big[\nabla_1\,\mathrm{G}\Big] E_z^{0*}(\boldsymbol{r}_1)E_z^0(\boldsymbol{r}_2)\\ &- k^2\alpha''^2\,\mathrm{G}^*\,E_z^{0*}(\boldsymbol{r}_2)\nabla_1 E_z^0(\boldsymbol{r}_1) + \mathcal{O}(\alpha^3)\Big\}\\ \boldsymbol{F}_2 = \frac{\epsilon\epsilon_0}{2}\,\mathrm{Re}\Big\{ &- i\alpha'' E_z^{0*}(\boldsymbol{r}_2)\nabla_2 E_z^0(\boldsymbol{r}_2) - k^2\alpha''^2\Big[\nabla_1\,\mathrm{G}\Big] E_z^{0*}(\boldsymbol{r}_2)E_z^0(\boldsymbol{r}_1)\\ &- k^2\alpha''^2\,\mathrm{G}^*\,E_z^{0*}(\boldsymbol{r}_1)\nabla_2 E_z^0(\boldsymbol{r}_2) + \mathcal{O}(\alpha^3)\Big\}\end{aligned} \tag{3.8}$$

The first terms in both equations vanish because they are the real part of a purely imaginary number. Furthermore, in our configuration, $E^0(\boldsymbol{r}_i)$ and $\nabla_i E^0(\boldsymbol{r}_i)$ are also pure imaginary numbers, so we have

$$E_z^{0*}(\boldsymbol{r}_1)E_z^0(\boldsymbol{r}_2) = E_z^{0*}(\boldsymbol{r}_2)E_z^0(\boldsymbol{r}_1) \tag{3.9}$$

and then, when adding both forces, the second terms cancel out and we can readily calculate the force on the center of mass as

$$\begin{aligned}\boldsymbol{F}_{cm} &= \boldsymbol{F}_1 + \boldsymbol{F}_2\\ &= -\frac{\epsilon\epsilon_0}{2}k^2\alpha''^2\Big[E_z^{0*}(\boldsymbol{r}_2)\nabla_1 E_z^0(\boldsymbol{r}_1) + E_z^{0*}(\boldsymbol{r}_1)\nabla_2 E_z^0(\boldsymbol{r}_2)\Big]\,\mathrm{Re}\Big\{\,\mathrm{G}\,\Big\} + \mathcal{O}(\alpha^3).\end{aligned} \tag{3.10}$$

From this equation we can obtain information about the dynamical behavior of the dimer:

First, the force on the center of mass is equal to zero if $\mathrm{Re}\,\{\mathrm{G}\}$ vanishes. For this particular situation, the diffusion of the dimer is purely Brownian and the existence of an external electromagnetic field is not going to modify the dynamics. The real part of the Green function is written as

$$\mathrm{Re}\Big\{\,\mathrm{G}\,\Big\} = \frac{1}{4\pi L}\left[\left(1 - \frac{1}{k^2L^2}\right)\cos kL - \frac{1}{kL}\sin kL\right]. \tag{3.11}$$

First two zeros of Equation (3.11) are given by $L = 0.72\lambda$ and $L = 1.2\lambda$, so we expect to find free Brownian dynamics for dimers with these lengths.

In second place, we can also obtain information about the behavior of the dimer when the force on the center of mass is different from zero. We will describe the dimer configuration in terms of its center-of-mass

coordinates (x, y) and an angular coordinate θ describing the angle of the dimer with respect to the x-axis. The relationship between the monomer's coordinates and the center of mass is given by

$$\boldsymbol{r}_1 = \boldsymbol{r} + \Delta\boldsymbol{r}_\theta \quad , \quad \boldsymbol{r}_2 = \boldsymbol{r} - \Delta\boldsymbol{r}_\theta$$
$$\Delta\boldsymbol{r}_\theta = (\frac{L}{2}\cos\theta, \frac{L}{2}\sin\theta).$$

if we consider now a fixed orientation of the dimer with respect to the electromagnetic field (fixed θ), then

$$\nabla_2 = \nabla_1 = \nabla \tag{3.12}$$

being ∇ the gradient with respect to the coordinates of the center of mass.

Then, going back to Equation (3.10), we can obtain an expression for the potential energy of the system for fixed θ,

$$\boldsymbol{F}_{cm} \simeq -\nabla U_\theta(x, y) \tag{3.13}$$

with

$$U_\theta(x, y) = -\frac{\epsilon\epsilon_0}{2}k^2\alpha''^2\Big[E_z^{0*}(\boldsymbol{r}_1)E_z^0(\boldsymbol{r}_2)\Big]\,\mathrm{Re}\Big\{\,\mathrm{G}(L)\Big\} \tag{3.14}$$
$$= -\frac{\epsilon\epsilon_0}{2}k^2\alpha''^2\Big[E_z^{0}(\boldsymbol{r}_1)E_z^{0*}(\boldsymbol{r}_2)\Big]\,\mathrm{Re}\Big\{\,\mathrm{G}(L)\Big\}. \tag{3.15}$$

Where Equations (3.14) and (3.15) are equivalent. In this approximation, although the forces are non-conservative, if the dimer moves at fixed angle, the system is conservative and the energy landscape is given by $U_\theta(x, y)$.

3.2 Dimer's diffusion

3.2.1 Dimer's Brownian diffusion

In this section we are going to obtain the diffusion constant of the dimer when no electromagnetic field is applied. First, we must write the equations of motion for the dimer by transforming the coordinates of the monomers (x_1, y_1, x_2, y_2) into the dimer coordinates (x, y, θ). The equations of motion for the angle θ and the center of mass for a pure Brownian motion of the

dimer are

$$2m\frac{d^2\boldsymbol{r}_{cm}}{dt^2} = -2\gamma\left(\dot{x}_{cm}\hat{i} + \dot{y}_{cm}\hat{j}\right) + \sigma\left[(\Psi_{x_1} + \Psi_{x_2})\hat{i} + (\Psi_{y_1} + \Psi_{y_2})\hat{j}\right] \tag{3.16a}$$

$$2mL^2\frac{d^2\alpha}{dt^2} = -2\gamma\dot{\alpha}L^2 + \sigma L\Big[(\Psi_{x_2} - \Psi_{x_1})\sin\alpha + (\Psi_{y_1} - \Psi_{y_2})\cos\alpha\Big]. \tag{3.16b}$$

being γ the friction coefficient ($\gamma = 6\pi a\eta$, η is the viscosity, $\eta = 0.89 \times 10^{-3}$kg m^{-1}s^{-1} for water at $T = 298$K) and $\sigma\Psi_i(t)$ a thermal force with zero mean and variance given by the fluctuation-dissipation theorem

$$\langle\sigma\Psi_i(t)\,\sigma\Psi_j(t')\rangle = \sigma^2\delta_{ij}\delta(t-t') = 2\gamma k_B T\delta_{ij}\delta(t-t') \tag{3.17}$$

with i and j equal to (x_1, y_1, x_2, y_2) and T being the system's temperature.

To obtain the diffusion relations we shall take the overdamped approximation, in which the masses m of the particles are set to zero. For the coordinates of the center of mass we will have

$$2\gamma\dot{x} = \sigma\Big(\Psi_{x_1} + \Psi_{x_2}\Big) \tag{3.18a}$$

$$2\gamma\dot{y} = \sigma\Big(\Psi_{y_1} + \Psi_{y_2}\Big). \tag{3.18b}$$

Given two Gaussian distributions $X \sim N(\mu_x, \sigma_x^2)$ and $Y \sim N(\mu_y, \sigma_y^2)$, it is a known result that their sum and difference U, V are also Gaussian distributions such that

$$U = X + Y \sim N(\mu_x + \mu_y, \sigma_x^2 + \sigma_y^2) \tag{3.19a}$$

$$V = X - Y \sim N(\mu_x - \mu_y, \sigma_x^2 + \sigma_y^2), \tag{3.19b}$$

then the equations of motion can be written in the form

$$\gamma\dot{x} = \frac{(\sqrt{2}\sigma)}{2}\Big(\Psi_{x_1} + \Psi_{x_2}\Big) = \frac{\sigma}{\sqrt{2}}\Psi^x \tag{3.20a}$$

$$\gamma\dot{y} = \frac{(\sqrt{2}\sigma)}{2}\Big(\Psi_{y_1} + \Psi_{y_2}\Big) = \frac{\sigma}{\sqrt{2}}\Psi^y. \tag{3.20b}$$

These are, formally, the equations that a sole particle would have when diffusing in two dimensions with $\sigma' = \sigma/\sqrt{2}$, then the diffusion relation for the coordinates of the center of mass will be

$$\Big\langle(\vec{r}(t) - \vec{r}(t_0))^2\Big\rangle = 4Dt \tag{3.21}$$

with

$$D = \frac{\sigma'^2}{2\gamma^2} = \left(\frac{\sigma}{\sqrt{2}}\right)^2 \frac{1}{2\gamma^2}. \tag{3.22}$$

or, taking into account that $\sigma = \sqrt{2\gamma k_B T}$,

$$D = \frac{2\gamma k_B T}{4\gamma^2} = \frac{k_B T}{2\gamma} \tag{3.23}$$

It can be noticed that this diffusion constant is exactly half of the diffusion constant that a sole particle would have when freely diffusing in two dimensions.

3.2.2 Langevin dynamics simulations in an optical lattice

Let us now analyze the dynamics of the system with no approximations when the optical field (3.1) is applied by means of Langevin molecular dynamics simulations. The equations of motiion are now given by

$$\begin{aligned}
2m\frac{d^2x}{d^2t} &= -2\gamma\frac{dx}{dt} + \xi_{x1} + \xi_{x2} + F_x \\
2m\frac{d^2y}{d^2t} &= -2\gamma\frac{dy}{dt} + \xi_{y1} + \xi_{y2} + F_y \\
2mL^2\frac{d^2\theta}{d^2t} &= -2\gamma\frac{d\theta}{dt}L^2 + \\
&\quad + L\Big(\xi_{x2} + F_{x2} - \xi_{x1} - F_{x1}\Big)\sin(\theta) \\
&\quad + L\Big(\xi_{y1} + F_{y1} - \xi_{y2} - F_{y2}\Big)\cos(\theta)
\end{aligned}$$

where $\xi_i = \sigma\Psi_i$. F_i, with $i = (x_1, x_2, y_1, y_2)$, are the components of the optical force on both particles obtained through Equation (3.2). We have considered particles $a = 5$nm radius, $\lambda = 387.585$nm wavelength in water, $n_w = \sqrt{1.8}$.

When the intensity P of the electromagnetic field, $(n/c)P \equiv \epsilon\epsilon_0|E_0|^2/2$, is different from zero, the diffusion constant decreases. In Figure 3.2a we show the mean square displacement versus time from 1000 different Langevin molecular dynamics simulations. We consider a resonant dimer of length $L = 0.6\lambda$ and several laser intensities $P = 0,\ 0.4,\ 0.6,\ 0.8 \times 10^5 \mathrm{W/cm}^2$. Note how, as the laser intensity increases, the dimer gets trapped and the diffusion constant strongly decreases.

From the long time behavior of the mean square displacement we can obtain the values of the diffusion constant as the laser intensity increases.

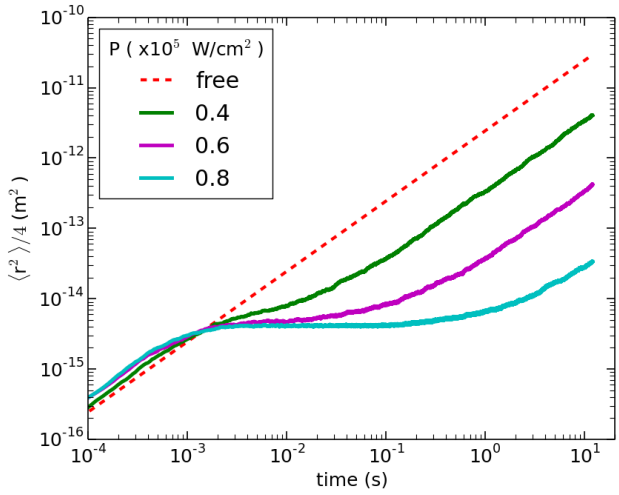

(A)

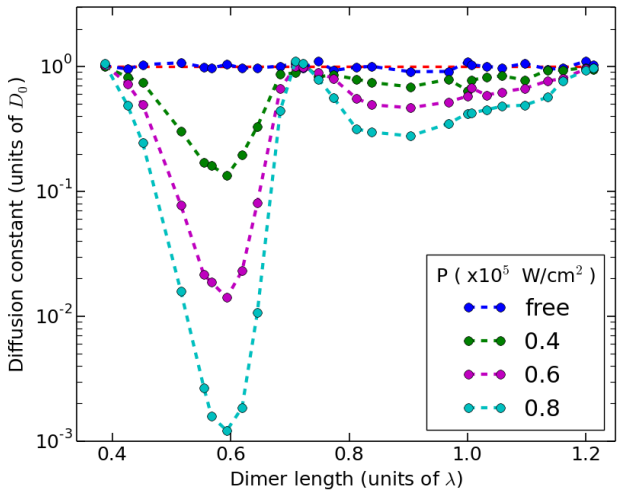

(B)

FIGURE 3.2: (A) Mean squared displacement versus time in logarithmic scale obtained from 1000 Langevin molecular dynamics simulations for a resonant dimer with length $L = 0.6\lambda$ and different laser intensities. The dimer is moving in water at a temperature $T = 298$K. (B) Effective diffusion constant versus dimer's length for different laser intensities in semi logarithmic scale. All diffusion constant are normalized by $D_0 = \frac{k_B T}{2\gamma}$. For rather small laser intensities the diffusion constant changes in several orders of magnitude.

We have done this for several values of L and the results are shown in Fig. 3.2b. Note how the value of the diffusion constant strongly depends on dimer's length. A maximum reduction of almost three orders of magnitude is obtained for the particular case of $L = 0.6\lambda$ with relatively small laser intensities, while for $L = 0.72\lambda$ and $L = 1.2\lambda$ there is no arrest due to the optical forces. This is in perfect agreement with the analytic results previously obtained. The present results indicate that dimers of different lengths would be easily sorted due to the great sensitivity of the system on dimer's dimension. Note that, since each isolated monomer feels no optical force at all, the decrease in the value of the diffusion constant is due only to the non symmetric scattering interaction among the monomers. That is, the interaction force exerted on particle 1 by 2 is not reciprocal to the interaction force exerted on particle 2 by 1. We already found in the literature a situation in which action-reaction in optical forces is not fulfilled (Sukhov et al., 2015) for a dimer made up of two different particles. In our case both particles are identical and the asymmetry in the interactions comes from the external field.

Figures 3.3a and 3.3b show typical Brownian trajectories of the dimer's center of mass together with a polar plot of the dimer orientation at specific points for dimer lengths $L = 0.6\lambda$ and $L = 0.84\lambda$. The mean square displacement, the reduction on the diffusion constant and the strong dependence of the main statistical features of the dynamics on the dimer's length L, can be understood in terms of the potential energy landscape obtained in Equation (3.14). First, we have performed statistics of the data collected from the Langevin molecular dynamics simulations to obtain the distribution function for the dimer orientation θ. The results are shown in Figure 3.4a for the particular case of a dimer of length $L = 0.6\lambda$ and a laser intensity $P = 0.4 \times 10^5 \mathrm{W/cm}^2$. For this particular length, the multiple scattering among monomers induces preferential orientations of the dimer along the x or y coordinates corresponding to $\theta = n\pi/2$ ($n = 0, 1, \dots$). The corresponding probability distribution for the position of the center of mass of the dimer is shown in Figure 3.5a.

We could understand the motion of the dimer's center of mass as a diffusing process in an effective potential energy landscape given by $U_0(x, y) = U_{\pi/2}(x, y)$ (both orientations given the same approximated potential energy landscape). This potential landscape, plotted in Figure 3.5b, shows various potential minima in agreement with the numerical probability distribution.

The positions where it is most probable to find the center of the dimer correspond to the positions where the potential given by Equation (3.14)

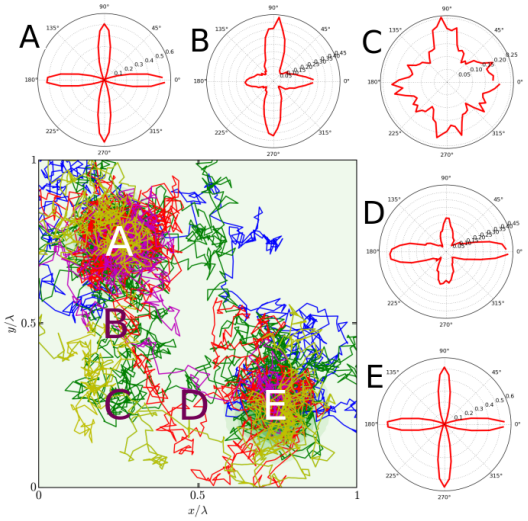

(A)

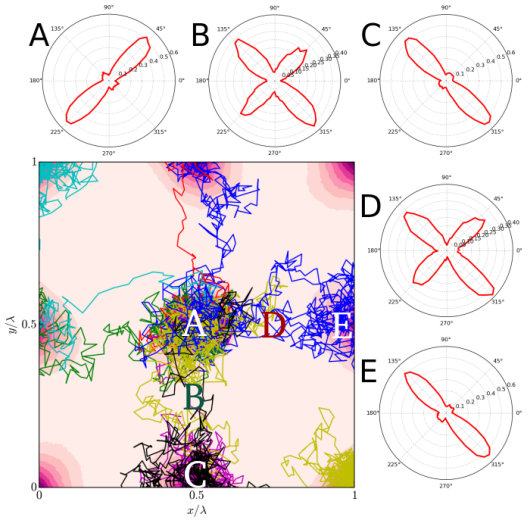

(B)

FIGURE 3.3: (A) Typical trajectories of the dimer's center of mass in $(x, y) \in [0, \lambda)$ obtained from Langevin molecular dynamics simulations for $L = 0.6\lambda$ and $P = 0.3 \times 10^5 \mathrm{W/cm^2}$. Polar plots of the dimer orientation probability distribution at specific points "A" to "E" are also shown. (B) The same as in (A), but for $L = 0.84\lambda$ and $P = 0.8 \times 10^5 \mathrm{W/cm^2}$.

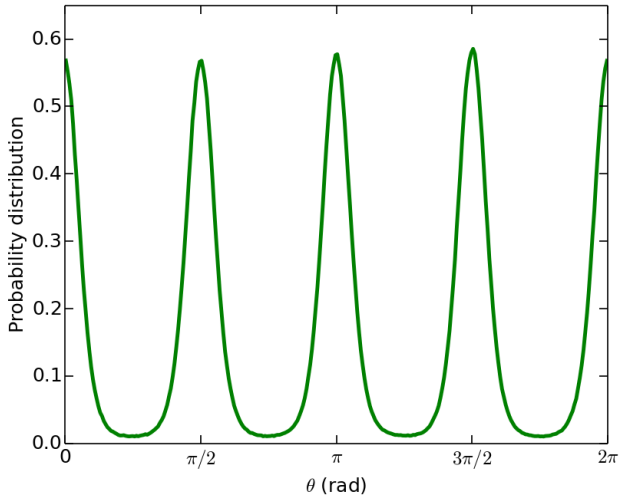

(A)

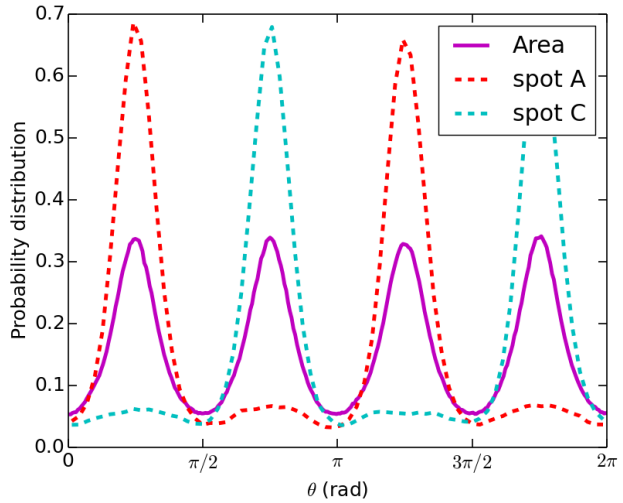

(B)

FIGURE 3.4: (A) Probability distribution for the orientation angle θ for a dimer with length $L = 0.6\lambda$ and laser intensity $P = 0.4 \times 10^5 \text{W/cm}^2$. (B) Continuous line corresponds to the probability distribution for a dimer length 0.84λ. Dashed lines are the distributions obtained at two fixed positions of the center of mass (labeled "A" and "C" in Figure3.3b).

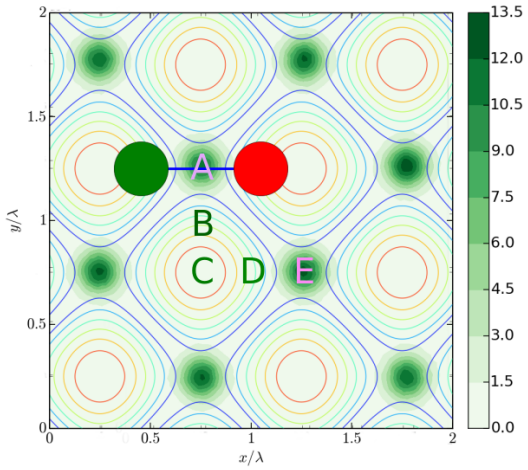

(A)

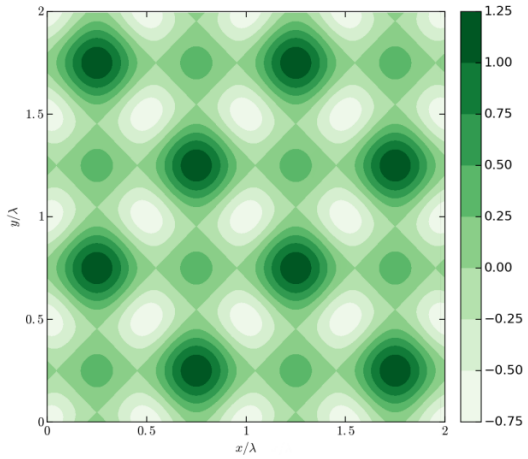

(B)

FIGURE 3.5: (A) Probability distribution for the dimer's center of mass in $x, y \in [0, \lambda)$ obtained from Langevin molecular dynamics simulations for $L = 0.6\lambda$ and $P = 0.3W/cm^2$. Darker regions correspond to a higher probability (the integral of the distribution over the area of the figure is normalized to 1). Typical Brownian trajectories form "A" to "E" are shown in Figure 3.3a. The contour map shows the underlying field intensity landscape (contour lines correspond to 0.15, 0.30, 0.45, 0.60, 0.75 and (red line) $0.90|\boldsymbol{E}^0|^2_{max}$) (B) Potential energy landscape $-U_\theta(x, y)/k_BT$ from Equation (3.14) for a fixed angle $\theta = 0$ or $\theta = \pi/2$ corresponding to the preferential angles observed in Figure 3.4a. Potential minima are located in the darker regions.

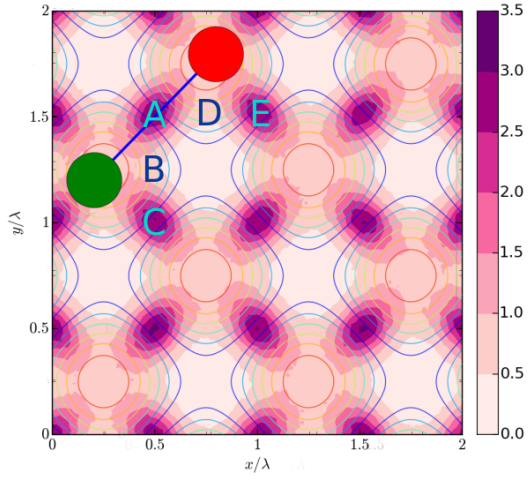

(A)

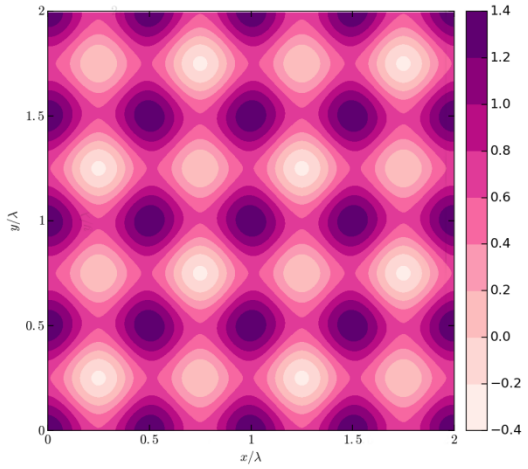

(B)

FIGURE 3.6: (A) Probability distribution for the dimer's center of mass in $x, y \in [0, \lambda)$ obtained from Langevin molecular dynamics simulations for $L = 0.84\lambda$ and $P = 0.8W/cm^2$. Darker regions correspond to a higher probability. Typical Brownian trajectories from "A" to "E" (or "A" to "C") are shown in Figure 3.3b. The contour lines show the underlying field intensity landscape as in Figure 3.5a. (B) Potential energy landscape $-U_\theta(x, y)/k_BT$ from Equation (3.14) for a fixed angle $\theta = \pi/4$ and $\theta = 3\pi/4$ corresponding to the preferential angles observed in Figure 3.4b.

has a minimum, indicating that the diffusion of the dimer is actually modified by the dynamical arrest produced by the potential wells in the energy landscape. Note that this potential landscape is felt by the system only when the two particles create the dimer. For the isolated dipoles there is no energy landscape at all.

The results for a different length $L = 0.84\lambda$ are sumarized in Figures. 3.3b, 3.4b and 3.6b. In this case, the preferred orientations of the dimer have tilted $\pi/4$, corresponding to the diagonals instead of the vertical and horizontal orientations and the locations of the maxima in the probability distribution for the dimer's center of mass have changed. Again, the effective potential landscape minima, with $\theta = \pi/4 + n\pi/2$, capture the most probable locations of the center of mass.

It is worth it to mention that, for computing the potential of Figure 3.6b, not only one orientation has to be taken into account but rather the two preferential orientations that appears in the probability distribution represented in Figure 3.4b. This is because, as can be seen in this Figure, each minimum has a different symmetry, while for the case of $L = 0.6\lambda$ shown in Figure 3.4a every minimum has the same angular probability distribution.

3.3 Conclusions

Two main conclusions can be extracted from the work of this chapter:

- Interactions between two dipolar nanoparticles forming a dimer are able to strongly modify the diffusion properties of the dimer moving in a lattice of optical wells.
- A model potential is proposed to capture the main features of this trapped diffusion. Even though the studied interaction is manifiestly non-conservative, this potential is able to satisfactorily describe the probability distribution of the positions of the center of mass.

Chapter 4

Many-particle dynamics in optical lattices

Many particle interactions of different physical origins have been extensively investigated during the last decades. Within the field of colloidal sciences, three- and many-particle interactions due to DLVO potentials (Russ et al., 2005) or to critical Casimir forces (Paladugu et al., 2016) are a topic of current major interest.

The study of complex systems, where a physical problem can not be understood just as the sum of its parts, but rather as a whole system evolving in time and space, is strongly cross-disciplinar. In this scenario, emergent phenomena such as synchronization (Arzola et al., 2014) or pinning effects (del Valle et al., 2017) show up enriching the fundamental theory and further applications of different fields in physical sciences.

In this chapter many particle interactions between NPs due to multiple scattering of light will be studied by using the simple case of three dipolar NPs under different electromagnetic fields. The influence of three-particle interactions on the force exerted on one of them, and the effect of three-particle interactions on the force on the center of mass of the system of particles will be discussed in detail.

Then, a system of many NPs illuminated by an optical vortex field, and subjected to optical and hydrodynamic interactions will be investigated. This will provide a specific realization of a complex system, where different collective dynamics are found. We present the results obtained from the simulations, and then discuss specifically the influence of optical interactions between NPs in the features of the dynamics. This part has been done in collaboration with Prof. Rafael Delgado-Buscalioni and Dr. Marc Meléndez, from the Department of Theoretical Condensed Matter Physics at Universidad Autónoma de Madrid.

4.1 Pair-wise interactions

To study the different contributions to the many-particle dynamics, we will need to define what we mean by pair-wise interactions and write a method for computing this contribution. We already saw in the theory section that, given a system of two particles located at $\boldsymbol{r}_1, \boldsymbol{r}_2$ respectively, with polarizability α, the incident field on any of them will be given by

$$\boldsymbol{E}(\boldsymbol{r}_i) = \Big[\mathbb{I} - [k^2 G(\boldsymbol{r}_i, \boldsymbol{r}_j)\alpha]^2\Big]^{-1}\Big(\boldsymbol{E}^0(\boldsymbol{r}_i) + k^2 G(\boldsymbol{r}_i, \boldsymbol{r}_j)\alpha \boldsymbol{E}^0(\boldsymbol{r}_j)\Big) \tag{4.1}$$

with $i = 1, 2, j \neq i$. We can use this solution to compute the field derivative and eventually compute the optical force on particle i due to particle j.

For a system of three nanoparticles located at $\boldsymbol{r}_1, \boldsymbol{r}_2, \boldsymbol{r}_3$, the following definition of pair-wise interaction force on particle 1 will be used

$$\boldsymbol{F}(\boldsymbol{r}_1) = \frac{\epsilon\epsilon_0}{2}\,\mathrm{Re}\left\{\alpha^* \Psi_{12}^* \cdot \nabla \Psi_2\right\} + \frac{\epsilon\epsilon_0}{2}\,\mathrm{Re}\left\{\alpha^* \Psi_{13}^* \cdot \nabla \Psi_3\right\} \tag{4.2}$$

where

$$\Psi_{12} = \Big[\mathbb{I} - [k^2 G(\boldsymbol{r}_1, \boldsymbol{r}_2)\alpha]^2\Big]^{-1}\Big(\boldsymbol{E}^0(\boldsymbol{r}_1) + k^2 G(\boldsymbol{r}_1, \boldsymbol{r}_2)\alpha \boldsymbol{E}^0(\boldsymbol{r}_2)\Big) \tag{4.3a}$$

$$\Psi_{13} = \Big[\mathbb{I} - [k^2 G(\boldsymbol{r}_1, \boldsymbol{r}_3)\alpha]^2\Big]^{-1}\Big(\boldsymbol{E}^0(\boldsymbol{r}_1) + k^2 G(\boldsymbol{r}_1, \boldsymbol{r}_3)\alpha \boldsymbol{E}^0(\boldsymbol{r}_3)\Big) \tag{4.3b}$$

$$\Psi_{21} = \Big[\mathbb{I} - [k^2 G(\boldsymbol{r}_2, \boldsymbol{r}_1)\alpha]^2\Big]^{-1}\Big(\boldsymbol{E}^0(\boldsymbol{r}_2) + k^2 G(\boldsymbol{r}_2, \boldsymbol{r}_1)\alpha \boldsymbol{E}^0(\boldsymbol{r}_1)\Big) \tag{4.3c}$$

$$\Psi_{31} = \Big[\mathbb{I} - [k^2 G(\boldsymbol{r}_3, \boldsymbol{r}_1)\alpha]^2\Big]^{-1}\Big(\boldsymbol{E}^0(\boldsymbol{r}_3) + k^2 G(\boldsymbol{r}_3, \boldsymbol{r}_1)\alpha \boldsymbol{E}^0(\boldsymbol{r}_1)\Big) \tag{4.3d}$$

and

$$\nabla \Psi_{12} = \nabla \boldsymbol{E}^0(\boldsymbol{r}_2) + k^2 \Big[\nabla G(\boldsymbol{r}_1, \boldsymbol{r}_2)\Big]\alpha\, \Psi_{21} \tag{4.4a}$$

$$\nabla \Psi_{13} = \nabla \boldsymbol{E}^0(\boldsymbol{r}_2) + k^2 \Big[\nabla G(\boldsymbol{r}_1, \boldsymbol{r}_3)\Big]\alpha\, \Psi_{31} \tag{4.4b}$$

and similarly for $\boldsymbol{F}(\boldsymbol{r}_2)$ and $\boldsymbol{F}(\boldsymbol{r}_3)$.

We use the variables Ψ_{ij} to emphasize that Ψ_{1j} is not the incident field on particle 1, since in this case particle 1 would have, for a fixed particle configuration, different incident fields depending on which particle j we are looking at, but rather the part of the total incident field that contributes to the pair-wise interaction force due to particle j. This reasoning can be generalized to N particle systems.

We will compare the full solution of the three-particle optical interactions with the pair-wise approximation, to see under which circumstances the pair-wise interaction approximation can be a suitable method to compute the dynamics of a system of several particles or, on the other hand, under which circumstances the many-body terms of the interaction have to be taken into account.

4.2 Three-particle interactions

In this Section we will use the simple case of a system formed by three identical particles to get an idea of the influence of many-particle interctions. Two different cases will be studied.

First, the three particles will be illuminated by a linearly polarized plane wave. We will study the three-particle and two-particle force on particle 3 when they are aligned parallel and perpendicular to the plane wave polarization. The force on the center of mass of the system of particles will also be analyzed.

Second, the three particles will be immersed in an optical vortex lattice. Again, three- and two-particle forces will be analyzed for particle 3, as well as the force exerted on the center of mass of the particle system.

The particles considered are, in all cases, described by an electric polarizability $\alpha \simeq (1.0+i2.0)\times 10^{-21}\mathrm{m}^3$ at an applied wavelength of $\lambda = 395\mathrm{nm}$ in water, which is close to the plasmon resonance of gold nanoparticles with radius $a = 50\mathrm{nm}$. This wavelength has been chosen to increase the relevance the effect of scattering forces against conservative forces in the optical vortex lattice setup, since the imaginary part of the polarizability is, approximately, twice as large as its real part.

4.2.1 Three particles illuminated by a plane wave

In this subsection we study the optical interaction forces in a system of three dipolar particles illuminated by a plane wave linearly polarized in the z-axis, propagating in the y-direction. We will analyze two different cases.

In the first one, the three particles will be aligned along the x-axis, perpendicular to the wave polarization. The x-component of the force on particle 3 due to two- and three-particle interactions is discussed. It is also studied the x-component of the force on the center of mass of the particle system. Particle 2 is set at the origin, and particle 1 at a position $x_1 = -x_{12}$, where x_{12} is the distance between particle 1 and 2, that will remain fixed.

Particle 3 will be displaced along the x-axis, a distance that will range from $x_{23}^{min} = 3a$ to $x_{23}^{max} = 1500$nm. The sketch of the configuration is shown in Figure 4.1a.

In the second case, the three particles will be aligned along the z-axis, parallel to the wave polarization. Now, the z-component of the force on particle 3 due to two- and three-particle interactions will be investigated, as well as the z-component of the force on the center of mass of the particle system. In this case, particle 2 is again set at the origin, particle 1 at a position $z_1 = -z_{12}$, where z_{12} is the distance between particle 1 and 2, that will remain fixed, and particle 3 will be displaced along the z-axis, in a distance range from $z_{23}^{min} = 3a$ to $z_{23}^{max} = 1500$nm. The sketch of the configuration is shown in Figure 4.1b.

These configurations have been chosen to simplify the analysis, since in both of them the selected components of the forces will only be due to optical interactions between the particles, and not to the applied electromagnetic field, since a sole particle would not experience any force along these directions.

First, the influence of three-particle interactions will be studied. To characterize this effect, the total force on particle 3 for each value of x_{23} and z_{23} will be calculated using the solution of the incident fields given by the CDA method. Then, the pair-wise force on particle 3 will be obtained using the Equation (4.2).

For the first configuration, described in Figure 4.1a, the results obtained for the x-component of the two- and three-particle force is depicted in Figure 4.2a. In this figure, two different values of x_{12} have been set, $x_{12} = 250$nm and $x_{12} = 320$nm. The three-particle force is more evident in the $x_{12} = 320$nm case. Specially for short distances ($x_{23} \sim \lambda$), an enhancement of the x-component of the force can be observed. In this figure and in all figures within this section, F_0 is an arbitrary unit defined as the x-component of the force exerted on particle 3 in this perpendicular configuration when $x_{12} = 320$nm and $x_{23} = 194$nm.

We can now analyze the sum of the forces on the ensemble of particles, to study the fulfillment of the third Newton's law. From a similar set up, it was concluded in the literature that two disimilar particles illuminated perpendicularly by a plane wave do not fulfill actio and reactio law, leading to a net linear momentum of the system of particles (Sukhov et al., 2015). The reason is that, since the polarizabilities of the particles are not equal, the radiation of the pair of particles will not be symmetric. Then some net linear momentum will be carried away by the electromagnetic

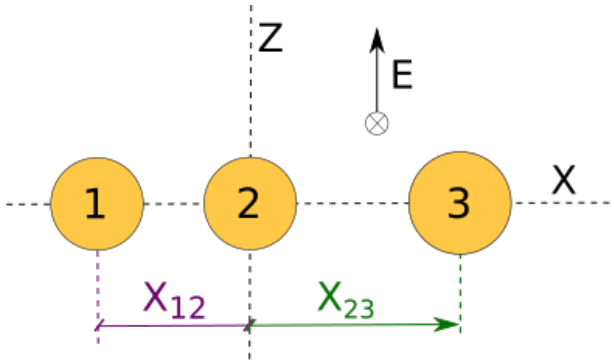

(A)

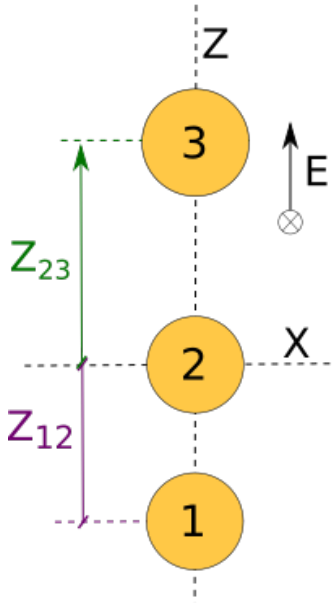

(B)

FIGURE 4.1: Sketch of the two different configurations used to study 2- and 3-particle forces. (A) Three NP aligned perpendicular to the plane wave polarization. Distance x_{12} is fixed. The x-component of the force on particle 3 is studied as a function of x_{23}. (B) Three NP aligned parallel to the plane wave polarization. Distance z_{12} is fixed. The z-component of the force on particle 3 is studied as a function of z_{23}. Electric field E is aligned along the z-direction.

field, resulting in a net linear momentum of the system of particles, guaranteeing the conservation of momentum of the particles-plus-field system.

Similarly, break of the actio and reactio law has been found in a dimer of similar particles diffusing through an optical lattice (Luis-Hita et al., 2016) leading to a trapping phenomenon mediated by the interactions. In this case both particles had the same polarizability, but now the applied fields on each of them were different, resulting again in a non-symetric scattering that enabled the electromagnetic field to carry away net linear momentum.

In this case, the three particles have identical polarizability, and all of them are illuminated by the same optical field. The difference is that the particle configuration is not symmetric in general, and then the resulting scattering along the x-axis is again non-symmetric. The results are shown in Figure 4.2b. It is seen that, for the specific cases in which $x_{12} = x_{23}$, the system of particles has again a symmetric configuration and actio and reactio law is recovered.

It is worth emphasizing that this effect is entirely a many-particle effect, since two identical particles perpendicularly illuminated by a plane wave would not break any symmetry of the system, and then the forces on both particles would be reciprocal, leading to a vanishing force on the center of mass of the particle system.

In the second configuration, described in Figure 4.1b, the results obtained for the z-component of the two- and three-particle force is depicted in Figure 4.3a. Similarly to the previous case, two different values of z_{12} have been set, $z_{12} = 250$nm and $z_{12} = 320$nm. In this case, very little effects of three-particle forces on the z-component of the force on particle 3 are observed.

However, in Figure 4.3b, it can be still notice a non-vanishing z-component of the force on the center of mass of the system of particles, pointing out that many-particle effects are still present in the dynamics of the system, as was argued in the prevoius configuration.

4.2.2 Three particles in an optical lattice

This system of plasmonic nanoparticles we are going to deal with will be subjected to the force field generated by two perpendicular standing electromagnetic waves, out-of-phase, in such a way that they produce a regular-spaced optical vortex lattice. The interaction of the particles with this electromagnetic field will provide the injection of external energy that is needed to produce a collective phenomenon.

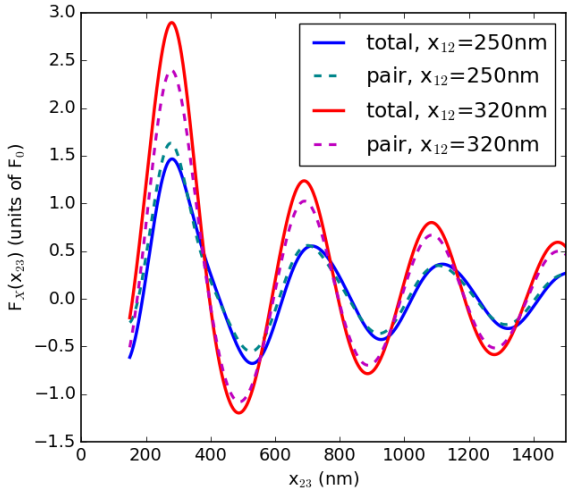

(A)

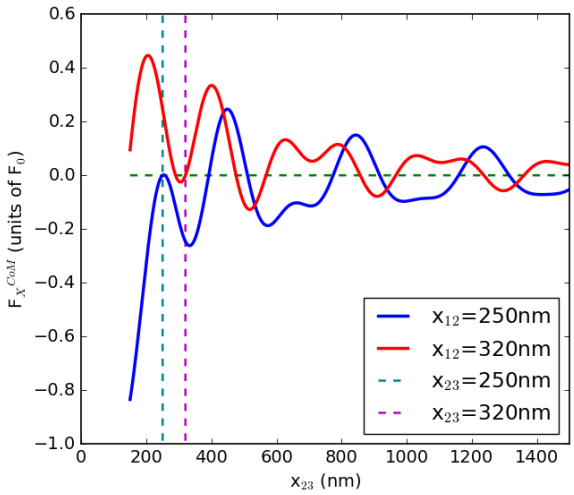

(B)

FIGURE 4.2: Forces along the x-axis when particles $1, 2, 3$ are aligned perpendicular to the plane wave polarization. (A) Comparision of 2- and 3-particle forces on particle 3. For short distances, three particle contribution becomes relevant. (B) x-component of the force on the center-of-mass of the system of particles. Reciprocity is recovered when the configuration becomes symmetric (dotted lines).

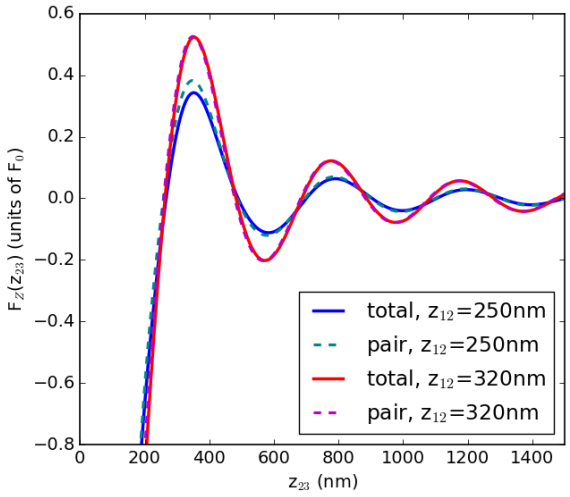

(A)

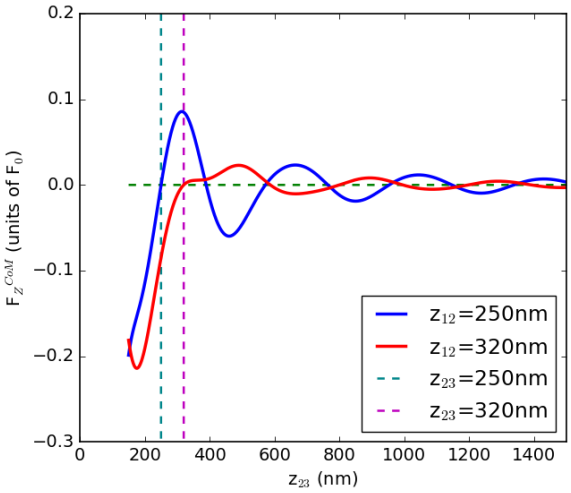

(B)

FIGURE 4.3: Forces along the z-axis when particles $1, 2, 3$ are aligned parallel to the plane wave polarization. (A) Comparision of 2- and 3-particle forces on particle 3. For this configuration, three particle contributions seem to be less relevant than in the previious case. (B) z-component of the force on the center-of-mass of the system of particles. Again, reciprocity is recovered when the configuration becomes symmetric (dotted lines).

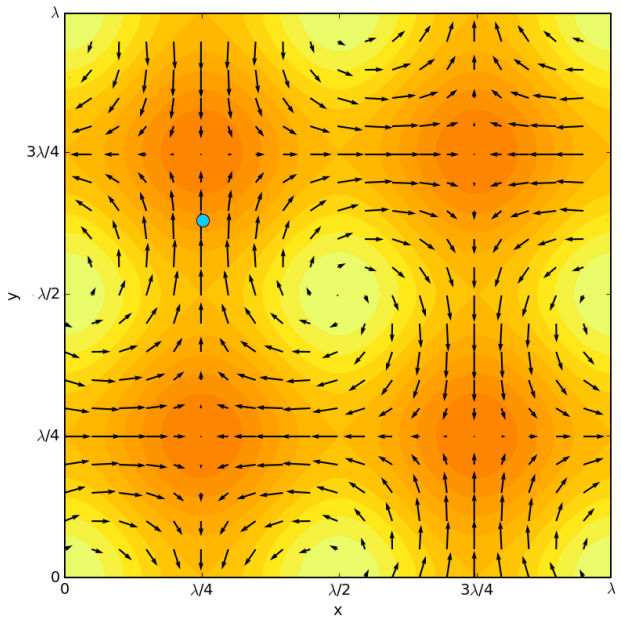

FIGURE 4.4: Diagram of the intensity of the electric field from Equation (4.5) (color map) and the vortex force field from Equation (4.6) (vector map). x and y coordinates are represented within the range $[0, \lambda)$. Darker colors correspond to higher intensities. The spot $(x, y) = (100, 250)$nm is marked in light blue.

The applied optical field is given by

$$\boldsymbol{E}^0(\boldsymbol{r}) = 2E_0\Big(-\sin ky + i\sin kx\Big)\hat{\boldsymbol{e}}_z \tag{4.5}$$

which is polarized in the z-direction. A sole particle immersed in this field would experience a force given by

$$\boldsymbol{F}(x,y) = 2\alpha'\frac{nI}{c}\nabla\Big(\sin^2 kx+\sin^2 ky\Big)+2\alpha''\frac{nI}{c}\nabla\times\Big[2\cos kx\,\cos ky\hat{\boldsymbol{e}}_z\Big] \tag{4.6}$$

where $k = 2\pi/\lambda$ is the wavenumber, c is the speed of light, n is the refractive index of water and I is the laser intensity.

To write this equation in this form, the identity

$$\frac{nI}{c} = \frac{\epsilon\epsilon_0}{2}|E_0|^2, \tag{4.7}$$

that relates two different forms of expressing the energy density u_E, has been used. The range of laser intensities considered in this work $I \sim 10^5\text{W/cm}^2$, can be achieved by focusing a 0.1W laser onto a $10\mu\text{m}\times 10\mu\text{m}$ region.

The intensity of the applied electric field described by Equation (4.5) and the vortex force map that would be exerted on a single particle described by Equation (4.6) is depicted in Figure 4.4. Darker colors correspond to higher intensities of the electric field. Both intensity and vortex forces have been represented in arbitrary units, just to give an idea of the structure of the system. Note that for each location (x, y) the electric field is constant along the z-axis, and then, there is no z-component of the force for a single particle.

The z-component of the force has been studied for a system of three particles lying on the same (x, y) vertical line. Particle 2 is located at $z_2 = 0$, particle 1 is located at a fixed position $z_1 = -z_{12}$, and particle 3 is displaced along the z-axis, from a minimum distance $z_{23}^{min} = 3a$ to a separation of several λ.

The results for the case $(x, y) = (100, 250)$nm are shown in Figure 4.5. Although for this particular configuration it can be seen in Figure 4.5a that the contribution of the three-particle force is only relevant when the three particles are close to each other, we see in Figure 4.5b that the z-component of the total force on the center of mass of the system of three particles does not vanish even when the particles are far away.

As in the previous subsection, it can be emphasize that this contribution is purely a many-particle interaction effect, since the polarizability

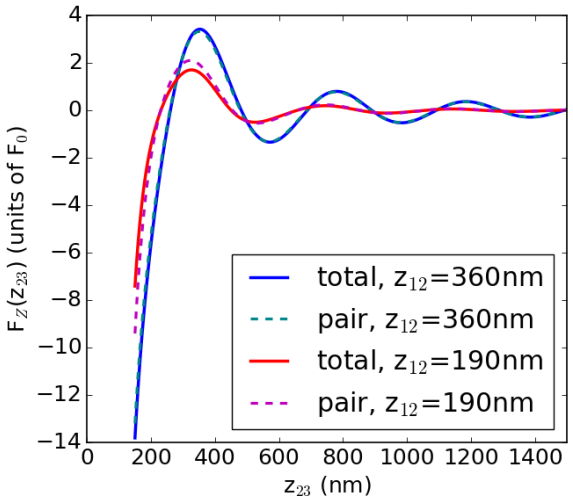

(A)

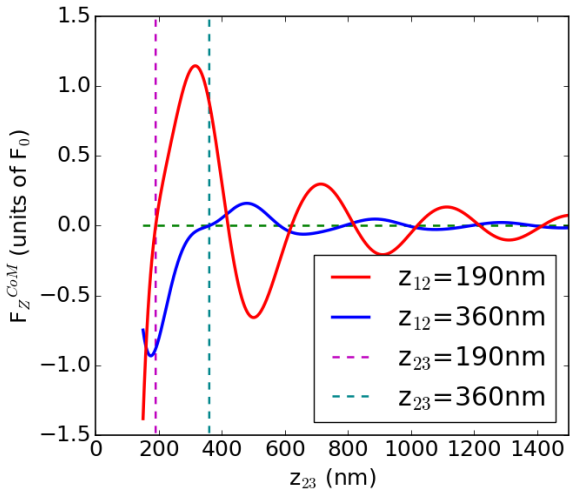

(B)

FIGURE 4.5: Forces along the z-axis when particles $1, 2, 3$ are located at $(x, y) = (100, 250)$nm. (A) Comparision of two- and three-particle forces on particle 3. It can be seen that, for this configuration, three particle contributions are almost negligible. (B) Sum of the z-component of the forces on particles $1, 2, 3$. Net forces are exerted on the center of mass of the system of three particles.

and applied electromagnetic field for every particle are identical. Then, the z-component of the pair-wise force on the center of mass of the system of particles would identically vanish.

The contribution of three-particle forces have not been depicted in the xy-plane since, except for very small separations, the forces produced by the optical vortex field are larger than the optical interaction forces between NPs. The behavior along the z-axis studied for $(x, y) = (100, 250)$nm is similar in any other point of the xy-plane, with the exception of the points analogous to $(x, y) = (\lambda/2, \lambda/2)$, where the z-component of the force vanishes.

4.3 Interplay between optical forces and hydrodynamics

Emergent phenomena in the scope of self-driven particles were modeled by Vicsek *et al.* (Vicsek et al., 1995). In this work, the authors proposed that collective behavior of an ensemble of particles requires individuality, connectivity and external injection of energy. On one hand, direct energy conversion is a characteristic feature of optical forces when applied to resonant nanoparticles. At resonance, scattering forces on nanoparticles are mainly associated to radiation pressure, which enables the system to take energy from the environment and convert it into direct motion of the particles. On the other hand, hydrodynamic interactions among these active nanoparticles show the kind of many-particle features that produces the required connectivity, being capable to provoke the emergent collective motion that is going to be the objective of this study.

In this section we present the study of one particular realization of these collective phenomena, within the field of optical forces in colloidal nanoparticles connected by hydrodynamic interactions, and will discuss specifically the role of the optical interaction between the nanoparticles in the system. This work has been done in collaboration with Prof. Rafael Delgado-Buscalioni and Dr. Marc Meléndez, from the Department of Theoretical Condensed Matter Physics at Universidad Autónoma de Madrid, who implemented the Brownian hydrodynamic interactions and carried out the numerical simulations and analysis. A detailed discussion on the statistical and hydrodynamic aspects of this study can be found in Reference (Delgado-Buscalioni et al., 2017).

In the numerical simulations of the system formed by the fluid and the ensemble of particles, optofluidic dynamics were numerically solved. The robustness of the results were verified by considering two different

geometries and two different techniques to handle with hydrodynamic interactions.

The first geometry consists in relatively large periodic domains ($L \in [8, 32)\lambda$). In order to mimic the bulk region of a large closed box, the total momentum in the system was imposed to be zero, so any mean current in the system induces flow reversal. In this periodic system, only the vortex force field, described by Equation (4.6), and hydrodynamic interactions were considered. Hydrodynamics were solved using the Fluctuating Immersed Boundary method (Balboa Usabiaga et al., 2014).

In the second geometry, particles move in a cubic box of size $L = 7.9\lambda$ modeled by a local-acting potential that mimics a laser trap confinement. Fluid is supposed to move freely without noticing the walls of the box. For this configuration, both hydrodynamics and full optical interactions are solved. To handle with the hydrodynamic part, Brownian Hydrodynamics were implemented in an infinite domain (Öttinger, 1996).

The system is similar to the vortex lattice system described in the previous section. A number N of gold nanoparticles, $a = 50$nm radius, are immersed in water and subject to the electric field formed by two perpendicular standing waves in the xy-plane, described by Equation (4.5), which produces an optical force field given by Equation (4.6).

The particles will interact via hydrodynamics. This hydrodynamic interaction will provide the kind of many-particle interaction that is needed to generate a collective phenomenon. The flow-field around a moving particle will affect the motion of the others, weakly coupling together the motion of every particle in the system. Then, the velocity of a certain particle now becomes a collective variable that influences its surroundings with an interction decaying as R^{-1}.

We consider a volume V of water at $T = 300$K filled with a number N of gold nanoparticles of radius $a = 50$nm at quite small volume fraction $\phi \sim 10^{-4}$, with $\phi = Nv_p/V$ and $v_p = 4\pi a^3/3$.

The power of the laser radiation is quantified by the non-dimensional quantity $u = U/k_BT$, being U the laser energy per particle given by the laser energy density and the particle's polarizability. If $u = 0$ then for large values of time t, the MSD of a tracer particle is proportional to t. However, as u becomes different from zero, the MSD becomes proportional to $t^{1+\beta}$, being β an exponent which equals zero for normal diffusion and gets close to 1 for superdiffusion.

The transition from incoherent motion to synchronized displacement shows up in the abrupt change β, signaling a dynamic transition from the

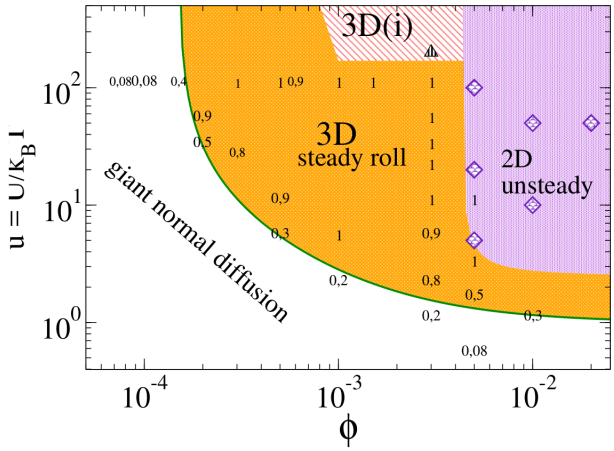

FIGURE 4.6: From (Delgado-Buscalioni et al., 2017). Dynamic phase diagram showing the β values in the non-dimensional laser energy u and volume fraction ϕ chart. NPs hydrodynamically interact and are driven by the primary force of the optical vortex lattice in Equation (4.6) in a periodic domain. Secondary forces were not taken into account. The critical line corresponds to the relation $\xi \equiv (u_{cr} - u^*)(\phi_{cr} - \phi^*)$. Below the threshold values no transition was observed. Shaded areas are explained in the main text.

optically enhanced normal diffusion to a collectively triggered superdiffusion with $\beta > 0$. A slight increase above the critical values of power u_{cr} and volume fraction ϕ_{cr} induces a drastic jump in the diffusion exponent towards the ballistic value $\beta = 1$.

Figure 4.6 illustrates the transition in the $u - \phi$-chart. Consistent with a critical phenomenon, the critical energy and volume fraction lie on the hyperbola $\xi_{cr} = (u_{cr} - u^*)(\phi_{cr} - \phi^*)$ being $\xi_{cr} = (1.55 \pm 0.05) \times 10^{-4}$ and the threshold values $\phi^* = (1.5 \pm 0.1) \times 10^{-4}$ and $u^* = 1.0$, respectively. In this Figure, several coherent dynamics can be found. In (3D) a steady convection roll occupies the whole box in z-direction, and the vorticity points along one of the diagonals of the optical plane. In (3Di) at large u this (3D) flow becomes intermittent with sudden stops. In (2D) at large ϕ NPs order in 2D vortical structures circulating in the optical plane, with vorticity along the z-direction.

During the whole analysis, the phenomenon of cavitation has been discarded. However, in recient years the heating of plasmon nanoparticles due to laser illumination has been deeply studied (Govorov et al., 2007; Baffou et al., 2010; Baffou et al., 2013). Since this heating is closely related to the dynamics of the cloud of electrons within the metal nanoparticle, the phenomenon turns out to be specially significant when the light wavelength is near the Surface Plasmon Resonance.

To estimate this heating, several works describe a model based on the heat equation. According to the work by (Baffou et al., 2013), the temperature increase for a spherical metal nanoparticle under continuous illumination is

$$\delta T = \frac{\sigma_{abs} I}{4\pi \kappa_s \, a} \tag{4.8}$$

being σ_abs the absorption cross section, I the laser intensity, κ_s the thermal conductivity of the surrounding medium and a the particle's radius. For the gold nanoparticle surrounded by water we are considering, Equation (4.8) would result in a temperature increase of $\delta T = 36$K at the particle's surface, significantly below the boiling point of water.

Even though we may claim that the phenomenon of cavitation is prevented for the range of laser intensities considered, it is not easy to foresee the effects of hot-diffusion on the present dynamics.

4.3.1 Optical interactions among particles

On the second geometry (confined setup) the particles will also interact optically. To simulate the interaction, I have implemented a specific module compute the optical forces between the nanoparticles. The incident

electric fields on every nanoparticle were computed using the Coupled Dipole Approximation.

For a system of $3N$ particles, this requires the solution of a system of $3N$ equations, which is performed with a LU decomposition algorithm. The accuracy of the solution of the MSP can be tested by checking the fulfillment of the condition

$$\sigma_{ext} = \sigma_{abs} + \sigma_{sca}, \tag{4.9}$$

where the cross sections are not the cross sections of a single particle but the cross sections of the system of N particles, given by Equations (2.16a), (2.16b), (2.16c), seen in Chapter 2. Once the fields and their derivatives have been computed, Equation (2.32) can be applied to obtain the optical forces.

To check if optical interactions are capable to alter, delay or impede the collective dynamics trigged by hydrodynamic interactions, extensive Brownian dynamics simulations have been performed. In these simulations four cases have been investigated: with and without hydrodynamics and with and without optical interactions. The vortex force field generated by the external applied light is always present. The study has been carried out using boundary conditions corresponding to a confined setup made of a cubic box of side $L = 7.9\lambda$.

We prevent nanoparticles from overlapping by the addition of exclude volume forces, which were modeled with the repulsive part of the Lennard-Jones potential. The hydrodynamic particle radius were chosen to be $a_h = 100$nm, indeed larger than the gold nanoparticle radius. This enlarged hydrodynamic radius guarantees that the dipole approximation condition $R > 3a$, being R the distance between particles, is fulfilled at any simulation step.

To analyze the onset of collective motion in the confined setup we measure, in the xy-plane, the MSD of the center of mass of the particle ensemble. Although at long enough times the MSD saturates to a fraction of the squared box size L^2, at intermediate times the effective collective diffusion coefficient may be calculated as

$$D_{cm} = \frac{1}{4t}\left\langle \left(\boldsymbol{r}''_{cm}(t+t_0) - \boldsymbol{r}''_{cm}(t_0) \right)^2 \right\rangle \tag{4.10}$$

with

$$\boldsymbol{r}''_{cm} = \frac{1}{N}\sum_{i=1}^{N} \Big(x_i, y_i \Big). \tag{4.11}$$

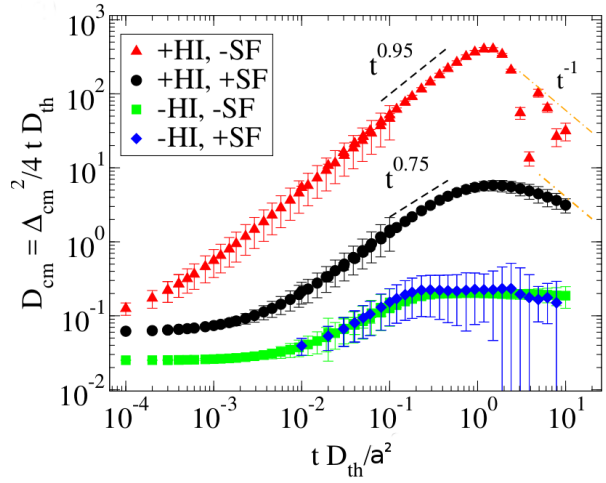

(A)

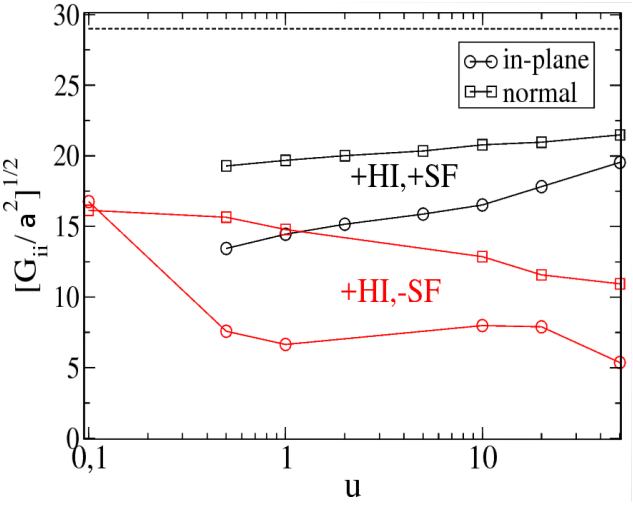

(B)

FIGURE 4.7: From (Delgado-Buscalioni et al., 2017). $\pm HI$ stands for with (without) hydrodynamic interactions. $\pm SF$ stands for with (without) optical interactions. (A) The center-of-mass diffusion coefficient D_{cm} from the (in-plane) MSD and scaled to the NP thermal diffusion coefficient D_{th}. The parameter values are $u = 1$, $\phi = 2 \times 10^{-3}$. (B) Gyration radius in the optical plane defined by the xy-plane, and in the normal direction defined by the z-axis.

This collective effective diffuson coefficient also reveals a transition from normal diffusion to superdiffusive motion $D_{cm}(t) \sim t^{\beta}$, with $\beta > 0$. The results have been depicted in Figure 4.7a for the different conditions assumed during the simulations. We can observe in the plot that, in absence of hydrodynamic interactions, the diffusion is enhanced with and without optical interactions, but no transition to a superdiffusive behaviour is found, since β remains equal to cero. This can be explained as the effect of the optical vortex force field applied to the particles, as is discussed in Reference (Albaladejo et al., 2009a), where an enhancement of the diffusion of a single particle was found.

On the other hand, hydrodynamic interactions do produce a transition to superdiffusive dynamics. We observe that this transition remains when optical interactions are taken into account, neither impeding nor delaying the collective dynamics. However, they do alter the collective motion. It can be noticed that the value of β is now modified, leading to a quantitative and qualitative difference in the effective diffusion constant.

When restricting the system to be in a cubic box of size $L = 7.9\lambda$, it is found that, in the absence of optical interactions among particles, the critical parameter ξ_{cr} is about four times larger than the one obtained for the periodic domain. However, this value does not change when optical interactions are taken into account, the critical control parameter $\xi_{cr} = (6 \pm 1) \times 10^{-4}$ has the same value than in the case with no optical interactions. In this respect, optical interactions do not alter the location of the transition. This backs the interpretation of the phase transition as a hydrodynamically-driven transition. The threshold energy u^* and volume fraction ϕ^* are in the same range as those found for periodic domains.

For the ensemble of particles, we can define a parameter which accounts for the mean squared distance between the nanoparticles' position and the position of the center of mass of the set of particles, known as the gyration radius

$$G_{\alpha,\alpha} = \frac{1}{N} \sum_{i=1}^{N} \left(r_i^{(\alpha)} - r_{cm}^{(\alpha)} \right)^2 \tag{4.12}$$

where α is a given direction x, y, z. The gyration radius gives idea of how dense or compact is the ensemble of particles.

When two NPs do not lie on the same xy-plane optical interactions appear in the z-direction. This interaction oscillates due to the e^{ikR} factor of the Green function for the electric field (see Appendix A), creating attractive and repulsive regions. Thus, optical interactions produce binding positions along the z-direction.

This effect effect can be seen in the gyration radius in the z-axis, depicted in Figure 4.7b. It can be noticed that optical interactions increase $G_{z,z}$, and also $G_{x,x}$ and $G_{y,y}$, which intuitively means that the ensemble of particles is now less compact, being expanded in all directions. This makes difficult the compresion of the swarm of particles, and points out that, when considering a confined geometry, the center of mass of the ensemble of NPs has less free space to move.

4.4 Conclusions

Two main conclusions can be extracted from the work of this chapter:

- Many-particle optical interactions are able to produce effects not predicted by pair-wise interactions, such as a net force on the center-of-mass of a system of nanoparticles, that may be responsible for some of the collective effects discussed in this chapter. The exact significance of many-particle optical interactions is object of further investigation.
- Hydrodynamics and optical forces from the vortex lattice are needed ingredients to trigger the observed dynamical phase transition. Optical interactions do not impede nor delay the mentioned phase transitions. the effect of optical interactions is to modify the diffusion properties and to provide certain structure to the ensemble of nanoparticles.

Chapter 5

Dipolar interactions in random electromagnetic fields

Forces due to random light illumination are being extensively studied during the last years, either concerning the dynamics of a sole particle (Zurita-Sánchez et al., 2004; Marqués, 2016) or pairs of particles under certain gauges (Brügger et al., 2015; Sukhov et al., 2013). They belong to the family of dispersion forces, which have shown to have remarkable applications in interdisciplinary topics as important as biology, chemistry or colloidal sciences, where it finds applications in the study of interaction between molecules (Thirunamachandran, 1980; McLachlan, 1963) or extended objects of spheroidal shape (Stiles, 1979; Schiller et al., 2011).

In this Chapter, we will study the case of two dipolar spherical particles separated along the z-axis and illuminated by an homogeneous and isotropic random electromagnetic field with wavelength λ. First, we study the case without absorption, for which we obtain the behavior of the interaction at short center-to-center interparticle distance. It is claim in the literature that, by assuming the imaginary part of the polarizability to be negligible, a R^{-2} gravitational-like interaction between the two objects can be obtained for separations much smaller than the applied wavelength $R \ll \lambda$. It was first proposed by (Thirunamachandran, 1980) in the study of the interaction between two molecules, and also proposed by (O'Dell et al., 2000) to study the interaction between atoms in a Bose-Einstein condensate illuminated by an extremely off-resonance electromagnetic field. It was also suggested within the field of optical interaction between nanoparticles (Sukhov et al., 2013).

We will discuss in detail the interaction between two dipolar NP under random light illumination (RLI) in the case of particles with no absorption. It will be shown that, out of the Frohlich Resonance Condition (FRC), for a physical model for the electric permittivity, it is not possible to get rid

of the contributions from the imaginary part of the polarizability. Then, in the short distance limit, they will be responsible of a departure from the expected gravity-like behavior.

The previous works on interactions due to RLI focused in the specific case of particles without absorption, putting aside the problem of the interaction between two absorbing particles. Then, we will study the interaction force between the two particles when absorption is taken into account. We introduce absorption by choosing non-vanishing values of the damping coefficient Γ_0 in a Lorentz model for electric permittivity, and obtain a new analytical expression for the interaction force for arbitrary values of absorption.

5.1 Electric fields and optical forces

The system of field equations for particle A and B is given by

$$\boldsymbol{E}(\boldsymbol{r}_A) = \boldsymbol{E}_0(\boldsymbol{r}_A) + k^2 G(\boldsymbol{r}_A, \boldsymbol{r}_B)\alpha \boldsymbol{E}(\boldsymbol{r}_B) \tag{5.1a}$$

$$\boldsymbol{E}(\boldsymbol{r}_B) = \boldsymbol{E}_0(\boldsymbol{r}_B) + k^2 G(\boldsymbol{r}_B, \boldsymbol{r}_A)\alpha \boldsymbol{E}(\boldsymbol{r}_A) \tag{5.1b}$$

being $\boldsymbol{E}(\boldsymbol{r}_{A,B})$ the incident fields on particles A, B, $\boldsymbol{E}_0(\boldsymbol{r}_{A,B})$ the applied fields on particles A, B, α the polarizability of the particles, k the wavenumber and $G(\boldsymbol{r}_A, \boldsymbol{r}_B) = G(\boldsymbol{r}_B, \boldsymbol{r}_A)$ the Green dyadic function of the electric field.

We can rewrite this equations in a more compact form

$$\boldsymbol{\psi}_B = \boldsymbol{\psi}_B^0 + G_{BA} T_A \boldsymbol{\psi}_A \tag{5.2a}$$

$$\boldsymbol{\psi}_A = \boldsymbol{\psi}_A^0 + G_{AB} T_B \boldsymbol{\psi}_B \tag{5.2b}$$

where $\boldsymbol{\psi}_{A,B}$ plays the role of $\boldsymbol{E}(\boldsymbol{r}_{A,B})$, $\boldsymbol{E}_0(\boldsymbol{r}_{A,B})$ is substituted by $\boldsymbol{\psi}_{A,B}^0$ and G_{AB} represents $G(\boldsymbol{r}_A, \boldsymbol{r}_B)$. The matrices $T_{A,B}$ are defined as

$$T_{A,B} = k^2 \begin{bmatrix} \alpha_{A,B} & 0 & 0 \\ 0 & \alpha_{A,B} & 0 \\ 0 & 0 & \alpha_{A,B} \end{bmatrix} \tag{5.3}$$

since we are dealing with spherical particles with diagonal polarizability tensor. The reason of this change in nomenclature is that it will be easier to track the indices A, B that accounts for the particles.

The solutions to these system of equations are

$$T_A\boldsymbol{\psi}_A = A^{-1}\Big(\boldsymbol{\psi}_A^0 + G_{AB}T_B\boldsymbol{\psi}_B^0\Big) \tag{5.4a}$$

$$T_B\boldsymbol{\psi}_B = B^{-1}\Big(\boldsymbol{\psi}_B^0 + G_{BA}T_A\boldsymbol{\psi}_A^0\Big) \tag{5.4b}$$

where we have defined the matrices

$$A = T_A^{-1} - G_{AB}T_B\mathbb{G}_{BA} \tag{5.5a}$$

$$B = T_B^{-1} - G_{BA}T_A\mathbb{G}_{AB} \tag{5.5b}$$

The derivatives of the fields are

$$\partial_{z_A}\boldsymbol{\psi}_A = \partial_{z_A}\boldsymbol{\psi}_A^0 + \Big[\partial_{z_A}G_{AB}\Big]B^{-1}\Big(\boldsymbol{\psi}_B^0 + G_{BA}T_A\boldsymbol{\psi}_A^0\Big) \tag{5.6a}$$

$$\partial_{z_B}\boldsymbol{\psi}_B = \partial_{z_B}\boldsymbol{\psi}_B^0 + \Big[\partial_{z_B}G_{BA}\Big]A^{-1}\Big(\boldsymbol{\psi}_A^0 + G_{AB}T_B\boldsymbol{\psi}_B^0\Big) \tag{5.6b}$$

As it has been seen in the introduction, the field-field correlations are (Setälä et al., 2003)

$$\Big\langle \boldsymbol{\psi}_B^{0*} \otimes \boldsymbol{\psi}_A^0 \Big\rangle = \frac{4\pi}{\epsilon\epsilon_0 k} u_E(\omega)\,\mathrm{Im}\Big\{G_{BA}\Big\} \tag{5.7a}$$

$$\Big\langle [\partial_{z_B}\boldsymbol{\psi}_B^{0*}] \otimes \boldsymbol{\psi}_A^0 \Big\rangle = \frac{4\pi}{\epsilon\epsilon_0 k} u_E(\omega)\,\mathrm{Im}\Big\{\partial_{z_B}G_{BA}\Big\} \tag{5.7b}$$

where $u_E(\omega)$ is the electromagnetic energy density and, for arbitrary matrices C, D,

$$\begin{aligned}\Big\langle \boldsymbol{\psi}_B^{0*} C\cdot D\boldsymbol{\psi}_A^0 \Big\rangle &= \frac{8\pi^2}{\epsilon\epsilon_0 k}\,\mathrm{Tr}\Big[CD\,\mathrm{Im}\Big\{G_{BA}\Big\}\Big] \\ &= \frac{8\pi^2}{\epsilon\epsilon_0 k}\,\mathrm{Tr}\Big[D\,\mathrm{Im}\Big\{G_{BA}\Big\}C\Big] = \frac{8\pi^2}{\epsilon\epsilon_0 k}\,\mathrm{Tr}\Big[\,\mathrm{Im}\Big\{G_{BA}\Big\}CD\Big]\end{aligned} \tag{5.8}$$

The time-averaged z-component of optical force on particle B can be expressed as

$$\langle F_B^z\rangle = \frac{\epsilon\epsilon_0}{2}\Big\langle\,\mathrm{Re}\Big\{\boldsymbol{\psi}_B^t\alpha^t\cdot\partial_{z_B}\boldsymbol{\psi}_B^*\Big\}\Big\rangle. \tag{5.9}$$

It can be checked numerically that the x- and y-components of the force will be zero. This is in agreement with symmetry considerations, since due to the isotropy of the random electromagnetic field, the only axis that

can be defined without ambiguity is the z-axis (the axis the particles are separated along). This kind of symmetry considerations will be used again when we discuss the conservativity of the interactions due to RLI.

It can be rewritten explicitly as

$$\begin{aligned}
\langle F_B^z \rangle &= \frac{\epsilon\epsilon_0}{2\,k^2} \left\langle \mathrm{Re}\left\{ \boldsymbol{\psi}_B^t T_B^t \cdot \partial_{z_B} \boldsymbol{\psi}_B^* \right\} \right\rangle \\
&= \frac{\epsilon\epsilon_0}{2\,k^2} \left\langle \mathrm{Re}\left\{ \left(\boldsymbol{\psi}_B^{0t} + \boldsymbol{\psi}_A^{0t} T_A^t G_{BA}^t \right) B^{-1t} \right.\right. \\
&\qquad \left.\left. \cdot \left(\partial_{z_B} \boldsymbol{\psi}_B^{0*} + \left[\partial_{z_B} G_{BA}^* \right] A^{-1*} \boldsymbol{\psi}_A^{0*} + \left[\partial_{z_B} G_{BA}^* \right] A^{-1*} G_{AB}^* T_B^* \boldsymbol{\psi}_B^{0*} \right) \right\} \right\rangle \\
&= \frac{\epsilon\epsilon_0}{2\,k^2} \left\langle \mathrm{Re}\left\{ \left(\boldsymbol{\psi}_B^{0t} + \boldsymbol{\psi}_A^{0t} T_A G_{AB} \right) B^{-1} \right.\right. \\
&\qquad \left.\left. \cdot \left(\partial_{z_B} \boldsymbol{\psi}_B^{0*} + \left[\partial_{z_B} G_{BA}^* \right] A^{-1*} \boldsymbol{\psi}_A^{0*} + \left[\partial_{z_B} G_{BA}^* \right] A^{-1*} G_{AB}^* T_B^* \boldsymbol{\psi}_B^{0*} \right) \right\} \right\rangle.
\end{aligned}$$

Since, in our case, G_{AB} and $T_{A,B}$ are symmetric matrices, the matrices A, B, A^{-1} and B^{-1} will be symmetric as well.

For the sake of simplicity, we decompose the force into $\langle F_B^z \rangle = F_1 + F_2$, being

$$F_1 = \frac{\epsilon\epsilon_0}{2k^2} \mathrm{Re}\left\{ \left\langle \left(\boldsymbol{\psi}_B^{0t} + \boldsymbol{\psi}_A^{0t} T_A G_{AB} \right) B^{-1} \cdot \partial_{z_B} \boldsymbol{\psi}_B^{0*} \right\rangle \right\} \tag{5.10}$$

and

$$\begin{aligned}
F_2 = \frac{\epsilon\epsilon_0}{2k^2} \mathrm{Re}\left\{ \left\langle \left(\boldsymbol{\psi}_B^{0t} + \boldsymbol{\psi}_A^{0t} T_A G_{AB} \right) B^{-1} \right.\right. \\
\left.\left. \cdot \left(\left[\partial_{z_B} G_{BA}^* \right] A^{-1*} \boldsymbol{\psi}_A^{0*} + \left[\partial_{z_B} G_{BA}^* \right] A^{-1*} G_{AB}^* T_B^* \boldsymbol{\psi}_B^{0*} \right) \right\rangle \right\}
\end{aligned} \tag{5.11}$$

The first part is calculated as follows

$$\begin{aligned}
F_1 &= \frac{2\pi u_E(\omega)}{k^3} \mathrm{Tr}\left[\mathrm{Im}\left\{ \partial_{z_B} G_{BB} \right\} \mathrm{Re}\left\{ B^{-1} \right\} \right. \\
&\qquad \left. + \mathrm{Im}\left\{ \partial_{z_B} G_{BA} \right\} \mathrm{Re}\left\{ T_A G_{AB} B^{-1} \right\} \right] \\
&= \frac{2\pi u_E(\omega)}{k^3} \mathrm{Tr}\left[\mathrm{Im}\left\{ \partial_{z_B} G_{BA} \right\} \mathrm{Re}\left\{ T_A G_{AB} B^{-1} \right\} \right]
\end{aligned} \tag{5.12}$$

because, as we see in Appendix A,

$$\mathrm{Im}\left\{ \partial_{z_B} G_{BB} \right\} = \mathbf{0} \tag{5.13}$$

And the second term is obtained as

$$F_2 = \frac{2\pi u_E(\omega)}{k^3}\,\mathrm{Re}\Big\{\,\mathrm{Tr}\Big[[\partial_{z_B} G^*_{BA}]A^{-1*}\Big(\,\mathrm{Im}\{G_{AB}\} + \mathrm{Im}\{G_{AA}\}T_A G_{AB} + G^*_{AB}T^*_B\,\mathrm{Im}\{G_{BB}\} + G^*_{AB}T^*_B\,\mathrm{Im}\{G_{BA}\}T_A G_{AB}\Big)B^{-1}\Big]\Big\} \tag{5.14}$$

Notice that no approximations have been made so far, but the dipolar approximation. Neither weak scattering nor lack of absorption have been assumed, and the polarizability may have whatever real and imaginary values.

5.2 The nonabsorbing case

If we are in a non-absorbing scenario, we can use the relation

$$\mathrm{Im}\left\{T_A^{-1}\right\} = \frac{1}{i2}\left(T_A^{-1} - T_A^{-1*}\right) = -\,\mathrm{Im}\left\{G_{AA}\right\} \tag{5.15}$$

to simplify the expression of the optical force F_2 obtained above. From Equation (5.14) we get

$$\begin{aligned} F_2 = \frac{2\pi u_E(\omega)}{k^3}\,\mathrm{Re}\Big\{\,\mathrm{Tr}\Big[[\partial_{z_B} G^*_{BA}]A^{-1*}\Big(\,&\mathrm{Im}\{G_{AB}\} \\ &- \mathrm{Im}\left\{T_A^{-1}\right\}T_A G_{AB} - G^*_{AB}T^*_B\,\mathrm{Im}\left\{T_B^{-1}\right\} \\ &+ G^*_{AB}T^*_B\,\mathrm{Im}\{G_{BA}\}T_A G_{AB}\Big)B^{-1}\Big]\Big\} \end{aligned} \tag{5.16}$$

And then

$$\begin{aligned} F_2 &= \frac{2\pi u_E(\omega)}{k^3}\,\mathrm{Re}\Big\{\,\mathrm{Tr}\Big[[\partial_{z_B} G^*_{BA}]A^{-1*}\Big(\frac{1}{i2}\Big(G_{AB} - G^*_{AB}\Big) \\ &\quad - \frac{1}{i2}\Big(T_A^{-1} - T_A^{-1*}\Big)T_A G_{AB} - \frac{1}{i2}G^*_{AB}T^*_B\Big(T_B^{-1} - T_B^{-1*}\Big) \\ &\quad + \frac{1}{i2}G^*_{AB}T^*_B\Big(G_{BA} - G^*_{BA}\Big)T_A G_{AB}\Big)B^{-1}\Big]\Big\} \\ &= \frac{2\pi u_E(\omega)}{k^3}\,\mathrm{Re}\Big\{\,\mathrm{Tr}\Big[[\partial_{z_B} G^*_{BA}]A^{-1*}\frac{1}{i2}\Big(A^*\,T_A G_{AB} - G^*_{AB}T^*_B B\Big)B^{-1}\Big]\Big\} \\ &= \frac{2\pi u_E(\omega)}{k^3}\,\mathrm{Re}\Big\{\,\mathrm{Tr}\Big[[\partial_{z_B} G^*_{BA}]\frac{1}{i2}\Big(T_A G_{AB}B^{-1} - A^{-1*}G^*_{AB}T^*_B\Big)\Big]\Big\} \end{aligned} \tag{5.17}$$

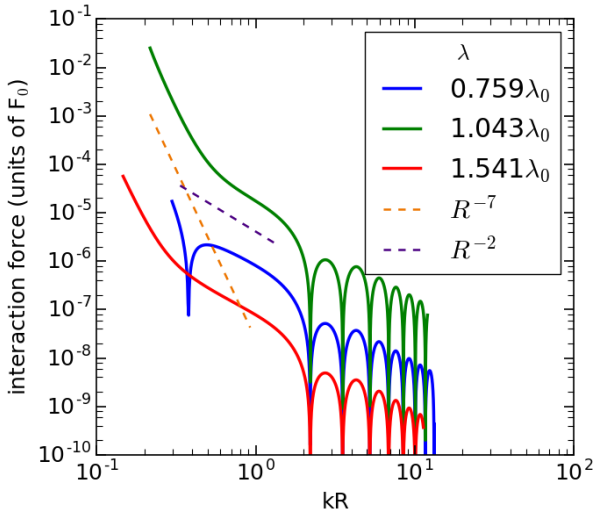

(A)

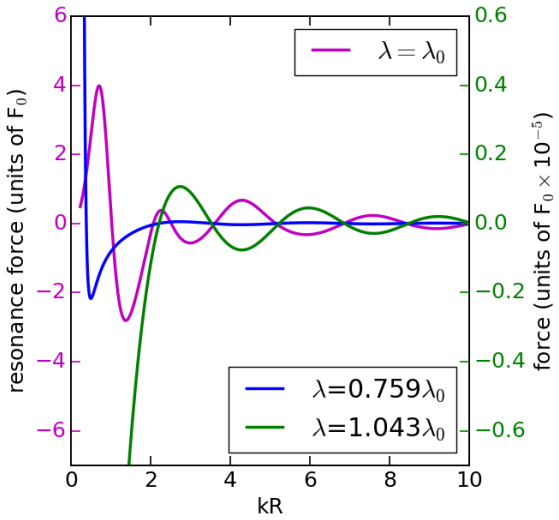

(B)

FIGURE 5.1: (A) Optical forces in logarithmic scale for an absorptionless Lorentz model particle around the FRC. It can be seen that there is a range for which $F(R) \sim R^{-2}$, but at short distances it is not possible to get rid of the term R^{-7}. (B) The interaction force at resonance shows a behavior $F_{\lambda_0}(R) \sim R^2$ when $R \to 0$. For $\lambda < \lambda_0$ ($\lambda > \lambda_0$) the force is repulsive (attractive) and shows an exponential growth at $R \to 3a$. Blue and green lines correspond to the right axis.

But, as it was stated in Chapter 2,

$$T_A G_{AB} B^{-1} = A^{-1} G_{AB} T_B \tag{5.18}$$

And then the second term of the force can be expressed as

$$\begin{aligned} F_2 &= \frac{2\pi u_E(\omega)}{k^3} \operatorname{Tr}\left[\operatorname{Re}\left\{\partial_{z_B} G^*_{BA}\right\} \operatorname{Im}\left\{T_A G_{AB} B^{-1}\right\}\right] \\ &= \frac{2\pi u_E(\omega)}{k^3} \operatorname{Tr}\left[\operatorname{Re}\left\{\partial_{z_B} G_{BA}\right\} \operatorname{Im}\left\{T_A G_{AB} B^{-1}\right\}\right] \end{aligned} \tag{5.19}$$

Finally, the z-component of force on particle B due to the interaction with particle A in absence of absorption under RLI is given by

$$\begin{aligned} \langle F^z_B \rangle &= \frac{2\pi u_E(\omega)}{k^3} \Big[\operatorname{Tr}\left[\operatorname{Im}\left\{\partial_{z_B} G_{BA}\right\} \operatorname{Re}\left\{T_A G_{AB} B^{-1}\right\}\right] \\ &\qquad + \operatorname{Tr}\left[\operatorname{Re}\left\{\partial_{z_B} G_{BA}\right\} \operatorname{Im}\left\{T_A G_{AB} B^{-1}\right\}\right]\Big] \\ &= \frac{2\pi u_E(\omega)}{k^3} \operatorname{Im}\left\{\operatorname{Tr}\left[[\partial_{z_B} G_{BA}] T_A G_{AB} B^{-1}\right]\right\} \end{aligned} \tag{5.20}$$

In this expression, we have not supposed weak scattering nor negligible imaginary part of the polarizability. Within the dipolar approximation, this equation of the force is valid for every value of the wavelength and every interparticle separation. In the literature, it is found that for a vanishing value of the imaginary part of the polarizability, the interaction force behaves at short distances as an inverse square force. This is because the terms that behaves as $(kR)^{-5}$, $(kR)^{-7}$ depend on α''.

But in a physical model for the electric polarizability, α'' cannot be identically zero. It can be as small as we want, but paying the price of using larger and larger wavelengths. Increasing the wavelength also reduces the wavenumber, and then the terms $(kR)^{-5}$, $(kR)^{-7}$ become more and more relevant. Then, there is a competition between reducing α'' and increasing the contribution of $(kR)^{-5}$, $(kR)^{-7}$ for a fixed interparticle separation.

In Figure 5.1a the interaction force between two dipolar particles with a polarizability described by a Lorentz model is depicted. The parameters that have been used are particle radius $a = 0.01186\,\lambda_0$, $\epsilon_\infty = 1.0$, $\epsilon_S = 2.9$, $\omega_0 = 0.7824\,\omega^*$, $\Gamma_0 = 0$. Being $\epsilon_0 = 1.0$ the permittivity of vacuum, λ_0 the wavelength for which $\alpha' = 0$, and $\omega^* = hc/\lambda_0$. The arbitrary value of F_0 has been set to $F_0 = 10^{-12}$N.

We can see in this graph that the $F \sim R^{-2}$ regime survives only up to a certain interparticle separation. For shorter distances, α'' is no longer

small enough to keep the gravitational-like behavior, and the terms $(kR)^{-5}$, $(kR)^{-7}$ begin to dominate the interaction. For two nonabsorbing particles, with a physical model of polarizability, we cannot then obtain a inverse square interaction at short distances. The inverse square interaction is achievable only in an intermediate range of interparticle separations.

In Figure 5.1b we show the interaction force at resonance wavelength λ_0, at a wavelength below λ_0 and at a wavelength above λ_0. It can be seen that, in the resonant case, the optical interaction is always oscillatory. For wavelengths below λ_0 the interaction is repulsive at short distances, while for wavelengths above λ_0 the interaction at short distances has an attractive behavior.

5.2.1 The $kR \to \infty$ limit (no absorption)

Let us write the Green dyadic function as

$$\mathbb{G}_{AB} = g_1 \mathbb{I} + g_2 \frac{\boldsymbol{R} \otimes \boldsymbol{R}}{R^2} \tag{5.21}$$

$$= \begin{bmatrix} g1 & & \\ & g_1 & \\ & & g_1 + g_2 (z_B - z_A)^2 / R^2 \end{bmatrix} \tag{5.22}$$

$$= \begin{bmatrix} g1 & & \\ & g_1 & \\ & & g_1 + g_2 \end{bmatrix} \tag{5.23}$$

since, in our problem, $R = |z_B - z_A|$. The functions g_1, g_2 are given by

$$g_1(R) = \frac{e^{ikR}}{4\pi R} \left(1 + \frac{i}{kR} - \frac{1}{k^2 R^2} \right), \quad g_2(R) = \frac{-e^{ikR}}{4\pi R} \left(1 + \frac{i3}{kR} - \frac{3}{k^2 R^2} \right) \tag{5.24}$$

Since B is a diagonal matrix, we can readily obtain

$$B^{-1} = \begin{bmatrix} \frac{k^2 \alpha_B}{1 - k^2 \alpha_B k^2 \alpha_A g_1^2} & & \\ & \frac{k^2 \alpha_B}{1 - k^2 \alpha_B k^2 \alpha_A g_1^2} & \\ & & \frac{k^2 \alpha_B}{1 - k^2 \alpha_B k^2 \alpha_A (g_1 + g_2)^2} \end{bmatrix}. \tag{5.25}$$

The derivative of the Green dyadic function can be written as

$$\partial_{z_B} \mathbb{G}_{AB} = \begin{bmatrix} \partial_{z_B} g_1 & & \\ & \partial_{z_B} g_1 & \\ & & \partial_{z_B} g_1 + [\partial_{z_B} g_2] \frac{(z_B - z_A)^2}{R^2} + g_2 [\partial_{z_B} \frac{(z_B - z_A)^2}{R^2}] \end{bmatrix}$$

But the last term can be simplified since

$$\partial_{z_B}\frac{(z_B-z_A)^2}{R^2}=\frac{2(z_B-z_A)R^2-(z_B-z_A)^2 2(z_B-z_A)}{R^4} \tag{5.26}$$

which is equal to zero when $R=|z_B-z_A|$. Then we get

$$\partial_{z_B}\mathbb{G}_{AB}=\begin{bmatrix}\partial_{z_B}g_1 & & \\ & \partial_{z_B}g_1 & \\ & & \partial_{z_B}g_1+\partial_{z_B}g_2\end{bmatrix} \tag{5.27}$$

The force (5.20) can then be written as

$$\begin{aligned}\langle F_B^z\rangle=\frac{2\pi u_E(\omega)}{k^3}\,\mathrm{Im}\Big\{&2k^2\alpha_A[\partial_{z_B}g_1]\frac{k^2\alpha_B\,g_1}{1-k^4\alpha_B\alpha_A g_1^2}\\&+k^2\alpha_A[\partial_{z_B}(g_1+g_2)]\frac{k^2\alpha_B\,(g_1+g_2)}{1-k^4\alpha_B\alpha_A(g_1+g_2)^2}\Big\}\end{aligned} \tag{5.28}$$

where $\partial_{z_B}g_1$, $\partial_{z_B}g_2$ are given by the expressions

$$\partial_{z_B}g_1=\frac{ke^{ikR}}{4\pi R}\left(i-\frac{2}{kR}-\frac{i3}{k^2R^2}+\frac{3}{k^3R^3}\right)\frac{z_B-z_A}{R} \tag{5.29}$$

$$\partial_{z_B}g_2=\frac{-ke^{ikR}}{4\pi R}\left(i-\frac{4}{kR}-\frac{i9}{k^2R^2}+\frac{9}{k^3R^3}\right)\frac{z_B-z_A}{R} \tag{5.30}$$

where the factors $(z_B-z_A)/R$ can be ommited since, in our case, they equal one.

It is easy to check that

$$\lim_{kr\to\infty}g_1\sim\frac{e^{ikR}}{4\pi R}\qquad\lim_{kr\to\infty}g_2\sim-\frac{e^{ikR}}{4\pi R} \tag{5.31}$$

Also, for the derivatives we obtain

$$\lim_{kr\to\infty}\partial_{z_B}g_1\sim i\frac{ke^{ikR}}{4\pi R}\qquad\lim_{kr\to\infty}\partial_{z_B}g_2\sim-i\frac{ke^{ikR}}{4\pi R} \tag{5.32}$$

and

$$\lim_{kr\to\infty}\left(1-k^4\alpha^2g_1^2\right)\sim 1\qquad\lim_{kr\to\infty}\left(1-k^4\alpha^2(g_1+g_2)^2\right)\sim 1 \tag{5.33}$$

so the $kR \to \infty$ limit for the nonabsorbing force, when the two particles are identical $\alpha_A = \alpha_B = \alpha$, is given by

$$\begin{aligned}\langle F_B^z \rangle &\sim \frac{2\pi u_E(\omega)}{k^3} \operatorname{Im}\left\{ 2k^2\alpha \left(i\frac{ke^{ikR}}{4\pi R} \right) k^2\alpha \left(\frac{e^{ikR}}{4\pi R} \right) \right\} \\ &\sim \frac{2\pi u_E(\omega)}{k^3} \frac{2k^5}{16\pi^2 R^2} \Big[\operatorname{Re}\{\alpha^2\} \cos(2kR) - \operatorname{Im}\{\alpha^2\} \sin(2kR) \Big] \\ &\sim \frac{k^2 u_E(\omega)}{4\pi R^2} \Big[\operatorname{Re}\{\alpha^2\} \cos(2kR) - \operatorname{Im}\{\alpha^2\} \sin(2kR) \Big] \end{aligned} \tag{5.34}$$

If the applied wavelength is large, the imaginary part of the polarizability gets very small compared to the real part, leading to a *weak scattering* approximation. Then, the dominant contribution in the previous equation comes from the cos term

$$\langle F_B^{ws} \rangle \sim \frac{k^2 u_E(\omega)}{4\pi R^2} \alpha'^2 \cos(2kR) \tag{5.35}$$

Similarly, if we are at the Frohlich resonance condition, $\alpha' = 0$, and then

$$\langle F_B^{res} \rangle \sim -\frac{k^2 u_E(\omega)}{4\pi R^2} \alpha''^2 \cos(2kR) \tag{5.36}$$

We see that both approximations lead to the same formal interaction force, with $\phi = \pi$ difference of phase between them.

5.2.2 Short distance expansions (no absorption)

From Equation (5.20) we can obtain the expansion of the optical force in the $R \to 0$ limit. In the resonant case, where $\alpha' = 0$, we obtain

$$\langle F_B^z \rangle \sim \frac{2\pi u_E(\omega)}{k^3} \Big[3k^3 R^2 \Big] = 6\pi u_E(\omega) R^2. \tag{5.37}$$

Note that this force does not depend on the applied wavelength, and it is always repulsive in the $R \to 0$ limit.

Actually, if we computed the expansion of the force described by Equation (5.20) when $\alpha'' \to 0$, we would obtain the same result. The difference is that, while for the resonant case this expansion is still valid for values of the interparticle separation compatible with the dipole approximation $R > 3a$, for the $\alpha'' \to 0$ case the distance must be set to non-physical values $R < 2a$.

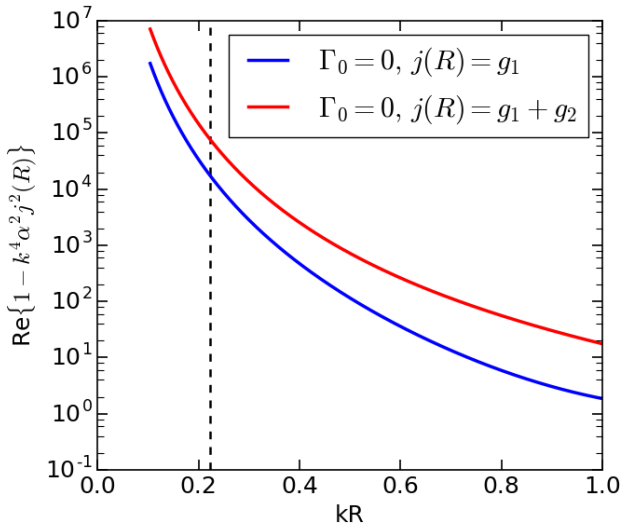

FIGURE 5.2: Value of the function $\mathrm{Re}\{1-k^4\alpha^2 j^2(R)\}$, with $j(R) = g_1, g_1 + g_2$, when the wavelength at which $\alpha' = 0$ has been used. It can be seen that the WSA is not valid for any distance range. This is the reason why the R^2 behaviour of the $R \to 0$ expansion can be observed at resonance, and also it shows that the R^{-2}-like interaction can not be found at any distance at resonance. Dotted line represents the limit of the validity of the dipole approximation $R = 3a$.

In Figure 5.1b, the force versus R is represented in the Frohlich Resonance Condition and in cases out of the resonance, taking as a minimum separation the condition $R_{min} = 3a$. It can be noticed that for FRC the $R \to 0$ limit of the force is physically observable.

One can define the expansion for an intermediate separation range by imposing the WSA

$$1 - k^4\alpha^2 g_1^2(R) \sim 1 \tag{5.38a}$$

$$1 - k^4\alpha^2 (g_1(R) + g_2(R))^2 \sim 1 \tag{5.38b}$$

in Equation (5.20) and then taking the limit $R \to 0$ of this new expresion. For a general polarizability we obtain

$$\begin{aligned}\lim_{R\to 0} F^{ws} &= \lim_{R\to 0} \frac{2\pi u_E(\omega)}{k^3} \operatorname{Im}\left\{2k^4\alpha^2[\partial_z g_1]g_1 + k^4\alpha^2[\partial_z(g_1+g_2)](g_1+g_2)\right\} \\ &\sim \frac{2\pi u_E(\omega)}{k^3}\frac{k^7}{\pi^2}\operatorname{Im}\Big\{-\frac{9}{8}\frac{\alpha^2}{k^7R^7} - \frac{1}{4}\frac{\alpha^2}{k^5R^5} - \frac{1}{8}\frac{\alpha^2}{k^3R^3} \\ &\qquad - \frac{i11}{120}\frac{\alpha^2}{k^2R^2} + \mathcal{O}(R^2)\Big\} \end{aligned} \tag{5.39}$$

In the cases $\alpha' = 0$ and $\alpha'' = 0$ one would expect this intermediate limit force to have a R^{-2} behavior, but two important features have to be taken into account. On the one hand, no range of applicability of the WSA can be found when λ is taken in the FRC, as has been represented in Figure 5.2, so this expansion would not correspond to the actual interaction between the two particles.

On the other hand, when using a physical model for the electric polarizability α'' can not be set to zero. It can be set very small by selecting large values of λ, but by enlarging λ, the terms $k^{-3,-5,-7}$ become more relevant, and then at short distances the interaction is no longer of the R^{-2} type, as is represented in Figure 5.1a. Then, in the case of no absorption, it is not possible to obtain a R^{-2} interaction between two dipolar NP at short distances, although it is possible to find a range of applicability of this R^{-2} interaction if λ is not in FRC.

5.3 The absorption case

If there is absorption, $\operatorname{Im}\{\alpha_0^{-1}\}$ and an additional term that will be later modeled with material parameters must be added

$$\begin{aligned} -\operatorname{Im}\left\{G_{AA}\right\} &= \operatorname{Im}\left\{T_A^{-1}\right\} - \operatorname{Im}\left\{\frac{1}{k^2\alpha_0}\right\} \\ &= \operatorname{Im}\left\{T_A^{-1}\right\} - \operatorname{Im}\left\{K^{-1}(\omega)\right\} \end{aligned} \tag{5.40}$$

where

$$K(\omega) = k^2\alpha_0 \tag{5.41}$$

We can then expand the terms of the forces F_1, F_2 obtained above. The first term, described by Equation (5.12), does not change. For the second

term of the force we have now

$$F_2 = \frac{2\pi u_E(\omega)}{k^3}\,\mathrm{Re}\Big\{\,\mathrm{Tr}\Big[B^{-1}[\partial_{z_B}G^*_{BA}]A^{-1*}\Big(\,\mathrm{Im}\{G_{AB}\} - \Big(\mathrm{Im}\Big\{T_A^{-1}\Big\} - \mathrm{Im}\Big\{K^{-1}(\omega)\Big\}\Big)T_AG_{AB} - G^*_{AB}T^*_B\Big(\mathrm{Im}\Big\{T_B^{-1}\Big\} - \mathrm{Im}\Big\{K^{-1}(\omega)\Big\}\Big) + G^*_{AB}T^*_B\,\mathrm{Im}\{G_{BA}\}T_AG_{AB}\Big)\Big]\Big\}$$

We can split it into two terms, $F_{2,nabs}$ given by Equation (5.19), and $F_{2,abs}$, which can be expressed as

$$F_{2,abs} = \frac{2\pi u_E(\omega)}{k^3}\,\mathrm{Re}\Big\{\,\mathrm{Tr}\Big[[\partial_{z_B}G^*_{BA}]A^{-1*}\Big(\,\mathrm{Im}\Big\{K^{-1}(\omega)\Big\}T_AG_{AB} + G^*_{AB}T^*_B\,\mathrm{Im}\Big\{K^{-1}(\omega)\Big\}\Big)B^{-1}\Big]\Big\}$$

From the calculations performed in the nonabsorbing scenario we already know that

$$F_1 + F_{2,nabs} = \frac{2\pi u_E(\omega)}{k^3}\,\mathrm{Im}\Big\{\,\mathrm{Tr}\Big[[\partial_{z_B}G_{BA}]T_A\mathbb{G}_{AB}B^{-1}\Big]\Big\}$$

The $F_{2,abs}$ can be further split into $F_{2a,abs}, F_{2b,abs}$

$$F_{2a,abs} = \frac{2\pi u_E(\omega)}{k^3}\,\mathrm{Re}\Big\{\,\mathrm{Tr}\Big[[\partial_{z_B}G^*_{BA}]A^{-1*}\,\mathrm{Im}\Big\{K^{-1}(\omega)\Big\}T_AG_{AB}B^{-1}\Big]\Big\}$$

$$F_{2b,abs} = \frac{2\pi u_E(\omega)}{k^3}\,\mathrm{Re}\Big\{\,\mathrm{Tr}\Big[[\partial_{z_B}G^*_{BA}]A^{-1*}G^*_{AB}T^*_B\,\mathrm{Im}\Big\{K^{-1}(\omega)\Big\}B^{-1}\Big]\Big\}$$

So the total force can be written as

$$\begin{aligned} F &= \Big(F_1 + F_{2,nabs}\Big) + F_{2a,abs} + F_{2b,abs} \\ &= \frac{2\pi u_E(\omega)}{k^3}\,\mathrm{Im}\Big\{\,\mathrm{Tr}\Big[[\partial_{z_B}G_{BA}]T_AG_{AB}B^{-1}\Big]\Big\} \\ &\quad + \frac{2\pi u_E(\omega)}{k^3}\,\mathrm{Re}\Big\{\,\mathrm{Tr}\Big[[\partial_{z_B}G^*_{BA}]A^{-1*}\,\mathrm{Im}\Big\{K^{-1}(\omega)\Big\}T_AG_{AB}B^{-1}\Big]\Big\} \\ &\quad + \frac{2\pi u_E(\omega)}{k^3}\,\mathrm{Re}\Big\{\,\mathrm{Tr}\Big[[\partial_{z_B}G^*_{BA}]A^{-1*}\mathbb{G}^*_{AB}T^*_B\,\mathrm{Im}\Big\{K^{-1}(\omega)\Big\}B^{-1}\Big]\Big\} \end{aligned} \tag{5.42}$$

We can see that, in the limit of zero absorption, the factor $\mathrm{Im}\Big\{K^{-1}(\omega)\Big\}$ goes to zero and the formal expression of the force is exactly the same that the one obtained in the previous section. This Equation is one of the main

results of this Chapter, since an equation for the interaction force between two absorbing particles under RLI can not be found in literature.

5.3.1 The $kR \to \infty$ limit (absorption)

For the sake of simplicity, we rewrite the force omiting A and B subscripts

$$\begin{aligned}\langle F_B^z \rangle &= \Big(F_1 + F_{2,nabs}\Big) + F_{2a,abs} + F_{2b,abs} \\ &= \frac{2\pi u_E(\omega)}{k^3} \operatorname{Im}\Big\{ \operatorname{Tr}\Big[(\partial_z G) T G B^{-1}\Big]\Big\} \\ &+ \frac{2\pi u_E(\omega)}{k^3} \operatorname{Im}\Big\{\frac{1}{k^2\alpha_0}\Big\} \operatorname{Re}\Big\{ \operatorname{Tr}\Big[(\partial_z G^*) A^{-1*} T G B^{-1}\Big]\Big\} \\ &+ \frac{2\pi u_E(\omega)}{k^3} \operatorname{Im}\Big\{\frac{1}{k^2\alpha_0}\Big\} \operatorname{Re}\Big\{ \operatorname{Tr}\Big[(\partial_z G^*) A^{-1*} T^* G^* B^{-1}\Big]\Big\}\end{aligned}$$

The limit of the first term $F_1 + F_{2,nabs}$ was already computed in the previous section, see Equation (5.34),

$$\begin{aligned}\lim_{R\to\infty} F_1 + F_{2,nabs} &= \lim_{R\to\infty} \frac{2\pi u_E(\omega)}{k^3} \operatorname{Im}\Big\{(\partial_z g_1)\frac{2k^4\alpha^2 g_1}{1-k^4\alpha^2 g_1^2} \\ &\qquad + (\partial_z(g_1+g_2))\frac{k^2\alpha(g_1+g_2)}{1-k^4\alpha^2(g_1+g_2)^2}\Big\} \\ &= \frac{2\pi u_E(\omega)}{k^3} \operatorname{Im}\Big\{ i2k^5\alpha^2 \frac{e^{ikR}}{4\pi R}\frac{e^{ikR}}{4\pi R} + 0\Big\} \\ &= \frac{u_E(\omega)}{8\pi}\frac{k^2}{R^2} \operatorname{Im}\Big\{ i2\alpha^2 e^{i2kR}\Big\} = \frac{u_E(\omega)}{8\pi}\frac{k^2}{R^2} \operatorname{Re}\Big\{ 2\alpha^2 e^{i2kR}\Big\}\end{aligned} \tag{5.43a}$$

The limit of the second term of the force is

$$\begin{aligned}\lim_{R\to\infty} F_{2a,abs} &= \lim_{R\to\infty} \frac{2\pi u_E(\omega)}{k^3} \operatorname{Im}\Big\{\frac{1}{k^2\alpha_0}\Big\} \operatorname{Re}\Big\{(\partial_z g_1^*)\frac{k^2\alpha^*}{1-k^4\alpha^{*2} g_1^{*2}}\frac{2k^4\alpha^2 g_1}{1-k^4\alpha^2 g_1^2} \\ &\qquad + (\partial_z(g_1^*+g_2^*))\frac{k^2\alpha^*}{1-k^4\alpha^{*2}(g_1^*+g_2^*)^2}\frac{k^4\alpha^2(g_1+g_2)}{1-k^4\alpha^2(g_1+g_2)^2}\Big\} \\ &= \frac{2\pi u_E(\omega)}{k^3} \operatorname{Im}\Big\{\frac{1}{k^2\alpha_0}\Big\} \operatorname{Re}\Big\{ -i2k^7\alpha^2\alpha^* \frac{e^{-ikR}}{4\pi R}\frac{e^{ikR}}{4\pi R} + 0\Big\} \\ &= \frac{u_E(\omega)}{8\pi}\frac{k^2}{R^2} \operatorname{Im}\Big\{\frac{2}{\alpha_0}\Big\} \operatorname{Re}\Big\{ -i\alpha^*\alpha\alpha\Big\} \\ &= \frac{u_E(\omega)}{8\pi}\frac{k^2}{R^2} \operatorname{Im}\Big\{\frac{2}{\alpha_0}\Big\} |\alpha|^2 \operatorname{Im}\Big\{\alpha\Big\}\end{aligned} \tag{5.43b}$$

And finally for the third term

$$\begin{aligned}\lim_{R\to\infty} F_{2b,abs} &= \lim_{R\to\infty} \frac{2\pi u_E(\omega)}{k^3} \operatorname{Im}\left\{\frac{1}{k^2\alpha_0}\right\} \operatorname{Re}\left\{(\partial_z g_1^*)\frac{k^2\alpha^*}{1-k^4\alpha^{*2}g_1^{*2}}\frac{2k^4\alpha\alpha^* g_1^*}{1-k^4\alpha^2 g_1^2}\right.\\ &\qquad \left. + (\partial_z(g_1^*+g_2^*))\frac{k^2\alpha^*}{1-k^4\alpha^{*2}(g_1^*+g_2^*)^2}\frac{k^4\alpha\alpha^*(g_1^*+g_2^*)}{1-k^4\alpha^2(g_1+g_2)^2}\right\}\\ &= \frac{2\pi u_E(\omega)}{k^3} \operatorname{Im}\left\{\frac{1}{k^2\alpha_0}\right\} \operatorname{Re}\left\{ -i2k^7\alpha^{*2}\alpha\frac{e^{-ikR}}{4\pi R}\frac{e^{-ikR}}{4\pi R} + 0\right\}\\ &= \frac{u_E(\omega)}{8\pi}\frac{k^2}{R^2} \operatorname{Im}\left\{\frac{2}{\alpha_0}\right\} \operatorname{Re}\left\{ -i\alpha^*\alpha^*\alpha e^{-i2kR}\right\}\\ &= \frac{u_E(\omega)}{8\pi}\frac{k^2}{R^2} \operatorname{Im}\left\{\frac{2}{\alpha_0}\right\} \operatorname{Re}\left\{i\alpha^2\alpha^* e^{i2kR}\right\} \end{aligned} \tag{5.43c}$$

It can be noticed that, in the $kR \to \infty$ limit, Equation (5.43b) does not oscillate, it has a genuine R^{-2} behaviour. It can also be noticed that the three terms have different dependence on the polarizability α. This will allow us to find new features of the interaction by using different values of λ.

5.3.2 Short distance expansions (absorption)

When the condition $\alpha' = 0$ is satisfied, the $R \to 0$ limit of the three different terms of the interaction force are written as

$$F_1 + F_{nabs} \sim 3k^3R^2 + 17k^5R^4 \tag{5.44a}$$

$$F_{2a,abs} \sim -108\frac{\pi^2R^5}{\alpha''^3} \tag{5.44b}$$

$$F_{2b,abs} \sim +108\frac{\pi^2R^5}{\alpha''^3}. \tag{5.44c}$$

Then, as in the case of no absorption, $R \to 0$ limit leads to a R^2 interaction. We will see that in this case, absorption will modify the range of applicability of this limit.

Now, the intermediate distance expansion of the interaction force will be performed whithin the WSA. From Equation (5.42) we study the three

different terms. From the first one

$$\begin{aligned}
&\lim_{R\to 0} F_1^{ws} + F_{2,nabs}^{ws} \qquad (5.45a)\\
&\quad = \lim_{R\to 0} \frac{2\pi u_E(\omega)}{k^3} \operatorname{Im}\Big\{2k^4\alpha^2[\partial_z g_1]g_1 + k^4\alpha^2[\partial_z(g_1+g_2)](g_1+g_2)\Big\}\\
&\quad \sim \frac{2\pi u_E(\omega)}{k^3}\frac{k^7}{\pi^2}\operatorname{Im}\Big\{-\frac{9}{8}\frac{\alpha^2}{k^7R^7} - \frac{1}{4}\frac{\alpha^2}{k^5R^5} - \frac{1}{8}\frac{\alpha^2}{k^3R^3} - \frac{i11}{120}\frac{\alpha^2}{k^2R^2} + \mathcal{O}(R^2)\Big\}
\end{aligned}$$

The expansion of the second term is given by

$$\begin{aligned}
\lim_{R\to 0} F_{2a,abs}^{ws} &= \lim_{R\to 0} \frac{2\pi u_E(\omega)}{k^3}\operatorname{Im}\Big\{\frac{1}{k^2\alpha_0}\Big\}|\alpha|^2\operatorname{Im}\Big\{2k^6\alpha[\partial_z g_1]g_1\\
&\qquad + k^6\alpha[\partial_z(g_1+g_2)](g_1+g_2)\Big\}\\
&\sim \frac{2\pi u_E(\omega)}{k^3}\frac{k^7|\alpha|^2}{\pi^2}\operatorname{Im}\Big\{\frac{1}{\alpha_0}\Big\}\operatorname{Im}\Big\{-\frac{9}{8}\frac{\alpha}{k^7R^7} - \frac{1}{4}\frac{\alpha}{k^5R^5} - \frac{1}{8}\frac{\alpha}{k^3R^3}\\
&\qquad - \frac{i1}{8}\frac{\alpha}{k^2R^2} + \mathcal{O}(R^2)\Big\} \qquad (5.45b)
\end{aligned}$$

And finally the expansion of the third term is expressed as

$$\begin{aligned}
\lim_{R\to 0} F_{2b,abs}^{ws} &= \lim_{R\to 0} \frac{2\pi u_E(\omega)}{k^3}\operatorname{Im}\Big\{\frac{1}{k^2\alpha_0}\Big\}|\alpha|^2\operatorname{Im}\Big\{2k^6\alpha^*[\partial_z g_1]g_1\\
&\qquad + k^6\alpha^*[\partial_z(g_1+g_2)](g_1+g_2)\Big\}\\
&\sim \frac{2\pi u_E(\omega)}{k^3}\frac{k^7|\alpha|^2}{\pi^2}\operatorname{Im}\Big\{\frac{1}{\alpha_0}\Big\}\operatorname{Im}\Big\{-\frac{9}{8}\frac{\alpha^*}{k^7R^7} - \frac{1}{4}\frac{\alpha^*}{k^5R^5} - \frac{1}{8}\frac{\alpha^*}{k^3R^3}\\
&\qquad + \frac{i11}{120}\frac{\alpha^*}{k^2R^2} + \mathcal{O}(R^2)\Big\} \qquad (5.45c)
\end{aligned}$$

It is interesting to note that, for these three expansions, the only coefficient that is different from one Equation to other is the coefficient proportional to the last term. This property will be used when exploring the features of the interaction between particles with absorption under RLI.

5.4 Conclusions

Two main conclusions can be extracted from the work of this chapter:

- By using a physical model for the electric permittivity, it is shown that, for two identical nonabsorbing particles, it is not possible to

get rid of the $R^{-3,-5,-7}$ terms in the short distance expansion of the interaction.

- A new closed formula for the interactions between two dipolar particles in a random light field can be obtained as a function of the term of the polarizability that accounts for absorption.

Chapter 6

Effects due to absorption: "Mock" gravity and nonconservativity

The inverse-square behavior of the gravitational interaction has been attempted to be described by different physical models along the centuries. A kinetic theory in which a huge number of tiny particles comming from every direction produce gravitational attraction between bigger bodies by provoking shadow effects was originally proposed by Nicolas Fatio de Duillier in 1690 and later by Georges-Louis Le Sage in 1748 (Edwards, 2002). In 1900, Lorentz extended this model to electromagnetic waves, making the remark that this model can not explain gravitational-like interactions if absorption is not taking into account (Lorentz, 1900). Some years later, it was found that absorption of radiation between two dust particles lead to a net attractive inverse-square force (Spitzer, 1941), which was named "Mock gravity" by George Gamow in a paper where proposed that this effect might play a role in galaxy formation (Gamow, 1949).

On the other hand, non-reciprocal forces in colloidal systems have been intensively investigated in the last years. The violation of action and reaction induced by non-equilibrium fluctuations (Buenzli et al., 2008), in a non-equilibrium Langevin many-body simulation (Hayashi et al., 2006) and in a system where two particles are subjected to depletion forces due to a flowing bath (Dzubiella et al., 2003) point out that this phenomena is strongly related to systems of particles immersed in a non-equilibrium environment (Ivlev et al., 2015).

In this chapter we will analyze two remarkable features of the optical interaction between two absorbing particles under Random Light Illumination.

First, we shall analyze the expansions in different regimes of the interaction between two identical particles under RLI obtained in the previous chapter. By imposing the mutual cancelation of the two oscillatory terms at large distances, we will obtain the conditions of the electric polarizability to obtain a monothonic inverse-square optical interaction between the particles. By applying these conditions to the intermediate limit expansion, we will see how absorption influences in the validity of the Weak Scattering Approximation, and how it aloow us to obtain a gravitational-like interaction at short distances. This permits us to obtain and analytically understand a full-range gravitational-like interaction between two identical particles under RLI.

Finally, we will analyze the case in which two absorbing particles with different polarizabilities interact in presence of random light. Non-reciprocal interactions will be analyze both analitical and numerically, giving an example of violation of action-reaction principle mediated by random light in the field of optical nanoparticles. By symmetry considerations, we will see that the rotational of the forces on each particle vanishes, since they are central forces. On the other hand, by means of an application of differential forms, we will see that no potential function for the system as a whole can be defined in the case of particles with different polarizabilities, but it can be found when the particles are identical. This will lead to the novel result that a system of identical absorbing particles under RLI is conservative, while the system of two particles with different polarizabilities is not. This results will be checked numerically.

6.1 The full-range $F \sim R^{-2}$ interaction

Once we have obtained the expansion of the force for different separation regimes, the $R \to \infty$ limit, given by Equations (5.43a), (5.43b) and (5.43c), the intermediate range, given by Equations (5.45a), (5.45b) and (5.45c), and the $R \to 0$, given by Equations (5.44a), (5.44b) and (5.44c), we analyze special behavior of the interaction that can be obtained by tuning the polarizability of the particles.

Among the three terms that describe the interaction between the particles when absorption is taken into account, expressed in Equation (5.42), there are two, $(F_1 + F_{2,nabs})$ and $F_{2b,abs}$, that have intrinsic oscillations and one, $F_{2a,abs}$, that do not oscillate.

Then, a question arises: Can the oscillations of $(F_1 + F_{2,nabs})$ and $F_{2b,abs}$

cancel out? The answer is yes. Under specific conditions of the polarizability of the particles we can get a monotonic behaviour of the interaction. Moreover, this monotonic behaviour is going to be inverse-squared and attractive, leading to a full-range gavitational-like interaction. This is possible only when absorption is considered.

Let us impose $(F_1 + F_{2,nabs}) + F_{2b,abs} = 0$ for the large-separation expansions of the force given by Equations (5.43a), (5.43b) and (5.43c); we obtain

$$\mathrm{Re}\left\{2\alpha^2 e^{i2kR}\right\} = -\,\mathrm{Im}\left\{\frac{2}{\alpha_0}\right\}\mathrm{Re}\left\{i\alpha^2\alpha^* e^{i2kR}\right\}$$

and then

$$\begin{aligned}\mathrm{Re}\left\{\alpha^2\right\}\mathrm{Re}\left\{e^{i2kR}\right\} - \mathrm{Im}\left\{\alpha^2\right\}\mathrm{Im}\left\{e^{i2kR}\right\} \\ = -\,\mathrm{Im}\left\{\frac{1}{\alpha_0}\right\}\mathrm{Re}\left\{i\alpha^2\alpha^*\right\}\mathrm{Re}\left\{e^{i2kR}\right\} \\ + \mathrm{Im}\left\{\frac{1}{\alpha_0}\right\}\mathrm{Im}\left\{i\alpha^2\alpha^*\right\}\mathrm{Im}\left\{e^{i2kR}\right\}\end{aligned}$$

The functions $\mathrm{Re}\{e^{i2kR}\}$ and $\mathrm{Im}\{e^{i2kR}\}$ are linearly independent. Thus, two different conditions have to be fulfilled

$$\mathrm{Re}\left\{\alpha^2\right\} = -\,\mathrm{Im}\left\{\frac{1}{\alpha_0}\right\}\mathrm{Re}\left\{i\alpha^2\alpha^*\right\}$$
$$\mathrm{Im}\left\{\alpha^2\right\} = -\,\mathrm{Im}\left\{\frac{1}{\alpha_0}\right\}\mathrm{Im}\left\{i\alpha^2\alpha^*\right\}$$

and then

$$\alpha^2 = -\,\mathrm{Im}\left\{\frac{1}{\alpha_0}\right\} i\alpha^*\alpha^2 \tag{6.1}$$

or

$$1 = -\,\mathrm{Im}\left\{\frac{1}{\alpha_0}\right\} i\alpha^* \tag{6.2}$$

That can be decomposed into two different conditions

$$\alpha' = 0 \tag{6.3a}$$

$$\mathrm{Im}\left\{\frac{1}{\alpha_0}\right\} = \frac{-1}{\alpha''} \tag{6.3b}$$

The first condition requires a vanishing real part of the polarizability, not necessary at the FRC, as we will see. The second condition is fulfilled for small dipolar particles when absorption is much larger than scattering.

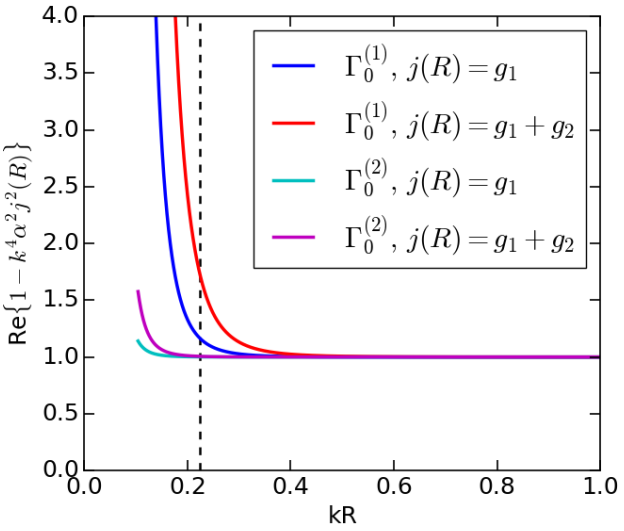

FIGURE 6.1: Range of validity of weak scattering approximation for two different values of Γ_0 in a Lorentz model. It can be seen that for larger absorption, the range on which weak scattering approximation is applicable goes below the $3a$ separation limit (dotted line).

Then, when these two conditions are fulfilled, we see that, in the large distance limit, the interaction will be inverse squared. What can we say about the intermediate distance regime, where WSA is applied, and about the $R \to 0$ limit?

When condition (6.3a) is introduced into the intermediate-distance expansions for $(F_1 + F_{2,nabs})$, $F_{2a,abs}$ and $F_{2b,abs}$, given by Equations (5.45a), (5.45b) and (5.45c), respectively, the only term that survives is the R^{-2} term. In the expansions (5.45b) and (5.45c), the $R^{-3,-5,-7}$ terms do not cancel by their own, but they do cancel each other, since $\mathrm{Im}\{\alpha\} = -\mathrm{Im}\{\alpha^*\}$. Then, by applying the same conditions than in the large distance limit, the only contribution that remains in the intermediate distance regime is the inverse squared term.

In the $R \to 0$ limit, these conditions do not modify the form of the interaction, given by Equations (5.44a), (5.44b) and (5.44c). This could seem to be a problem, since as it has been shown in the nonabsorbing case, this regime is specially important at the FRC, where the condition (6.3a) is fulfilled.

However, condition (6.3b) requires absorption to be larger than scattering. Increasing the absorption decreases the polarizability, which means

that the range of applicability of the WSA increases as well. Then, by imposing condition (6.3b) at the FRC, the range of applicability of the intermediate range can go beyond the distance limit of the dipolar approximation $R > 3a$, allowing a full range R^{-2} behavior of the interaction, since the short distance expansion is now valid only for distances $R < 3a$.

This can be seen in Figure 6.1. In this Figure, we check the validity of the WSA at the FRC for two different set of parameters of a Lorentz model for electric permittivity. In one case we set $a = 0.01186\,\lambda_0$, $\epsilon_\infty = 1.0$, $\epsilon_S = 2.9$, $\omega_0 = 0.7824\,\omega^*$ and $\Gamma_0^{(1)} = 0.0340\,\omega^*$, being $\epsilon_0 = 1.0$ the permittivity of vacuum, λ_0 the wavelength for which $\alpha' = 0$, and $\omega^* = hc/\lambda_0$. And in the other case we set the same parameters except Γ_0, which now takes the value $\Gamma_0^{(2)} = 0.3742\,\omega^*$. It can be noticed that, just by increasing the parameter Γ_0, which accounts for absorption, the range of applicability of the WSA goes beyond the $R = 3a$ limiting condition.

In Figure 6.2a and Figure 6.2b optical interactions between two dipolar particles described by a Lorentz model for electric permittivity have been depicted. The absorption parameters are $\Gamma_0^{(1)}$ and $\Gamma_0^{(2)}$ respectively. For wavelengths below the FRC (λ_0), we find again a characteristic peak at short distances indicating that the force is changing sign, leading to a binding interaction at short distances. We can readily see that, for FRC, an inverse-squared interaction is obtained. The arbitrary value of F_0 has been set to the same value than in the previous chapter, $F_0 = 10^{-12}$N.

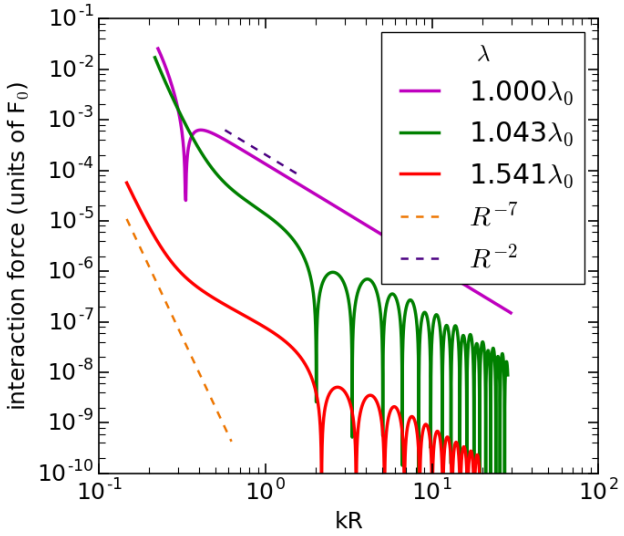

(A)

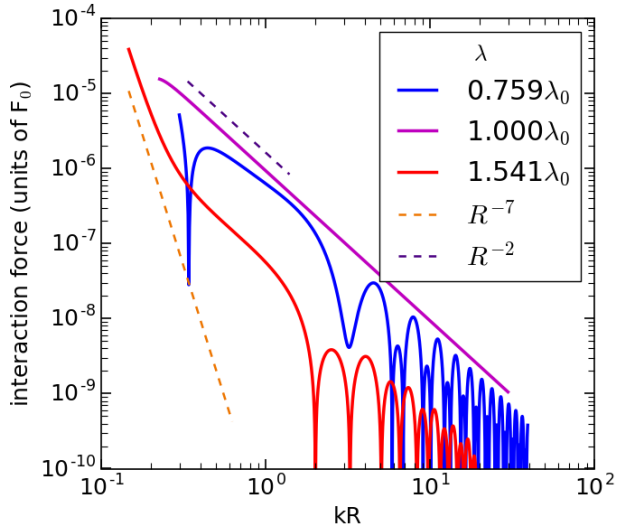

(B)

FIGURE 6.2: (A) Optical interaction between two particles described with a Lorentz model for electric permittivity with $\Gamma_0^{(1)}$. (B) The same with $\Gamma_0^{(2)}$. It can be seen that now the R^{-2} behaviour is enhanced at short distances.

6.1.1 The case of gold and silver

The numerical results of the previous section were based in a theoretical model for electric permittivity, known as Lorentz model. It is interesting to check the validity of this results in a more realistic scenario, by using experimental values of the electric permittivity for a given material.

Then, in this section we study the interaction under RLI between two NPs described by polarizabilities corresponding to gold and silver nanoparticles. Experimental values of electric permittivity for these materials were obtained from the literature (Palik, 1997). With these values of electric permittivity, electric polarizability for gold and silver nanoparticles $a = 5$nm radius were obtained using Equation (2.13).

The polarizabilities of gold and silver in vacuum calculated in this manner are represented in Figure 6.3a and Figure 6.3b, respectively. Taking into account the results of the first part of this section, it can be noticed that gold polarizability does not fulfill the condition $\alpha' = 0$ for any wavelength, while silver polarizability has two different wavelengths for which these condition is satisfied since, as was previously mentioned, condition (6.3a) does not necessary imply FRC.

Hence, we would not expect gold nanoparticles to show a gravitational-like interaction for any value of the system parameters, while silver NPs should show this kind of interaction for the two wavelengths at which condition (6.3a) is fulfilled.

This is what we observe in Figure 6.4a and Figure 6.4b, respectively. In the case of gold, we always find the R^{-7} interaction when the particles get close to each other. Moreover, since the real part of the polarizability does not change sign, it is not possible to find a value of λ for which this interaction is repulsive.

In the case of silver, we see that for $\lambda = \lambda_0$, the behaviour is the expected gravitational-like interaction, except when the particles are very close to each other, where the interaction differs from the R^{-2} interaction. This is because absorption is not large enough to enlarge the WSA range, as in the case of the model particles described by Lorentz permittivity when $\Gamma_0 = \Gamma_0^{(1)}$, represented in Figure 6.2a. This problem could be remedied by adding a polymer cover to the particle.

However, for $\lambda = 0.906\lambda_0$, absorption is much larger than scattering, and then the range of applicability of the WSA is beyond the $R = 3a$ limiting condition. We can then find a full-range gravitational behaviour.

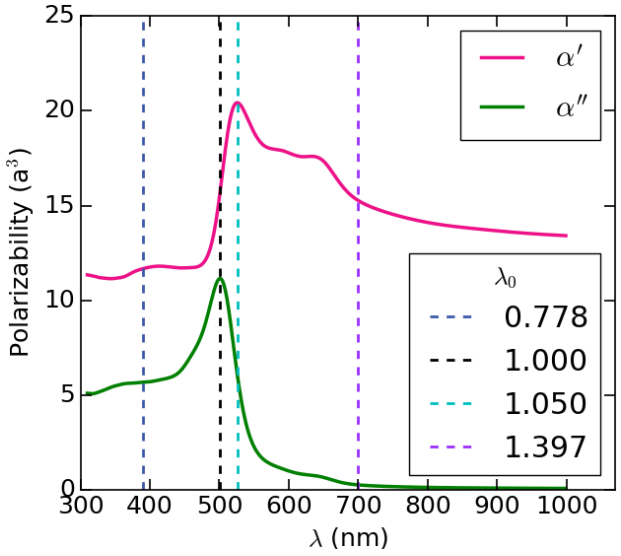

(A)

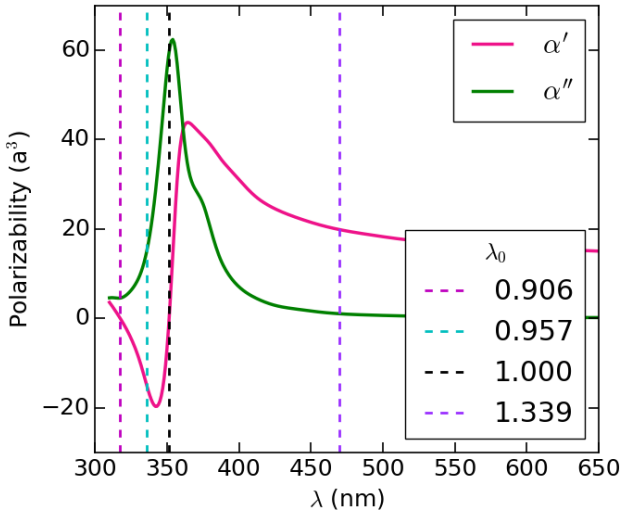

(B)

FIGURE 6.3: (A) Polarizability of a gold nanoparticle of $a = 5$nm radius in vacuum. The curve is an interpolation from experimental values obtained from the literature (Palik, 1997). (B) The same for a silver nanoparticle of $a = 5$nm radius.

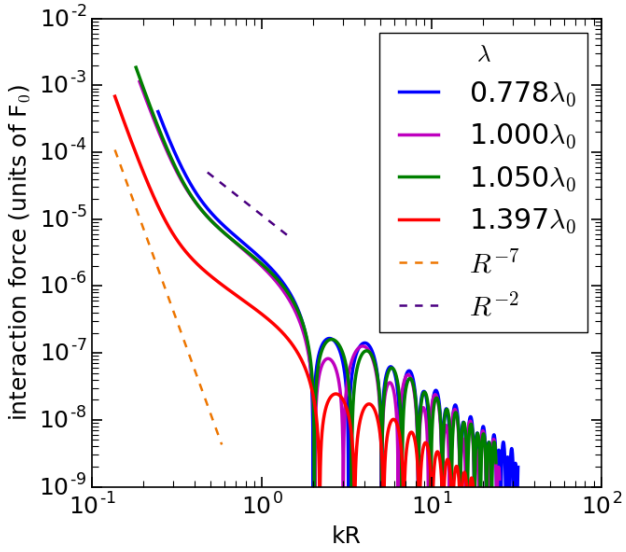

(A)

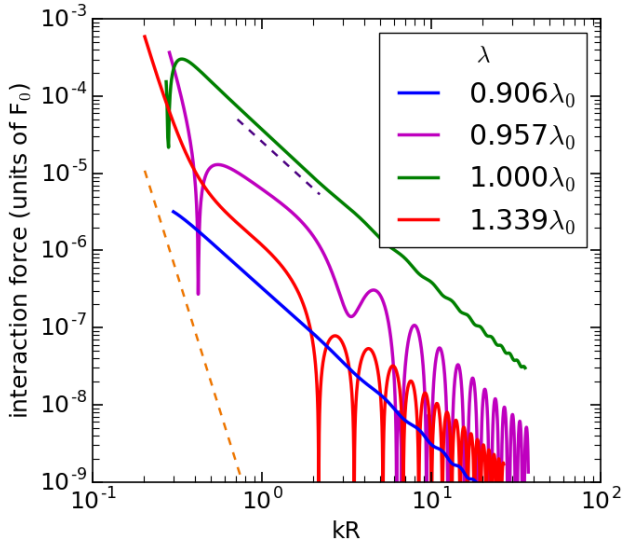

(B)

FIGURE 6.4: (A) Optical interaction between two gold nanoparticles in random light illumination. A gravitational-like interaction can not be obtained for any λ. (B) Optical interaction between two silver nanoparticles. Two different λ for which interaction is approximately gravitational-like can be found.

6.2 Nonreciprocity and nonconservativity under RLI

In this section, the interaction between two nanoparticles when illuminated by a random light field will be analized in the case of different electric polarizabilities for the two particles. At least one of them should include absorption.

First, the force on the center of mass of the two particles will be studied in order to show that this force is in general different from zero. We will analitically handle the simplest case in which one of the particles does not have absorption. Then, to analyze the results for the force on the center of mass in a general case, a system of one gold NP and one silver NP will be numerically studied. The particles will be described by the polarizabilities obtained in the previous section, and their radii will be $a = 5$nm.

Moreover, the conservativeness of the optical interaction between the two particles will be also studied. It will be shown that the force acting in one of them is conservative, as long as the other particle is not allowed to move. When the two particles can move under the influence of the forces exerted on each of them, the analysis will probe that no potential function can describe the forces acting on the system, pointing out that we are dealing with a nonconservative interaction.

Let us now rewrite the expressions for the optical forces on particles A and B, taking into account that both particles absorb with different electric polarizabilities. Considering that

$$\begin{aligned} -\operatorname{Im}\left\{\mathbb{G}_{AA}\right\} &= \operatorname{Im}\left\{T_A^{-1}\right\} - \operatorname{Im}\left\{\frac{1}{k^2\alpha_{0A}}\right\} \\ &= \operatorname{Im}\left\{T_A^{-1}\right\} - \operatorname{Im}\left\{K_A^{-1}(\omega)\right\} \end{aligned} \tag{6.4a}$$

$$\begin{aligned} -\operatorname{Im}\left\{\mathbb{G}_{BB}\right\} &= \operatorname{Im}\left\{T_B^{-1}\right\} - \operatorname{Im}\left\{\frac{1}{k^2\alpha_{0B}}\right\} \\ &= \operatorname{Im}\left\{T_B^{-1}\right\} - \operatorname{Im}\left\{K_B^{-1}(\omega)\right\} \end{aligned} \tag{6.4b}$$

where

$$K_i(\omega) = k^2\alpha_{0i} \tag{6.5}$$

and following the steps of the calculation detailed in Chapter 5, the force on particle B is obtained as

$$\begin{aligned} F^B &= \left(F_1^B + F_{2,nabs}^B\right) + F_{2a,abs}^B + F_{2b,abs}^B \\ &= \frac{2\pi u_E(\omega)}{k^3}\,\mathrm{Im}\left\{\,\mathrm{Tr}\left[[\partial_{z_B}\mathbb{G}_{BA}]T_A\mathbb{G}_{AB}B^{-1}\right]\right\} \\ &\quad + \frac{2\pi u_E(\omega)}{k^3}\,\mathrm{Re}\left\{\,\mathrm{Tr}\left[[\partial_{z_B}\mathbb{G}^*_{BA}]A^{-1*}\,\mathrm{Im}\left\{K_A^{-1}(\omega)\right\}T_A\mathbb{G}_{AB}B^{-1}\right]\right\} \\ &\quad + \frac{2\pi u_E(\omega)}{k^3}\,\mathrm{Re}\left\{\,\mathrm{Tr}\left[[\partial_{z_B}\mathbb{G}^*_{BA}]A^{-1*}\mathbb{G}^*_{AB}T_B^*\,\mathrm{Im}\left\{K_B^{-1}(\omega)\right\}B^{-1}\right]\right\} \end{aligned} \tag{6.6}$$

Similarly, the optical force acting on particle A will be

$$\begin{aligned} F^A &= \left(F_1^A + F_{2,nabs}^A\right) + F_{2a,abs}^A + F_{2b,abs}^A \\ &= \frac{2\pi u_E(\omega)}{k^3}\,\mathrm{Im}\left\{\,\mathrm{Tr}\left[[\partial_{z_A}\mathbb{G}_{AB}]T_B\mathbb{G}_{BA}A^{-1}\right]\right\} \\ &\quad + \frac{2\pi u_E(\omega)}{k^3}\,\mathrm{Re}\left\{\,\mathrm{Tr}\left[[\partial_{z_A}\mathbb{G}^*_{AB}]B^{-1*}\,\mathrm{Im}\left\{K_B^{-1}(\omega)\right\}T_B\mathbb{G}_{BA}A^{-1}\right]\right\} \\ &\quad + \frac{2\pi u_E(\omega)}{k^3}\,\mathrm{Re}\left\{\,\mathrm{Tr}\left[[\partial_{z_A}\mathbb{G}^*_{AB}]B^{-1*}\mathbb{G}^*_{BA}T_A^*\,\mathrm{Im}\left\{K_A^{-1}(\omega)\right\}A^{-1}\right]\right\} \end{aligned} \tag{6.7}$$

It can be noticed that the absorption of each particle contributes explicitly to different terms with different characteristics since, as was shown in Equation (5.42), the first and third term of the force oscillates while the second term does not.

6.2.1 The force on the center of mass

The explicit dependence on $K_{A,B}^{-1}(\omega)$ of the oscillatory and nonoscillatory terms of the force in Equations (6.6) and (6.7) suggests that, by selecting different values of the polarizability of the particles, new features will be found in the interaction between two distinct NPs.

Let us study the force on the center of mass of the system of particles. To simplify the analysis a specific condition will be imposed: Particle B is required to have no absorption, so the matrix K_B^{-1} will vanish. Then we have

$$\begin{aligned} F^B &= \frac{2\pi u_E(\omega)}{k^3}\,\mathrm{Im}\left\{\,\mathrm{Tr}\left[[\partial_{z_B}G_{BA}]T_AG_{AB}B^{-1}\right]\right\} \\ &\quad + \frac{2\pi u_E(\omega)}{k^3}\,\mathrm{Re}\left\{\,\mathrm{Tr}\left[[\partial_{z_B}G^*_{BA}]A^{-1*}\,\mathrm{Im}\left\{K_A^{-1}(\omega)\right\}T_AG_{AB}\,B^{-1}\right]\right\} \end{aligned} \tag{6.8a}$$

and

$$F^A = \frac{2\pi u_E(\omega)}{k^3}\,\mathrm{Im}\left\{\mathrm{Tr}\left[[\partial_{z_A}G_{AB}]T_BG_{BA}A^{-1}\right]\right\} \tag{6.8b}$$
$$+\frac{2\pi u_E(\omega)}{k^3}\,\mathrm{Re}\left\{\mathrm{Tr}\left[[\partial_{z_A}G^*_{AB}]B^{-1*}\,G^*_{BA}T^*_A\,\mathrm{Im}\left\{K_A^{-1}(\omega)\right\}A^{-1}\right]\right\}$$

The sum of the first terms $\left(F_1^{cm}+F_{2,nabs}^{cm}\right)$ is given by

$$\begin{aligned}&\left(F_1^{cm}+F_{2,nabs}^{cm}\right)\\ &\quad=\frac{2\pi u_E(\omega)}{k^3}\,\mathrm{Im}\left\{\mathrm{Tr}\left[[\partial_{z_B}G_{BA}]T_AG_{AB}B^{-1}+[\partial_{z_A}G_{AB}]T_BG_{BA}A^{-1}\right]\right\}\\ &\quad=\frac{2\pi u_E(\omega)}{k^3}\,\mathrm{Im}\left\{\mathrm{Tr}\left[A^{-1}G_{AB}T_B[\partial_{z_B}G_{BA}]-[\partial_{z_B}G_{BA}]T_BG_{BA}A^{-1}\right]\right\}\end{aligned}$$

But, by using Equations (2.42) and (A.5), and the property

$$\mathrm{Tr}\left[M-M^t\right]=0, \tag{6.9}$$

being M an arbitrary square matrix, we find that $\left(F_1^{cm}+F_{2,nabs}^{cm}\right)=0$.

The sum of the terms $F^B_{2a,abs}+F^A_{2b,abs}$ is what will provoke a net force on the center of mass of the particles. It can be written as

$$\begin{aligned}F_2^{cm}&=F^B_{2a,abs}+F^A_{2b,abs}\\ &=\frac{2\pi u_E(\omega)}{k^3}\,\mathrm{Re}\left\{\mathrm{Tr}\left[[\partial_{z_B}G^*_{BA}]A^{-1*}\,\mathrm{Im}\left\{K_A^{-1}(\omega)\right\}T_AG_{AB}\,B^{-1}\right.\right.\\ &\qquad\left.\left.+[\partial_{z_A}G^*_{AB}]B^{-1*}\,G^*_{BA}T^*_A\,\mathrm{Im}\left\{K_A^{-1}(\omega)\right\}A^{-1}\right]\right\}\\ &=\frac{2\pi u_E(\omega)}{k^3}\,\mathrm{Re}\left\{\mathrm{Tr}\left[[\partial_{z_B}G^*_{BA}]\,\mathrm{Im}\left\{K_A^{-1}(\omega)\right\}\right.\right.\\ &\qquad\left.\left.\left(A^{-1*}T_AG_{AB}B^{-1}-B^{-1*}G^*_{BA}T^*_AA^{-1}\right)\right]\right\}\end{aligned} \tag{6.10}$$

which in general does not vanish.

The result of the force on the center of mass F^{cm} obtained using Equations (6.7) and (6.6) for the general case are shown in Figure 6.5. In this calculation, a gold NP and a silver NP have been used. The applied wavelength is $\lambda = 354$nm. Their polarizabilities are shown in Figures 6.3a and 6.3b, respectively. In Figure 6.6, the three different contributions to the force on particle A (silver) and particle B (gold) are depicted. It can be noticed that terms $\left(F_1^{A,B}+F_{2,nabs}^{A,B}\right)$ and $F^{A,B}_{2b,abs}$ for both particles show an

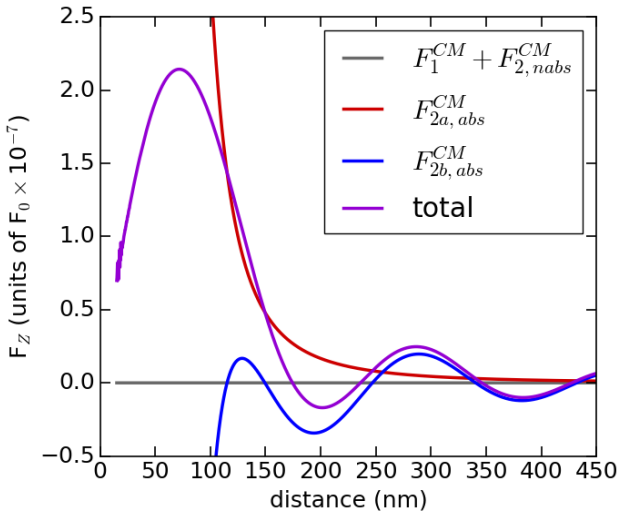

FIGURE 6.5: The sum of the different contributions to the force on the center of mass and the total force on the center of mass. The total force has an oscillatory behavior. Particle A (B) is a silver (gold) nanoparticle. The applied wavelength is $\lambda = 354$nm.

oscillatory behavior while terms $F_{2a,abs}^{A,B}$ shows a monotonic behavior at large distances for both particles.

The non-vanishing contributions to the force on the center of mass comes from terms $F_{2a,abs}^{cm}$ and $F_{2b,abs}^{cm}$. Since terms $F_{2b,abs}^{A,B}$ are oscillatory, the total force will have an oscillatory behavior too, depending on the separation between both particles. Similarly to what was found in Chapters 3 and 4, the linear momentum of the particle-particle system is not conserved. The remarkable feature in this case is that now there is spherical symmetry in the system, i.e. the particle positions do not have to be resticted to a specific line, as in the case of particles illuminated by a plane wave. They can freely rotate mantaining this characteristic feature, since the applied random field is homogeneous and isotropic.

6.2.2 Nonconservativity

In this section, the conservativity of the interaction between two different NPs under random light illumination (RLI) will be discussed. First, we will analyze the nature of the force acting on one of the two particles, and then, we will study the nature of the system as a whole.

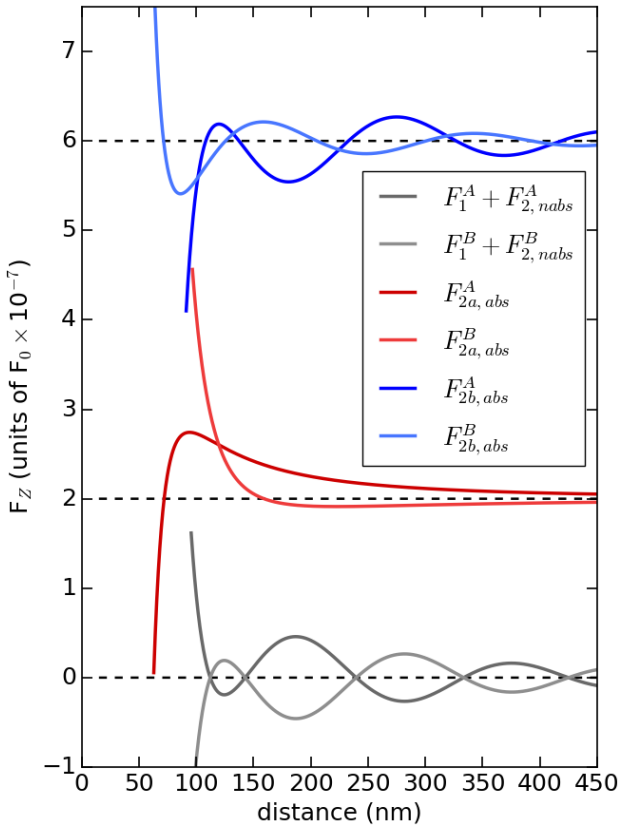

FIGURE 6.6: The different contributions to force on particle A (silver) and particle B (gold) are depicted. It can be seen that only terms $(F_1^{A,B} + F_{2,nabs}^{A,B})$ are reciprocal, and that the terms $F_{2a,abs}^{A,B}$ are not oscillatory. The applied wavelength is $\lambda = 354$nm.

It is known that, when dealing with a force acting on a particle, the conservativity of this force can be ensure by checking that the rotational of the force is identically zero. Moreover, central forces are by definition irrotational forces, which means that if the force on a particle depends only on the distance to a fixed point then the force can be written as the gradient of a potential function (Fasano et al., 2006).

Then, by symmetry considerations, we can see that in both cases, when the particles A and B are identical and when they have different polarizabilities, the forces F^A and F^B are going to be conservative forces. Since the applied random field is homogeneous and isotropic, the only axis that is defined without ambiguity is the z-axis, in which they are separated. Then, the x- and y-components of the force must vanish, and the forces depend only on z_A, z_B, implying that $\nabla \times \boldsymbol{F}^{A,B} = 0$. This can be checked numerically by performing the line integral of $\boldsymbol{F}^B$ over a close path for particle B while particle A is set at the origin (or *vice versa*) and bearing out that this line integral always vanishes.

On the other hand, it is also known that, given a scalar function $Q(\phi_1, \phi_2, \phi_3)$, its differential dQ is obtained as (Do Carmo, Manfredo P., 1994)

$$dQ \equiv \left(\frac{\partial Q}{\partial \phi_1}\right) d\phi_1 + \left(\frac{\partial Q}{\partial \phi_2}\right) d\phi_2 + \left(\frac{\partial Q}{\partial \phi_3}\right) d\phi_3 \tag{6.11}$$

In three dimensions, a differential form

$$A(\phi_1, \phi_2, \phi_3)d\phi_1 + B(\phi_1, \phi_2, \phi_3)d\phi_2 + C(\phi_1, \phi_2, \phi_3)d\phi_3 \tag{6.12}$$

is an exact differential form in a domain $D \in R^3$ if there exists a scalar function $Q(\phi_1, \phi_2, \phi_3)$ defined in D such that

$$dQ \equiv \left(\frac{\partial Q}{\partial \phi_1}\right) d\phi_1 + \left(\frac{\partial Q}{\partial \phi_2}\right) d\phi_2 + \left(\frac{\partial Q}{\partial \phi_3}\right) d\phi_3 \tag{6.13}$$

$$= A(\phi_1, \phi_2, \phi_3)d\phi_1 + B(\phi_1, \phi_2, \phi_3)d\phi_2 + C(\phi_1, \phi_2, \phi_3)d\phi_3 \tag{6.14}$$

in every point $x \in D$. This is equivalent to say that the vector field $\boldsymbol{J} = (A, B, C)$ is a conservative field, being Q its potential function.

Then, the field field $\boldsymbol{J} = (A, B, C)$ is a conservative field if all the following conditions are satisfied

$$\left(\frac{\partial A}{\partial \phi_2}\right) = \left(\frac{\partial B}{\partial \phi_1}\right), \qquad \left(\frac{\partial A}{\partial \phi_3}\right) = \left(\frac{\partial C}{\partial \phi_1}\right), \qquad \left(\frac{\partial B}{\partial \phi_3}\right) = \left(\frac{\partial C}{\partial \phi_2}\right) \tag{6.15}$$

This can be generalized to a vector field in N dimensions. Note that for 3 dimensions, this conditions are equivalent to the condition $\nabla \times \boldsymbol{J} = 0$.

What we are going to do is to try to find a potential function U that describes simultaneously the dynamics of particles A and B. Then, its differential would be written as

$$dU = F_x^A dx_A + F_y^A dy_A + F_z^A dz_A + F_x^B dx_B + F_y^B dy_B + F_z^B dz_B \tag{6.16}$$

since F_x^A, F_y^A and F_x^B, F_y^B identically vanish, and $F_z^{A,B}$ only depend on $z_{A,B}$, the set of conditions (6.15) reduces to

$$\left(\frac{\partial F_z^A}{\partial z_B}\right) = \left(\frac{\partial F_z^B}{\partial z_A}\right) \tag{6.17}$$

This will be the condition for the system of particles A and B to be conservative.

It can be noticed that, in the case of two identical particles, this condition fulfills identically, since $F_z^A = F_z^B$. This means that, when $\alpha_A = \alpha_B$, a potential function for the system of particles can be found, and any line integral performed over a path with the same initial and final configurations would be zero. This is, by itself, an interesting result, since in the literature there are no works assuring that the system of two identical absorbing particles under RLI is fully conservative.

In the case of two particles with different polarizabilities, it is shown in Equations (6.6) and (6.7) that the forces (F_z^A, F_z^B) depend on (z_A, z_B) in a different manner, so the condition (6.17) is not fulfilled, and then, it is not possible to find a potential function U describing the dynamics of the system, and the system of particles A and B is going to be nonconservative.

It is worth emphasizing that, although forces (F^A, F^B) always point along the line separating both particles and then it is possible to obtain separated potentials (U_A, U_B), the system as a whole turns out to be nonconservative. This is because it is not possible to describe (F^A, F^B) from a unique potential function U.

To show this nonconservative property explicitly we will perform a displacement of the particles originally separated a distance $d = 3a$ along the z-axis, being a the radius of the particles. Several paths will be studied. In the 1-step process, particle B will be displaced a distance D along the y-axis and then, particle A will be displaced the same distance D along the y-axis. The final configuration will then be the same than the original configuration, but a nonzero work will be done in the process. This procedure is shown in Figure 6.7a.

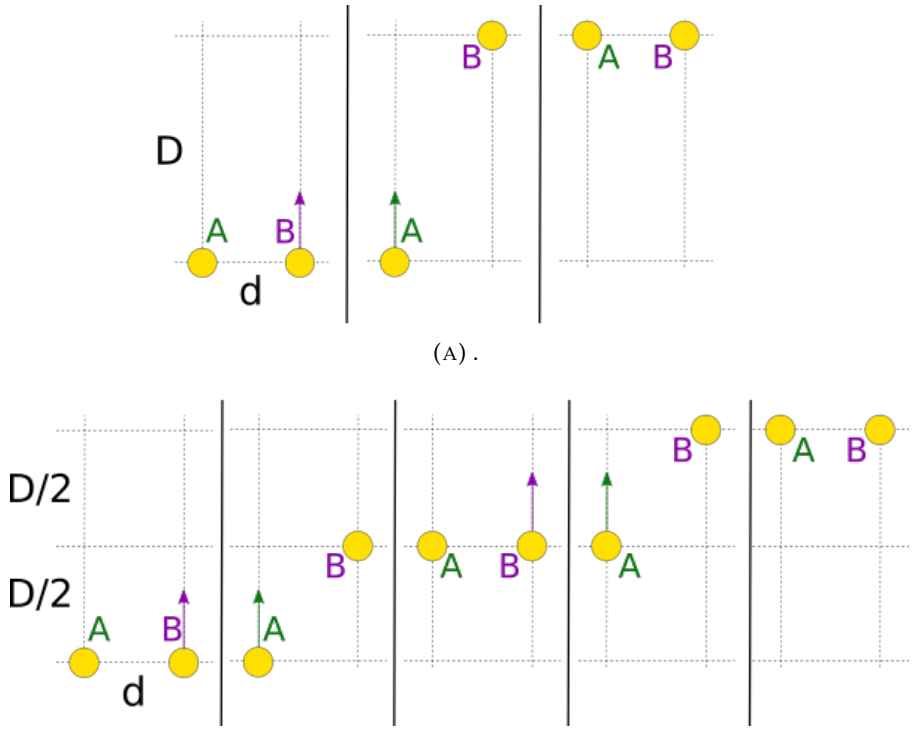

(A) .

(B) .

FIGURE 6.7: (A) 1-step process considered to study the work done by the system due to optical interactions. (B) 2-step process considered to study the work due to optical interactions. The distance traveled by particles A and B will be D in both cases, and the final configuration is the same than the initial one. The work done by the system is nonzero, and depends on the number of steps, showing the nonconservativity of the optical interaction.

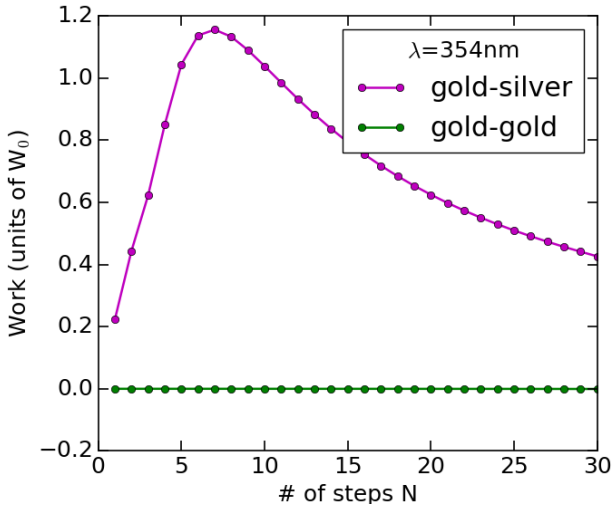

FIGURE 6.8: Work done by the system as a function of the number of intermediate steps. The case of identical particles and the case of different particles have been studied. The applied wavelength is $\lambda = 354$nm. Nonconservativity of the case of different particles is shown.

In the N-step process, particle B will be displaced a distance D/N along the y-axis, and then particle A will also be displaced a distance D/N along the y-axis. This will be repeated N times, so the final distance traveled by particle A and B will be a distance D, the same than in the 1-step process. The particular case of the 2-step process is depicted in Figure 6.7b.

The results are shown in Figure 6.8. The work done by the system has been represented as a function of the number of steps in the process. It can be noticed that, for large number of steps, the work approaches zero. This is because we are displacing the particles in a line that is perpendicular to the initial direction of separation and then, as the step size approaches zero, $\boldsymbol{F} \cdot d\boldsymbol{r}$ approaches zero as well. The arbitrary value W_0 has been set to $W_0 = 10^{-25}$J.

6.3 Conclusions

Three main conclusions can be extracted from the work of this chapter:

- It can be found, both for model polarizabilities and for silver, certain conditions for the polarizability that generate a full-range gravitational behavior of the interaction between the two particles.

- The interaction between identical particles due to random ligth illumination turns out to be conservative, even in the case of non-zero absorption.
- When the particles are not identical, no potential function can be used to describe the entire system, even though two different potential functions can be found for each of the two particles independently.

Chapter 7

Conclusions

Next, the main conclusions obtained in this Thesis are highlighted:

The Chapter 3 of this Thesis deals with the study of the dynamics of a diffusing dimer moving in an optical well lattice. The particles were identical, and modelled as non absorbing dipolar particles at Frohlich Resonance Condition, so their electric polarizabilities were given by $\alpha = i6\pi/k^3$, being $k = 2\pi/\lambda$ the wavenumber and λ the wavelength of the applied electromagnetic field. This polarizability was chosen to cancel the force that a sole particle would experience in an optical well lattice described by an electric field

$$\boldsymbol{E}^0(x, y, z) = E_z^0 \hat{\boldsymbol{e}}_z = i2E_0(\sin kx + \sin ky)\, \hat{\boldsymbol{e}}_z, \tag{7.1}$$

where $\hat{\boldsymbol{e}}_z$ is the unitary vector along the z-direction and E_0 the field's amplitude. Then, the effect on the diffusion purely produced by the optical dipolar interactions can be study. The dynamics were simulated with a Langevin algorithm, where the particles were subject to the effect of viscosity and to thermal fluctuations, modelled with Gaussian white noise, and related to the viscosity via the fluctuation-dissipation theorem.

With these tools, extensive numerical simulations have been performed for different values of the dimer length and different values of the intensity of the applied electromagnetic field. It has been shown that optical interactions have a remarkable effect on the diffusion of the dimer, that strongly depends on the dimer's length. A model potential has been proposed to capture the essential features of the dimer dynamics, leading to a correct description of the probability distribution of the dimer's center of mass.

In Chapter 4, many-particle interactions between dipolar NP were studied. Now, the polarizability mimics the one of a gold NP with $a = 50$nm radius. Simple configurations of three NPs illuminated by a linearly polarized plane wave have been proposed. It has been found that, although

the contribution of the three-particle term to the total force on a NP is generally not very relevant, other effects such as a nonvanishing force on the center of mass of the system of particles are entirely due to the three-particle interactions. The case of three particles immersed in an optical vortex lattice has also been discussed.

The more complex case of a system of N NPs immersed in an optical vortex lattice and subjected to optical and hydrodynamic interactions have been investigated in collaboration with Prof. Rafael Delgado-Buscalioni and Dr. Marc Meléndez. The system was proposed as a realization of a complex system in which NPs were able to take energy from the environment and to communicate via hydrodynamic and optical interactions. A rich variety of collective dynamics were found, mostly due to hydrodynamic interactions. Optical interactions between NPs was shown not to be able to produce a collective phase transition dynamics. However, it induces different effects on the swarm of particles, such as the expansion of the swarm, preventing the NPs to aggregate, and modifying quantitatively and qualitatively the diffusion properties.

In Chapter 5 of this Thesis, dipolar interactions between NPs due to Random Light Illumination have been investigated. First, the interaction between two nonabsorbing particles has been studied. It has been found that the behavior at short distances is not the expected behavior from the literature. This is because if a physical model of electric permittivity is used then, the imaginary part of the electric polarizability can never be equal to zero, and then the terms $R^{-3,-5,-7}$ (being R the separation between the two particles) play a crucial role in the short distance limit of the interaction.

The interaction between two absorbing particles has been also studied, and a new general analytical formula for the interaction between particles with arbitrary polarizabilities has been obtained.

Finally, in Chapter 6, two different features of the interaction between two absorbing particles due to Random Light Illumination have been studied. These properties were studied both numerically and analytically, thanks to the closed formula obtained in the previous chapter.

First, it has been discovered that, for certain conditions on the electric polarizability, a gravity-like interaction between the particles can be obtained not only at short distances but at a full-range of distances, cancelling out the characteristic oscillations of the dipolar interaction. The conditions are a vanishing real part of the polarizability α

$$\mathrm{Re}\left\{\alpha\right\} = 0 \tag{7.2}$$

and absorption cross section to be larger than scattering cross section. Then, the only contribution comes from a non-oscillating term that appears in the analytical expression of the force between absorbing particles.

Finally, the case where the two particles have distinct polarizabilities has been studied. In this case, it is not possible to describe the interaction as a conservative force. This can be deduced from symmetry considerations, and has been numerically analyzed by performing the line integral of the force along a close path which, as expected, does not vanish in the general case. This result points out a nonconservative nature of the dipolar interaction between two different particles under random light illumination.

Eight essential conclusions can be extracted from this work

- By their own, interactions between dipolar nanoparticles are able to strongly modify the diffusion properties of a dimer moving in a lattice of optical wells.
- The features of the trapped diffusion of a dimer in an optical lattice can be captured with a potential, even though the studied interaction is manifiestly non-conservative.
- Many-particle interactions between nanoparticles are able to produce effects not expected from pair-wise interactions, such as a net force on the center of mass of a system of three particles aligned perpendicularly to the wave direction of propagation.
- Optical interactions modify the diffusion properties and provide certain structure to an ensemble of particles subjected to hydrodynamic interactions diffusing in an optical vortex lattice. Forces produced by the vortex field are necessary to trigger a phase transition, while optical interactions between particles do not impede nor delay the phase transition.
- A new closed formula for the interactions between two dipolar particles in a random light field can be obtained as a function of the term of the polarizability that accounts for absorption.
- A full-range gravitational behavior of the interaction between two absorbing particles under random light illumination is found and understood both for model polarizabilities and for silver.

- The interaction between identical particles due to random ligth illumination turns out to be conservative, even in the case of non-zero absorption.
- The interaction between different particles due to random ligth illumination can not be described by a potential function, even though two different potential functions can be found for each of the two particles independently.

Chapter 8

Conclusiones (Spanish)

En este capítulo se presentan las principales conclusiones extraídas a lo largo de esta Tesis:

El Capítulo 3 de esta Tesis trata sobre el estudio de la dinámica de difusión de un dímero moviéndose a través de una red óptica de pozos. Las partículas son idénticas y modeladas como partículas sin absorción en la condición de resonancia de Frohlich, por lo que sus polarizabilidades eléctricas vienen dadas por $\alpha = i6\pi/k^3$, siendo $k = 2\pi/\lambda$ el número de onda y λ la longitud de onda del campo electromagnético aplicado. Se eligió esta polarizabilidad para cancelar la fuerza que sentiría una única partícula en el seno de la red óptica de pozos cuyo campo eléctrico viene dado por

$$\boldsymbol{E}^0(x,y,z) = E_z^0 \hat{\boldsymbol{e}}_z = i2E_0(\sin kx + \sin ky)\,\hat{\boldsymbol{e}}_z, \tag{8.1}$$

donde $\hat{\boldsymbol{e}}_z$ es el vector unitario a lo largo de la dirección z y E_0 es la amplitud del campo eléctrico. Por tanto, se puede estudiar el efecto sobre la difusión del dímero producido únicamente por las interacciones ópticas dipolares entre las dos partículas. La dinámica se simuló numéricamente mediante un algoritmo tipo Langevin, en el que las partículas sufren el efecto de la viscosidad del líquido que las rodea y de las fuerzas debidas fluctuaciones térmicas, modeladas con un término de ruido blanco Gaussiano y relacionado con la viscosidad a través del teorema de fluctuación-disipación.

Con estas herramientas se han desarrollado vastas simulaciones numéricas para diferentes valores de la longitud del dímero y de la intensidad del campo electromagnético aplicado. Se ha mostrado que las interacciones ópticas tienen un efecto extraordinario sobre las propiedades de difusión del dímero, con una gran dependencia en el valor de su longitud. Se ha propuesto un potencial modelo para capturar las principales características de la difusión del dímero, consiguiendo una descripción correcta de la distribución de probabilidad de las coordenadas del centro de masas del

dímero.

En el Capítulo 4 se han estudiado las interacciones entre varias partículas dipolares. En este caso, la polarizabilidad imita la que tendría una nanopartícula de oro de $a = 50$nm de radio. Se proponen unas configuraciones simples en las que una onda plana linealmente polarizada ilumina un sistema de tres partículas. Se ha encontrado que, aunque la contribución de los términos de tres cuerpos a la fuerza total sobre una de las nanopartículas no es en general de gran relevancia, otros efectos como la aparición de una fuerza neta sobre el centro de masas del sistema de partículas se explican únicamente mediante la existencia de estos términos a tres cuerpos. También se estudia el caso de tres partículas en el seno de una red óptica de vórtices.

En colaboración con el Prof. Rafael Delgado-Buscalioni y el Dr. Marc Meléndez se ha realizado el estudio del caso más complejo en el que N nanopartículas se introducen en una red óptica de vórtices, quedando sujetas a interacciones de tipo óptico y de tipo hidrodinámico. El sistema es una propuesta de realización de un sistema complejo en el que las partículas son capaces de tomar energía de su entorno y convertirla en movimiento, a la vez que se comunican entre ellas mediante interacciones ópticas e hidrodinámicas. Se encuentra una amplia variedad de dinámicas colectivas, principalmente debidas a las interacciones hidrodinámicas. Por los resultados de las simulaciones, se deduce que las interacciones ópticas entre partículas no pueden por sí solas provocar estas dinámicas colectivas. Sin embargo, producen diferentes efectos en el conjunto de partículas, como la expansión del conjunto, dificultando la agregación de nanopartículas y modificando cualitativa y cuantitativamente las propiedades de difusión.

En el Capítulo 5 de esta Tesis se han investigado las interacciones dipolares entre nanopartículas debidas a iluminación con luz aleatoria. En primer lugar, se ha estudiado la interacción entre dos partículas sin absorción. Se ha encontrdo que el comportamiento a distancias cortas no es el esperado en la literatura. Esto se debe a que se ha utilizado un modelo físico para la permitividad eléctrica y, por tanto, la parte imaginaria de la polarizabilidad eléctrica no toma valores nulos para ningún valor de λ. Como consecuencia, los términos $R^{-3,-5,-7}$ (siendo R la separación entre partículas) juega un papel fundamental en el límite a corta distancia de la interacción óptica.

También se ha estudiado la interacción entre dos partículas absorbentes, obteniéndose una nueva fórmula analítica de carácter general, capaz de

describir la interacción entre dos partículas con polarizabilidades arbitrarias.

Finalmente, en el Capítulo 6, se han estudiado dos propiedades características de la interacción entre dos partículas absorbentes debida a iluminación con luz aleatoria. Estas propiedades se han estudiado analítica y numéricamente, utilizando para ello la fórmula cerrada que se obtuvo en el capítulo anterior.

En primer lugar, se ha descubierto que imponiendo determinadas condiciones en la polarizabilidad eléctrica, es posible obtener una interacción de tipo gravitatorio entre las partículas. Esta propiedad no sólo es válida en el límite de cortas distancias, sino en todo el rango de separaciones físicamente admisible, cancelando las típicas oscilaciones de las interacciones dipolares. Las condiciones son: Una parte real de la polarizabilidad α nula

$$\mathrm{Re}\left\{\alpha\right\} = 0 \tag{8.2}$$

y una sección eficaz de absorción mayor que la sección eficaz de scattering. Cuando esto se cumple, la única contribución viene del término no oscilante que aparece en la expresión analítica de la fuerza entre dos partículas absorbentes.

En segundo lugar, se ha estudiado el caso en el que las dos partículas absorbentes tienen diferentes polarizabilidades. En este caso, se deduce analíticamente que, en general, no se cumple la ley de acción y reacción entre las dos partículas, señalando un nuevo escenario en el que esta propiedad no se cumple dentro del campo de las interacciones ópticas. También se deduce que, contrariamente a lo que pasa en el caso de dos partículas id"enticas, no es posible describir la interacción como un sistema completamente conservativo. Estos resultados se pueden deducir de consideraciones de simetría, y han sido comprobados numéricamente realizando la integral de línea de la fuerza a lo largo de una trayectoria cerrada que, tal como se esperaba, no tiene en general un resultado nulo. Este resultado señala la naturaleza no conservativa de la interacción entre dos partículas absorbentes con diferente polarizabilidad debido a iluminación con luz aleatoria.

Del trabajo de esta Tesis se pueden extraer ocho conclusiones principales

- Por sí solas, las interacciones entre nanopartículas dipolares son capaces de modificar extraordinariamente las propiedades de difusión de un dímero moviéndose a lo largo de una red óptica de pozos.

- Las pricipales características de esta difusión atrapada se pueden describir satisfactoriamente por medio de un potencial, incluso aunque la interacción estudiada sea manifiestamente no conservativa.

- Las interacciones de muchos cuerpos entre nanopartículas son capaces de producir efectos no esperados de las interaciones a pares, como la aparición de una fuerza neta sobre el centro de masas de un sistema de tres partículas alineadas perpendicularmente a la dirección de propagación de una onda plana.

- Las interacciones ópticas modifican las propiedades de difusión y proporcionan cierta estructura a un sistema de partículas sujetas a interacciones hidrodinámicas que difunden en una red óptica de vórtices. Las fuerzas producidas por el campo de vórtices son necesarias para generar una transición de fase dinámica, mientras que las interacciones ópticas no modifican ni impiden dicha transición.

- Se ha obtenido una nueva expresión para describir las interacciones entre partículas dipolares iluminadas con luz aleatoria en función del término de la polarizabilidad que da cuenta de la absorción de la partícula.

- Se ha obtenido y entendido una interacción tipo gravitatoria para todo el rango de separaciones entre dos partículas idénticas bajo iluminación de luz aleatoria tanto para partículas modelo como para partículas de plata.

- La interacción debida a iluminación con luz aleatoria entre partículas idénticas resulta ser una interacción conservativa, incluso en el caso con absorción.

- La interacción entre dos partículas diferentes bajo iluminación con luz aleatoria no puede describirse con una función potencial, incluso aunque se puedan encontrar dos potenciales que describan las fuerzas sobre las dos partículas por separado.

Appendix A

The Green dyadic function

In this appendix we shall detail some properties of the Green dyadic function for the electric field and of its derivatives. These properties will be useful for the analytical and numerical treatment of optical interactions.

From the literature (Novotny et al., 2012), we know that the Green dyadic function can be written as

$$\begin{aligned} G(\boldsymbol{r}_A, \boldsymbol{r}_B) &= \left[\mathbb{I} + \frac{1}{k^2}\nabla\nabla\right]\frac{e^{ikR}}{4\pi R} \\ &= \frac{e^{ikR}}{4\pi R}\left[\left(1 + \frac{i}{kR} - \frac{1}{k^2R^2}\right)\mathbb{I} - \left(1 + \frac{i3}{kR} - \frac{3}{k^2R^2}\right)\frac{\boldsymbol{R}\otimes\boldsymbol{R}}{R^2}\right] \end{aligned} \tag{A.1}$$

where $k = 2\pi/\lambda$ is the wavenumber, $\boldsymbol{R} = \boldsymbol{r}_A - \boldsymbol{r}_B$ is the separation vector between particles a and B,

$$R = \sqrt{(x_A - x_B)^2 + (y_A - y_B)^2 + (z_A - z_B)^2} \tag{A.2}$$

is its modulus, $\mathbb{I}$ is the 3×3 identity matrix and

$$\boldsymbol{R}\otimes\boldsymbol{R} = \begin{bmatrix} (x_A - x_B)^2 & (x_A - x_B)(y_A - y_B) & (x_A - x_B)(z_A - z_B) \\ (y_A - y_B)(x_A - x_B) & (y_A - y_B)^2 & (y_A - y_B)(z_A - z_B) \\ (z_A - z_B)(x_A - x_B) & (z_A - z_B)(y_A - y_B) & (z_A - z_B)^2 \end{bmatrix} \tag{A.3}$$

is the outer product of $\boldsymbol{R}$ by itself.

It can be readily seen that the Green dyadic function defined by Equation (A.1) is a symmetric matrix.

$$G(\boldsymbol{r}_A, \boldsymbol{r}_B) = G^t(\boldsymbol{r}_A, \boldsymbol{r}_B) \tag{A.4}$$

and that it is also symmetric with respect to the permutation of variables $\boldsymbol{r}_A \leftrightarrow \boldsymbol{r}_B$

$$G(\boldsymbol{r}_A, \boldsymbol{r}_B) = G(\boldsymbol{r}_B, \boldsymbol{r}_A) \tag{A.5}$$

The last property will be used in the numerical computation of incident fields. The former one will be useful in the analytical computation of forces between two NPs under RLI.

The derivative of the Green dyadic function with respect to a variable ϕ_A, being $\phi = x, y, z$ can be written as

$$\begin{aligned}\partial_{\phi_A} G(\boldsymbol{r}_A, \boldsymbol{r}_B) = &\left[\partial_{\phi_A} G_0(\boldsymbol{r}_A, \boldsymbol{r}_B)\right] \mathbb{I} \\ &+ \left[\partial_{\phi_A} G_1(\boldsymbol{r}_A, \boldsymbol{r}_B)\right] \boldsymbol{R} \otimes \boldsymbol{R} + G_1(\boldsymbol{r}_A, \boldsymbol{r}_B)\, \mathcal{R}_{\phi_1}\end{aligned} \tag{A.6}$$

where

$$G_0(\boldsymbol{r}_A, \boldsymbol{r}_B) = \frac{e^{ikR}}{4\pi R}\left(1 + \frac{i}{kR} - \frac{1}{k^2R^2}\right) \tag{A.7a}$$

$$G_1(\boldsymbol{r}_A, \boldsymbol{r}_B) = -\frac{e^{ikR}}{4\pi R}\left(1 + \frac{i3}{kR} - \frac{3}{k^2R^2}\right)\frac{1}{R^2} \tag{A.7b}$$

and the derivatives are given by

$$\partial_{\phi_A} G_0(\boldsymbol{r}_A, \boldsymbol{r}_B) = \left(i - \frac{2}{kR} - \frac{i3}{k^2R^2} + \frac{3}{k^3R^3}\right)\frac{\phi_A - \phi_B}{R}\frac{ke^{ikR}}{4\pi R} \tag{A.8a}$$

$$\partial_{\phi_A} G_1(\boldsymbol{r}_A, \boldsymbol{r}_B) = -\frac{ke^{ikR}}{4\pi R}\frac{\phi_A - \phi_B}{R^3}\left(i - \frac{6}{kR} - \frac{i15}{k^2R^2} + \frac{15}{k^3R^3}\right) \tag{A.8b}$$

And the derivatives of the outer product of $\boldsymbol{R}$ by itself are

$$\mathcal{R}_{x_A} = \begin{bmatrix} 2(x_A - x_B) & (y_A - y_B) & (z_A - z_B) \\ (y_A - y_B) & 0 & 0 \\ (z_A - z_B) & 0 & 0 \end{bmatrix} \tag{A.9}$$

$$\mathcal{R}_{y_A} = \begin{bmatrix} 0 & (x_A - x_B) & 0 \\ (x_A - x_B) & 2(y_A - y_B) & (z_A - z_B) \\ 0 & (z_A - z_B) & 0 \end{bmatrix} \tag{A.10}$$

$$\mathcal{R}_{z_A} = \begin{bmatrix} 0 & 0 & (x_A - x_B) \\ 0 & 0 & (y_A - y_B) \\ (x_A - x_B) & (y_A - y_B) & 2(z_A - z_B) \end{bmatrix} \tag{A.11}$$

From these results, the following relations between the derivatives of the Green dyadic function can be obtained

$$\begin{aligned}\partial_{\phi_A} G(\boldsymbol{r}_A, \boldsymbol{r}_B) &= \partial_{\phi_A} G(\boldsymbol{r}_B, \boldsymbol{r}_A) \\ &= -\partial_{\phi_B} G(\boldsymbol{r}_A, \boldsymbol{r}_B) = -\partial_{\phi_B} G(\boldsymbol{r}_B, \boldsymbol{r}_A)\end{aligned} \tag{A.12}$$

These relations will be useful to simplify the numerical calculation of optical interactions and to analytically study the forces on the center of mass of a pair of particles.

We also have the following relations

$$\mathrm{Im}\left\{G(\boldsymbol{r}_i\boldsymbol{r}_i)\right\} = \frac{k}{6\pi}\mathbb{I}, \qquad \mathrm{Im}\left\{\partial_{z_i}G(\boldsymbol{r}_i\boldsymbol{r}_i)\right\} = 0 \tag{A.13}$$

Appendix B

The Coupled Dipole Approximation

The Couple Dipole Approximation is a volume integral method to numerically compute the incident fields on a set of separated dipolar nanoparticles. It is closely related to the Discrete Dipole Approximation, a method first implemented (Purcell et al., 1973) and further developed by (Draine et al., 1994).

In this method, a system of N individual dipolar particles is handled. The different particles are located at $\boldsymbol{r}_i$, and show a response given by its electric polarizability α_i. When they are illuminated by an applied field, that is expressed at every point $\boldsymbol{r}_i$ as $\boldsymbol{E}^0(\boldsymbol{r}_i)$, the incident field on every particle $\boldsymbol{E}(\boldsymbol{r}_i)$ can be calculated as

$$\begin{aligned}
\boldsymbol{E}(\boldsymbol{r}_1) &= \boldsymbol{E}^0(\boldsymbol{r}_1) + k^2 G(\boldsymbol{r}_1, \boldsymbol{r}_2)\, \alpha_2 \boldsymbol{E}(\boldsymbol{r}_2) + \ldots + k^2 G(\boldsymbol{r}_1, \boldsymbol{r}_N)\, \alpha_N \boldsymbol{E}(\boldsymbol{r}_N) \\
\boldsymbol{E}(\boldsymbol{r}_2) &= k^2 G(\boldsymbol{r}_2, \boldsymbol{r}_1)\, \alpha_1 \boldsymbol{E}(\boldsymbol{r}_1) + \boldsymbol{E}^0(\boldsymbol{r}_2) + \ldots + k^2 G(\boldsymbol{r}_2, \boldsymbol{r}_N)\, \alpha_N \boldsymbol{E}(\boldsymbol{r}_N) \\
&\vdots \\
\boldsymbol{E}(\boldsymbol{r}_N) &= k^2 G(\boldsymbol{r}_N, \boldsymbol{r}_1)\, \alpha_1 \boldsymbol{E}(\boldsymbol{r}_1) + k^2 G(\boldsymbol{r}_N, \boldsymbol{r}_2)\, \alpha_2 \boldsymbol{E}^0(\boldsymbol{r}_2) + \ldots + \boldsymbol{E}^0(\boldsymbol{r}_N).
\end{aligned}$$

Which represents an autoconsistent set of equations. Two vectors that contain the components of the applied field and of the incident field on every particle can be defined as

$$\psi = \begin{bmatrix} \boldsymbol{E}_1 \\ \boldsymbol{E}_2 \\ \vdots \\ \boldsymbol{E}_N \end{bmatrix}, \quad \psi^0 = \begin{bmatrix} \boldsymbol{E}_1^0 \\ \boldsymbol{E}_2^0 \\ \vdots \\ \boldsymbol{E}_N^0 \end{bmatrix}. \tag{B.1}$$

Then, the system of Equations can be written in a more compact form

$$T\psi = \psi^0 \tag{B.2}$$

where the matrix T^{-1} is defined as

$$T = \begin{bmatrix} \mathbb{I} & -k^2 G(\boldsymbol{r}_1, \boldsymbol{r}_2)\alpha_2 & \dots & -k^2 G(\boldsymbol{r}_1, \boldsymbol{r}_N)\alpha_N \\ -k^2 G(\boldsymbol{r}_2, \boldsymbol{r}_1)\alpha_1 & \mathbb{I} & \dots & -k^2 G(\boldsymbol{r}_2, \boldsymbol{r}_N)\alpha_N \\ \vdots & \vdots & & \vdots \\ -k^2 G(\boldsymbol{r}_N, \boldsymbol{r}_1)\alpha_1 & -k^2 G(\boldsymbol{r}_N, \boldsymbol{r}_2)\alpha_2 & \dots & \mathbb{I} \end{bmatrix} \tag{B.3}$$

where $\mathbb{I}$ is the 3×3 identity matrix.

And then, the incident fields will be given by the solution ψ in Equation (B.2). The matrix T only depends on the relative positions of the particles. Then, if the system of particles are set at fixed separations, it is possible to compute the inverse matrix T^{-1} and apply this inverse matrix to obtain the incident fields for arbitrary applied fields

$$\psi = T^{-1}\psi^0. \tag{B.4}$$

However, if the system of particles will vary their relative positions, it might be recommended to solve Equation (B.2) not by computing the inverse matrix T^{-1}, but by solving the system of equations using, for example, a LU decomposition algorithm.

In the computation of matrix T, expressed in Equation (B.3), it is useful to remind that the Green dyadic function is symmetric under permutation of variables, as was shown in Equation (A.5). This allows us to compute only $N(N-1)/2$ Green dyadic functions.

The accuracy of the solution can be tested by illuminating the system of particles with a plane wave and checking the validity of

$$\sigma_{ext} = \sigma_{sca} + \sigma_{abs}, \tag{B.5}$$

where the extinction, scattering and absorption cross sections are computed using Equations (2.16a), (2.16b) and (2.16c), mentioned in Chapter 2.

Bibliography

Albaladejo, Silvia et al. (2009a). "Giant Enhanced Diffusion of Gold Nanoparticles in Optical Vortex Fields". In: *Nano Letters* 9.10. PMID: 19673533, pp. 3527–3531. DOI: 10.1021/nl901745a. eprint: http://dx.doi.org/10.1021/nl901745a. URL: http://dx.doi.org/10.1021/nl901745a.

Albaladejo, Silvia et al. (2009b). "Scattering Forces from the Curl of the Spin Angular Momentum of a Light Field". In: *Physical Review Letters* 102 (11), p. 113602. DOI: 10.1103/PhysRevLett.102.113602. URL: https://link.aps.org/doi/10.1103/PhysRevLett.102.113602.

Albaladejo, Silvia et al. (2010). "Radiative corrections to the polarizability tensor of an electrically small anisotropic dielectric particle". In: *Opt. Express* 18.4, pp. 3556–3567. DOI: 10.1364/OE.18.003556. URL: http://www.opticsexpress.org/abstract.cfm?URI=oe-18-4-3556.

Albaladejo, Silvia, Manuel I. Marqués, and Juan José Sáenz (2011). "Light control of silver nanoparticle's diffusion". In: *Optics Express* 19.12, pp. 11471–11478. DOI: 10.1364/OE.19.011471. URL: http://www.opticsexpress.org/abstract.cfm?URI=oe-19-12-11471.

Arias-González, J. Ricardo and Manuel Nieto-Vesperinas (2003). "Optical forces on small particles: attractive and repulsive nature and plasmon-resonance conditions". In: *Journal of the Optical Society of America A* 20.7, pp. 1201–1209. DOI: 10.1364/JOSAA.20.001201. URL: http://josaa.osa.org/abstract.cfm?URI=josaa-20-7-1201.

Arzola, Alejandro V. et al. (2014). "Rotation, oscillation and hydrodynamic synchronization of optically trapped oblate spheroidal microparticles". In: *Optics Express* 22.13, pp. 16207–16221. DOI: 10.1364/OE.22.016207. URL: http://www.opticsexpress.org/abstract.cfm?URI=oe-22-13-16207.

Ashcroft, N.W. and N.D. Mermin (1976). *Solid State Physics*. HRW international editions. Holt, Rinehart and Winston. ISBN: 9780030839931.

Ashkin, Arthur (1970). "Acceleration and Trapping of Particles by Radiation Pressure". In: *Physical Review Letters* 24 (4), pp. 156–159. DOI: 10.

1103/PhysRevLett.24.156. URL: https://link.aps.org/doi/10.1103/PhysRevLett.24.156.

Ashkin, Arthur et al. (1986). "Observation of a single-beam gradient force optical trap for dielectric particles". In: *Optics Letters* 11.5, pp. 288–290. DOI: 10.1364/OL.11.000288. URL: http://ol.osa.org/abstract.cfm?URI=ol-11-5-288.

Baffou, Guillaume, Romain Quidant, and F. Javier García de Abajo (2010). "Nanoscale Control of Optical Heating in Complex Plasmonic Systems". In: *ACS Nano* 4.2. PMID: 20055439, pp. 709–716. DOI: 10.1021/nn901144d. eprint: http://dx.doi.org/10.1021/nn901144d. URL: http://dx.doi.org/10.1021/nn901144d.

Baffou, Guillaume and Romain Quidant (2013). "Thermo-plasmonics: using metallic nanostructures as nano-sources of heat". In: *Laser & Photonics Reviews* 7.2, pp. 171–187. ISSN: 1863-8899. DOI: 10.1002/lpor.201200003. URL: http://dx.doi.org/10.1002/lpor.201200003.

Balboa Usabiaga, Florencio et al. (2014). "Inertial coupling method for particles in an incompressible fluctuating fluid". In: *Computer Methods in Applied Mechanics and Engineering* 269, pp. 139 –172. ISSN: 0045-7825. DOI: http://dx.doi.org/10.1016/j.cma.2013.10.029. URL: http://www.sciencedirect.com/science/article/pii/S0045782513002818.

Barton, J. P., D. R. Alexander, and S. A. Schaub (1989). "Theoretical determination of net radiation force and torque for a spherical particle illuminated by a focused laser beam". In: *Journal of Applied Physics* 66.10, pp. 4594–4602. DOI: 10.1063/1.343813. eprint: http://dx.doi.org/10.1063/1.343813. URL: http://dx.doi.org/10.1063/1.343813.

Bechinger, Clemens, Matthias Brunner, and Paul Leiderer (2001). "Phase Behavior of Two-Dimensional Colloidal Systems in the Presence of Periodic Light Fields". In: *Physical Review Letters* 86.5, pp. 930–933. DOI: 10.1103/PhysRevLett.86.930. URL: https://link.aps.org/doi/10.1103/PhysRevLett.86.930.

Berry, Michael V. and Pragya Shukla (2013). "Physical curl forces: dipole dynamics near optical vortices". In: *Journal of Physics A: Mathematical and Theoretical* 46.42, p. 422001. DOI: 10.1088/1751-8113/46/42/422001. URL: http://stacks.iop.org/1751-8121/46/i=42/a=422001.

— (2015). "Hamiltonian curl forces". In: *Proceedings of the Royal Society of London A: Mathematical, Physical and Engineering Sciences* 471.2176. DOI:

10.1098/rspa.2015.0002. URL: http://rspa.royalsocietypublishing.org/content/471/2176/20150002.

Bewerunge, Jörg and Stefan U. Egelhaaf (2016). "Experimental creation and characterization of random potential-energy landscapes exploiting speckle patterns". In: *Physical Review A* 93 (1), p. 013806. DOI: 10.1103/PhysRevA.93.013806. URL: https://link.aps.org/doi/10.1103/PhysRevA.93.013806.

Bouchaud, Jean-Philippe and Antoine Georges (1990). "Anomalous diffusion in disordered media: Statistical mechanisms, models and physical applications". In: *Physics Reports* 195.4, pp. 127 –293. ISSN: 0370-1573. DOI: http://dx.doi.org/10.1016/0370-1573(90)90099-N. URL: http://www.sciencedirect.com/science/article/pii/037015739090099N.

Brito, R., R. Soto, and U. Marini Bettolo Marconi (2007). "Casimir forces in granular and other non equilibrium systems". In: *Granular Matter* 10.1, pp. 29–36. ISSN: 1434-7636. DOI: 10.1007/s10035-007-0056-0. URL: http://dx.doi.org/10.1007/s10035-007-0056-0.

Brügger, Georges et al. (2015). "Controlling dispersion forces between small particles with artificially created random light fields". In: *Nature Communications* 6:7460. DOI: 10.1038/ncomms8460. URL: http://dx.doi.org/10.1038/ncomms8460.

Brzobohatỳ, Oto et al. (2013). "Experimental demonstration of optical transport, sorting and self-arrangement using a /'tractor beam/'". In: *Nature Photonics* 7.2, pp. 123–127. DOI: 10.1038/nphoton.2012.332. URL: http://dx.doi.org/10.1038/nphoton.2012.332.

Buenzli, Pascal R. and Rodrigo Soto (2008). "Violation of the action-reaction principle and self-forces induced by nonequilibrium fluctuations". In: *Physical Review E* 78 (2), p. 020102. DOI: 10.1103/PhysRevE.78.020102. URL: https://link.aps.org/doi/10.1103/PhysRevE.78.020102.

Burns, Michael M., Jean-Marc Fournier, and Jene A. Golovchenko (1990). "Optical Matter: Crystallization and Binding in Intense Optical Fields". In: *Science* 249.4970, pp. 749–754. ISSN: 0036-8075. DOI: 10.1126/science.249.4970.749. eprint: http://science.sciencemag.org/content/249/4970/749.full.pdf. URL: http://science.sciencemag.org/content/249/4970/749.

Chaumet, Patrick C. and Manuel Nieto-Vesperinas (2000). "Time-averaged total force on a dipolar sphere in an electromagnetic field". In: *Optics Letters* 25.15, pp. 1065–1067. DOI: 10.1364/OL.25.001065. URL: http://ol.osa.org/abstract.cfm?URI=ol-25-15-1065.

Chowdhury, Aslam, Bruce J. Ackerson, and Noel A. Clark (1985). "Laser-Induced Freezing". In: *Physical Review Letters* 55 (8), pp. 833–836. DOI: 10.1103/PhysRevLett.55.833. URL: https://link.aps.org/doi/10.1103/PhysRevLett.55.833.

de Sousa, Nuno et al. (2016). "Magneto-optical activity in high index dielectric nanoantennas". In: *Scientific Reports* 6.6 Pt 1, p. 60401. ISSN: 30803. DOI: 10.1038/srep30803. URL: http://pre.aps.org/abstract/PRE/v77/i6/e060401.

del Valle, Javier et al. (2017). "Different approaches to generate matching effects using arrays in contact with superconducting films." In: *Superconductor Science and Technology* 30.2, p. 025014. DOI: 10.1088/1361-6668/30/2/025014. URL: http://stacks.iop.org/0953-2048/30/i=2/a=025014.

Delgado-Buscalioni, Rafael et al. (2017). "Collective motion of gold nanoparticles in an optical vortex lattice". In: *In preparation*.

Depasse, Françoise and Jean-Marie Vigoureux (1994). "Optical binding force between two Rayleigh particles". In: *Journal of Physics D: Applied Physics* 27.5, p. 914. URL: http://stacks.iop.org/0022-3727/27/i=5/a=006.

Descharmes, Nicolas et al. (2013). "Observation of Backaction and Self-Induced Trapping in a Planar Hollow Photonic Crystal Cavity". In: *Physical Review Letters* 110 (12), p. 123601. DOI: 10.1103/PhysRevLett.110.123601. URL: https://link.aps.org/doi/10.1103/PhysRevLett.110.123601.

Dholakia, Kishan and Pavel Zemánek (2010). "Colloquium: Gripped by light: Optical binding". In: *Reviews of Modern Physics* 82 (2), pp. 1767–1791. DOI: 10.1103/RevModPhys.82.1767. URL: https://link.aps.org/doi/10.1103/RevModPhys.82.1767.

Do Carmo, Manfredo P. (1994). *Differential Forms and Applications*. Springer-Verlag Berlin Heidelberg. ISBN: 978-3-540-57618-1.

Dogariu, Aristide, Sergey Sukhov, and Juan José Sáenz (2013). "Optically induced 'negative forces'". In: *Nature Photonics* 7, pp. 24–27. DOI: 10.1038/nphoton.2012.315. URL: http://dx.doi.org/10.1038/nphoton.2012.315.

Douglass, Kyle M., Sergey Sukhov, and Aristide Dogariu (2012). "Superdiffusion in optically controlled active media". In: *Nature Photonics* 6, pp. 834–837. DOI: 10.1038/nphoton.2012.278. URL: http://dx.doi.org/10.1038/nphoton.2012.278.

Draine, Bruce T. and Piotr J. Flatau (1994). "Discrete-Dipole Approximation For Scattering Calculations". In: *Journal of the Optical Society of*

America A 11.4, pp. 1491–1499. DOI: 10.1364/JOSAA.11.001491. URL: http://josaa.osa.org/abstract.cfm?URI=josaa-11-4-1491.

Draine, B.T. and J. Goodman (1993). "Beyond Clausis-Mosotti: Wave propagation on a polarizable point lattice and the Discrete Dipole Approximation". In: *Astrophysical Journal* 405.2, pp. 685–697.

Dzubiella, J., H. Löwen, and C. N. Likos (2003). "Depletion Forces in Nonequilibrium". In: *Physical Review Letters* 91 (24), p. 248301. DOI: 10.1103/PhysRevLett.91.248301. URL: https://link.aps.org/doi/10.1103/PhysRevLett.91.248301.

Eckhardt, B. et al. (1999). "Correlations of electromagnetic fields in chaotic cavities". In: *EPL (Europhysics Letters)* 46.2, p. 134. URL: http://stacks.iop.org/0295-5075/46/i=2/a=134.

Edwards, M.R. (2002). *Pushing Gravity: New Perspectives on Le Sage's Theory of Gravitation*. C. Roy Keys Incorporated. ISBN: 9780968368978.

Evers, Florian et al. (2013). "Colloids in light fields: Particle dynamics in random and periodic energy landscapes". In: *The European Physical Journal Special Topics* 222.11, pp. 2995–3009. ISSN: 1951-6401. DOI: 10.1140/epjst/e2013-02071-2. URL: http://dx.doi.org/10.1140/epjst/e2013-02071-2.

Fasano, A., S. Marmi, and B. Pelloni (2006). *Analytical Mechanics: An Introduction*. Oxford Graduate Texts. OUP Oxford. ISBN: 9780191513596.

Frimmer, Martin et al. (2017). "Levitated nanoparticle as a classical two-level atom". In: *Journal of the Optical Society of America B* 34.6, pp. C52–C57. DOI: 10.1364/JOSAB.34.000C52. URL: http://josab.osa.org/abstract.cfm?URI=josab-34-6-C52.

Gamow, George (1949). "On Relativistic Cosmogony". In: *Rev. Mod. Phys.* 21 (3), pp. 367–373. DOI: 10.1103/RevModPhys.21.367. URL: https://link.aps.org/doi/10.1103/RevModPhys.21.367.

Gieseler, Jan et al. (2014). "Dynamic relaxation of a levitated nanoparticle from a non-equilibrium steady state". In: *Nature Nanotechnology* 9, pp. 358–364. DOI: 10.1038/nnano.2014.40. URL: http://dx.doi.org/10.1038/nnano.2014.40.

— (2015). "Dynamic relaxation of a levitated nanoparticle from a non-equilibrium steady state". In: *Nature Nanotechnology* 9, pp. 358–364. ISSN: 1748-3387. DOI: 10.1038/nnano.2014.40. URL: http://dx.doi.org/10.1038/nnano.2014.40.

Gómez-Medina, Raquel et al. (2001). "Resonant Radiation Pressure on Neutral Particles in a Waveguide". In: *Physical Review Letters* 86 (19), pp. 4275–

4277. DOI: 10.1103/PhysRevLett.86.4275. URL: https://link.aps.org/doi/10.1103/PhysRevLett.86.4275.

Gómez-Medina, Raquel and Juan José Sáenz (2004). "Unusually Strong Optical Interactions between Particles in Quasi-One-Dimensional Geometries". In: *Physical Review Letters* 93 (24), p. 243602. DOI: 10.1103/PhysRevLett.93.243602. URL: https://link.aps.org/doi/10.1103/PhysRevLett.93.243602.

Gómez-Medina, Raquel, Manuel Nieto-Vesperinas, and Juan José Sáenz (2011). "Nonconservative electric and magnetic optical forces on submicron dielectric particles". In: *Physical Review A* 83 (3), p. 033825. DOI: 10.1103/PhysRevA.83.033825. URL: https://link.aps.org/doi/10.1103/PhysRevA.83.033825.

Gómez-Santos, G. (2009). "Thermal van der Waals interaction between graphene layers". In: *Physical Review B* 80 (24), p. 245424. DOI: 10.1103/PhysRevB.80.245424. URL: https://link.aps.org/doi/10.1103/PhysRevB.80.245424.

Govorov, Alexander O. and Hugh H. Richardson (2007). "Generating heat with metal nanoparticles". In: *Nano Today* 2.1, pp. 30 –38. ISSN: 1748-0132. DOI: http://dx.doi.org/10.1016/S1748-0132(07)70017-8. URL: http://www.sciencedirect.com/science/article/pii/S1748013207700178.

Haefner, David, Sergey Sukhov, and Aristide Dogariu (2009). "Conservative and Nonconservative Torques in Optical Binding". In: *Physical Review Letters* 103 (17), p. 173602. DOI: 10.1103/PhysRevLett.103.173602. URL: https://link.aps.org/doi/10.1103/PhysRevLett.103.173602.

Han, Xiang and Philip H. Jones (2015). "Evanescent wave optical binding forces on spherical microparticles". In: *Optics Letters* 40.17, pp. 4042–4045. DOI: 10.1364/OL.40.004042. URL: http://ol.osa.org/abstract.cfm?URI=ol-40-17-4042.

Hänggi, Peter and Fabio Marchesoni (2009). "Artificial Brownian motors: Controlling transport on the nanoscale". In: *Reviews of Modern Physics* 81 (1), pp. 387–442. DOI: 10.1103/RevModPhys.81.387. URL: https://link.aps.org/doi/10.1103/RevModPhys.81.387.

Hayashi, Kumiko and Shin ichi Sasa (2006). "The law of action and reaction for the effective force in a non-equilibrium colloidal system". In: *Journal of Physics: Condensed Matter* 18.10, p. 2825. URL: http://stacks.iop.org/0953-8984/18/i=10/a=008.

Hemmerich, Andreas and Theodor W. Hänsch (1992). "Radiation pressure vortices in two crossed standing waves". In: *Physical Review Letters* 68

(10), pp. 1492–1495. DOI: 10.1103/PhysRevLett.68.1492. URL: https://link.aps.org/doi/10.1103/PhysRevLett.68.1492.

— (1993). "Two-dimesional atomic crystal bound by light". In: *Physical Review Letters* 70 (4), pp. 410–413. DOI: 10.1103/PhysRevLett.70.410. URL: https://link.aps.org/doi/10.1103/PhysRevLett.70.410.

Ivlev, A. V. et al. (2015). "Statistical Mechanics where Newton's Third Law is Broken". In: *Physical Review X* 5 (1), p. 011035. DOI: 10.1103/PhysRevX.5.011035. URL: https://link.aps.org/doi/10.1103/PhysRevX.5.011035.

Jackson, John David (1999). *Classical electrodynamics*. 3rd ed. New York, NY: Wiley. ISBN: 9780471309321.

Jones, Philip, Onofrio Maragó, and Giovanni Volpe (2015). *Optical Tweezers: Principles and Applications*. Cambridge University Press. ISBN: 9781107051164. URL: http://opticaltweezers.org/.

Juan, Mathieu L. et al. (2009). "Self-induced back-action optical trapping of dielectric nanoparticles". In: *Nature Physics* 5.12, pp. 915–919. DOI: 10.1038/nphys1422. URL: http://dx.doi.org/10.1038/nphys1422.

Kirkpatrick, T. R., J. M. Ortiz de Zárate, and J. V. Sengers (2016). "Nonequilibrium fluctuation-induced Casimir pressures in liquid mixtures". In: *Physical Review E* 93 (3), p. 032117. DOI: 10.1103/PhysRevE.93.032117. URL: https://link.aps.org/doi/10.1103/PhysRevE.93.032117.

Korda, Pamela T., Michael B. Taylor, and David G. Grier (2002). "Kinetically Locked-In Colloidal Transport in an Array of Optical Tweezers". In: *Physical Review Letters* 89 (12), p. 128301. DOI: 10.1103/PhysRevLett.89.128301. URL: https://link.aps.org/doi/10.1103/PhysRevLett.89.128301.

Ladavac, K., K. Kasza, and D. G. Grier (2004). "Sorting mesoscopic objects with periodic potential landscapes: Optical fractionation". In: *Physical Review E* 70 (1), p. 010901. DOI: 10.1103/PhysRevE.70.010901. URL: https://link.aps.org/doi/10.1103/PhysRevE.70.010901.

Lee, Sang-Hyuk and David G. Grier (2006). "Giant Colloidal Diffusivity on Corrugated Optical Vortices". In: *Physical Review Letters* 96 (19), p. 190601. DOI: 10.1103/PhysRevLett.96.190601. URL: https://link.aps.org/doi/10.1103/PhysRevLett.96.190601.

Lorentz, Hendrik A. (1900). "Considerations on Gravitation". In: *Koninklijke Nederlandse Akademie van Wetenschappen Proceedings Series B Physical Sciences* 2, pp. 559–574. URL: http://adsabs.harvard.edu/full/1899KNAB....2..559L.

Luis-Hita, Jorge, Juan José Sáenz, and Manuel I. Marqués (2016). "Arrested Dimer's Diffusion by Self-Induced Back-Action Optical Forces". In: *ACS Photonics* 3.7, pp. 1286–1293. DOI: 10.1021/acsphotonics.6b00259. eprint: http://dx.doi.org/10.1021/acsphotonics.6b00259. URL: http://dx.doi.org/10.1021/acsphotonics.6b00259.

MacDonald, Michael P., Gabriel C. Spalding, and Kishan Dholakia (2003). "Microfluidic sorting in an optical lattice". In: *Nature* 426.November, pp. 421–424. DOI: 10.1038/nature02144. URL: http://dx.doi.org/10.1038/nature02144.

Markel, Vadim A. and Andrey K. Sarychev (2007). "Propagation of surface plasmons in ordered and disordered chains of metal nanospheres". In: *Physical Review B* 75 (8), p. 085426. DOI: 10.1103/PhysRevB.75.085426. URL: https://link.aps.org/doi/10.1103/PhysRevB.75.085426.

Marqués, Manuel I. (2016). "Dynamics of a small particle in a fluctuating random light field". In: *Optics Letters* 41.4, pp. 796–799. DOI: 10.1364/OL.41.000796. URL: http://ol.osa.org/abstract.cfm?URI=ol-41-4-796.

McLachlan, A. D. (1963). "Retarded Dispersion Forces in Dielectrics at Finite Temperatures". In: *Proceedings of the Royal Society of London A: Mathematical, Physical and Engineering Sciences* 274.1356, pp. 80–90. ISSN: 0080-4630. DOI: 10.1098/rspa.1963.0115. eprint: http://rspa.royalsocietypublishing.org/content/274/1356/80.full.pdf. URL: http://rspa.royalsocietypublishing.org/content/274/1356/80.

Mikhael, Jules et al. (2008). "Archimedean-like tiling on decagonal quasicrystalline surfaces". In: *Nature* 454.7203, pp. 501–504. ISSN: 0028-0836. DOI: 10.1038/nature07074. URL: http://dx.doi.org/10.1038/nature07074.

Miljković, Vladimir D. et al. (2010). "Optical Forces in Plasmonic Nanoparticle Dimers". In: *The Journal of Physical Chemistry C* 114.16, pp. 7472–7479. DOI: 10.1021/jp911371r. eprint: http://dx.doi.org/10.1021/jp911371r. URL: http://dx.doi.org/10.1021/jp911371r.

Nieto-Vesperinas, Manuel (2015). "Optical torque on small bi-isotropic particles". In: *Optics Letters* 40.13, pp. 3021–3024. DOI: 10.1364/OL.40.003021. URL: http://ol.osa.org/abstract.cfm?URI=ol-40-13-3021.

Novotny, L and B Hecht (2012). *Principles of nano-optics*. Cambridge: Cambridge University Press.

Novotny, Lukas and Bert Hecht (2006). *Principles of Nano-Optics*. Cambridge University Press. ISBN: 9781139452052.

O'Dell, D. et al. (2000). "Bose-Einstein Condensates with $1/r$ Interatomic Attraction: Electromagnetically Induced "Gravity"". In: *Physical Review Letters* 84 (25), pp. 5687–5690. DOI: 10.1103/PhysRevLett.84.5687. URL: https://link.aps.org/doi/10.1103/PhysRevLett.84.5687.

Ohlinger, Alexander et al. (2012). "Optically Trapped Gold Nanoparticle Enables Listening at the Microscale". In: *Physical Review Letters* 108 (1), p. 018101. DOI: 10.1103/PhysRevLett.108.018101. URL: https://link.aps.org/doi/10.1103/PhysRevLett.108.018101.

Öttinger, Hans C. (1996). *Stochastic Processes in Polymeric Fluids: Tools and Examples for Developing Simulation Algorithms*. Springer-Verlag Berlin Heidelberg. ISBN: 978-3-540-58353-0.

Padgett, Miles J., Justin Molloy, and David McGloin (2010). *Optical Tweezers: Methods and Applications*. Chapman and Hall/CRC. ISBN: 9781420074123.

Paladugu, Sathyanarayana et al. (2016). "Nonadditivity of critical Casimir forces". In: *Nature Communications* 7, p. 11403. DOI: 10.1038/ncomms11403. URL: http://dx.doi.org/10.1038/ncomms11403.

Palik, Edward D. (1997). *Handbook of Optical Constants of Solids*. Burlington: Academic Press. ISBN: 978-0-12-544415-6.

Polin, Marco et al. (2005). "Optimized holographic optical traps". In: *Optics Express* 13.15, pp. 5831–5845. DOI: 10.1364/OPEX.13.005831. URL: http://www.opticsexpress.org/abstract.cfm?URI=oe-13-15-5831.

Purcell, E. M. and C. R. Pennypacker (1973). "Scattering and Absorption of Light by Nonspherical Dielectric Grains". In: *Astrophysical Journal* 186.2, pp. 705–714.

Reichhardt, Charles and Franco Nori (1999). "Phase Locking, Devil's Staircases, Farey Trees, and Arnold Tongues in Driven Vortex Lattices with Periodic Pinning". In: *Physical Review Letters* 82 (2), pp. 414–417. DOI: 10.1103/PhysRevLett.82.414. URL: https://link.aps.org/doi/10.1103/PhysRevLett.82.414.

Reimann, Peter (2002). "Brownian motors, noisy transport far from equilibrium". In: *Phys. Rep.* 361.2, pp. 57–265. DOI: 10.1016/S0370-1573(01)00081-3.

Reimann, Peter et al. (2001). "Giant Acceleration of Free Diffusion by Use of Tilted Periodic Potentials". In: *Physical Review Letters* 87 (1), p. 010602. DOI: 10.1103/PhysRevLett.87.010602. URL: https://link.aps.org/doi/10.1103/PhysRevLett.87.010602.

Risken, Hannes and Till Frank (1996). *The Fokker-Planck Equation: Methods of Solution and Applications*. Springer Series in Synergetics. Springer Berlin Heidelberg. ISBN: 9783540615309.

Rodríguez-Sevilla, Paloma et al. (2016). "Optical Torques on Upconverting Particles for Intracellular Microrheometry". In: *Nano Letters* 16.12. PMID: 27960460, pp. 8005–8014. DOI: 10.1021/acs.nanolett.6b04583. eprint: http://dx.doi.org/10.1021/acs.nanolett.6b04583. URL: http://dx.doi.org/10.1021/acs.nanolett.6b04583.

Rohrbach, Alexander et al. (2004). "Trapping and tracking a local probe with a photonic force microscope". In: *Review of Scientific Instruments* 75.6, pp. 2197–2210. DOI: 10.1063/1.1753097. eprint: http://dx.doi.org/10.1063/1.1753097. URL: http://dx.doi.org/10.1063/1.1753097.

Roichman, Yohai et al. (2008). "Optical Forces Arising from Phase Gradients". In: *Physics Review Letters* 100 (1), p. 013602. DOI: 10.1103/PhysRevLett.100.013602. URL: https://link.aps.org/doi/10.1103/PhysRevLett.100.013602.

Russ, Carsten et al. (2005). "Three-body forces at work: Three-body potentials derived from triplet correlations in colloidal suspensions". In: *EPL (Europhysics Letters)* 69.3, p. 468. URL: http://stacks.iop.org/0295-5075/69/i=3/a=468.

Sahimi, Muhammad (1993). "Flow phenomena in rocks: from continuum models to fractals, percolation, cellular automata, and simulated annealing". In: *Reviews of Modern Physics* 65 (4), pp. 1393–1534. DOI: 10.1103/RevModPhys.65.1393. URL: https://link.aps.org/doi/10.1103/RevModPhys.65.1393.

Schiller, P. et al. (2011). "Interactions between Spheroidal Colloidal Particles". In: *Langmuir* 27.17. PMID: 21780779, pp. 10429–10437. DOI: 10.1021/la2015918. eprint: http://dx.doi.org/10.1021/la2015918. URL: http://dx.doi.org/10.1021/la2015918.

Setälä, Tero, Matti Kaivola, and Ari T. Friberg (2003). "Spatial correlations and degree of polarization in homogeneous electromagnetic fields". In:

Optics Letters 28.13, pp. 1069–1071. DOI: 10.1364/OL.28.001069. URL: http://ol.osa.org/abstract.cfm?URI=ol-28-13-1069.

Šiler, Martin and Pavel Zemánek (2010). "Particle jumps between optical traps in a one-dimensional (1D) optical lattice". In: *New Journal of Physics* 12.8, p. 083001. DOI: 10.1088/1367-2630/12/8/083001. URL: http://stacks.iop.org/1367-2630/12/i=8/a=083001.

Spitzer, Lyman Jr. (1941). "The Dynamics of the Interstellar Medium. II. Radiation Pressure." In: *Astrophysical Journal* 94, p. 232. URL: http://adsabs.harvard.edu/doi/10.1086/144328.

Stiles, P.J. (1979). "Dipolar van der Waals forces between molecules of ellipsoidal shape". In: *Molecular Physics* 38.2, pp. 433–447. DOI: 10.1080/00268977900101791. eprint: http://dx.doi.org/10.1080/00268977900101791. URL: http://dx.doi.org/10.1080/00268977900101791.

Sukhov, Sergey and Aristide Dogariu (2011). "Negative Nonconservative Forces: Optical "Tractor Beams" for Arbitrary Objects". In: *Physical Review Letters* 107 (20), p. 203602. DOI: 10.1103/PhysRevLett.107.203602. URL: https://link.aps.org/doi/10.1103/PhysRevLett.107.203602.

Sukhov, Sergey, Kyle M. Douglass, and Aristide Dogariu (2013). "Dipole-dipole interaction in random electromagnetic fields". In: *Optics Letters* 38.14, pp. 2385–2387. DOI: 10.1364/OL.38.002385. URL: http://ol.osa.org/abstract.cfm?URI=ol-38-14-2385.

Sukhov, Sergey et al. (2015). "Actio et reactio in optical binding". In: *Optics Express* 23.1, pp. 247–252. DOI: 10.1364/OE.23.000247. URL: http://www.opticsexpress.org/abstract.cfm?URI=oe-23-1-247.

Thirunamachandran, T. (1980). "Intermolecular interactions in the presence of an intense radiation field". In: *Molecular Physics* 40.2, pp. 393–399. DOI: 10.1080/00268978000101561. eprint: http://dx.doi.org/10.1080/00268978000101561. URL: http://dx.doi.org/10.1080/00268978000101561.

Vicsek, Tamás et al. (1995). "Novel Type of Phase Transition in a System of Self-Driven Particles". In: *Physical Review Letters* 75 (6), pp. 1226–1229. DOI: 10.1103/PhysRevLett.75.1226. URL: https://link.aps.org/doi/10.1103/PhysRevLett.75.1226.

Volpe, Giorgio et al. (2014). "Speckle optical tweezers: micromanipulation with random light fields". In: *Optics Express* 22.15, pp. 18159–18167.

DOI: 10.1364/OE.22.018159. URL: http://www.opticsexpress.org/abstract.cfm?URI=oe-22-15-18159.

Volpe, Giovanni and Dmitri Petrov (2006). "Torque Detection using Brownian Fluctuations". In: *Physical Review Letters* 97 (21), p. 210603. DOI: 10.1103/PhysRevLett.97.210603. URL: https://link.aps.org/doi/10.1103/PhysRevLett.97.210603.

Witten, Thomas A. and Leonard M. Sander (1981). "Diffusion-Limited Aggregation, a Kinetic Critical Phenomenon". In: *Physical Review Letters* 47 (19), pp. 1400–1403. DOI: 10.1103/PhysRevLett.47.1400. URL: https://link.aps.org/doi/10.1103/PhysRevLett.47.1400.

Wu, Pinyu et al. (2009). "Direct Measurement of the Nonconservative Force Field Generated by Optical Tweezers". In: *Physical Review Letters* 103 (10), p. 108101. DOI: 10.1103/PhysRevLett.103.108101. URL: https://link.aps.org/doi/10.1103/PhysRevLett.103.108101.

Xiao, Ke and David G. Grier (2010). "Sorting colloidal particles into multiple channels with optical forces: Prismatic optical fractionation". In: *Physical Review E* 82 (5), p. 051407. DOI: 10.1103/PhysRevE.82.051407. URL: https://link.aps.org/doi/10.1103/PhysRevE.82.051407.

Xu, Hongxing and Mikael Käll (2002). "Surface-Plasmon-Enhanced Optical Forces in Silver Nanoaggregates". In: *Physical Review Letters* 89 (24), p. 246802. DOI: 10.1103/PhysRevLett.89.246802. URL: https://link.aps.org/doi/10.1103/PhysRevLett.89.246802.

Zapata, Ivar et al. (2009). "Deterministic ratchet from stationary light fields". In: *Physical Review Letters* 103, p. 130601. DOI: 10.1103/PhysRevLett.103.130601. URL: https://link.aps.org/doi/10.1103/PhysRevLett.103.130601.

Zapata, Ivar, Rafael Delgado-Buscalioni, and Juan José Sáenz (2016). "Control of diffusion of nanoparticles in an optical vortex lattice". In: *Physical Review E* 93 (6), p. 062130. DOI: 10.1103/PhysRevE.93.062130. URL: https://link.aps.org/doi/10.1103/PhysRevE.93.062130.

Zurita-Sánchez, Jorge R., Jean-Jacques Greffet, and Lukas Novotny (2004). "Friction forces arising from fluctuating thermal fields". In: *Physical Review A* 69 (2), p. 022902. DOI: 10.1103/PhysRevA.69.022902. URL: https://link.aps.org/doi/10.1103/PhysRevA.69.022902.